AL-MAHTOT, O.B. 1999. *An experimental investigation on Archie parameters at ambient and overburden conditions of clean reservoir rocks*. Robert Gordon University, PhD thesis. Hosted on OpenAIR [online]. Available from: https://doi.org/10.48526/rgu-wt-2807275

An experimental investigation on Archie parameters at ambient and overburden conditions of clean reservoir rocks.

AL-MAHTOT, O.B.

1999

THE ROBERT GORDON UNIVESIRTY

FACULTY OF SCIENCE AND TECHNOLOGY

SCHOOL OF MECHANICAL AND OFFSHORE ENGINEERING

"AN EXPERIMENTAL INVESTIGATION ON ARCHIE PARAMETERS AT AMBIENT AND OVERBURDEN CONDITIONS OF CLEAN RESERVOIR ROCKS"

Ph. D. THESIS

A thesis submitted in partial fulfilment of the requirements for the degree of
Doctor of Philosophy

BY:

O. B. AL-MAHTOT

(B. Sc. & M. Sc. in Petroleum Engineering)

JUNE 1999

DEDICATION

"I dedicate this work to my parents, my wife and to whole my family.

ABSTRACT

This thesis presents an experimental investigation of the effect of overburden pressure, porosity type and experimental conditions on the electrical properties (Archie's parameters) of clean reservoir rocks. The samples were from sandstone formations (North Sea), and carbonate formations (Sirte Basin, Libya). Although much work has been carried out on the electrical properties of sandstones (which are considered as ideal representatives of clean reservoir rocks) few experimental studies have been made for carbonate rocks.

The continuous injection technique was used to study the effects of flow displacement mechanisms and fluid characteristics on the resistivity-saturation relationships for both sandstone and carbonate samples. The results showed that the saturation exponent is dependent on both the injection rate of the displacing phase and the fluid viscosities, and it is demonstrated that large errors in water/hydrocarbon saturation can arise if conditions used for the core analysis differ widely from those in the formation. The classical Archie's equation does not take into account the effects of these variables, and therefore it is recommended that the saturation exponent to be used in log analysis should be evaluated with great caution.

The Archie's equation parameters of carbonate rocks were found to vary with porosity type. Samples with mainly interparticle porosity type had $m \cong 2$, while moldic and/or vuggy samples gave higher values, and n was found to be

only weakly dependent on porosity type. These results are of particular significance, as little work has previously been carried out on carbonate rocks, which show greater variations in porosity type than the sandstones which have been studied in considerable detail.

Measurements of the effect of overburden pressure showed that this has a significant effect on the values of the Archie parameters, depending on rock type and pressure applied, as well as on rock porosity. A better understanding of the mechanism of this effect has been achieved which will aid in improved formation evaluation.

The study has permitted a critical evaluation of the applicability of Archie's equation for different experimental conditions and rocks of different porosity types. It has been demonstrated that the equation has significant limitations and its applicability depends to a major extent on the experimental conditions used in core analysis.

TABLE OF CONTENTS

Contents Page No.

Abstract 3

Table of contents 5

List of Figures 11

List of Tables 15

Acknowledgement 16

Nomenclature 18

CHAPTER 1

INTRODUCTION 21

1.1 Introduction 21

1.2 Research Objectives 25

1.3 Approaches 25

1.4 Arrangement of Thesis 26

CHAPTER 2

LITERATURE SURVEY 28

2.1 Introduction to Literature Survey 28

2.2 Electrical Resistivity in Porous Media 30

2.3 Archie's Equations 31

2.31 Variations in the Values of Archie Parameters 34

2.32 Factors Affecting the Cementing Factor 38

2.33 Effect of Porosity Type 39

2.34 The Second Archie's Equation 40

2.4 Effect of Pressure and Temperature 44

2.41 Effect of Pressure on Physical Properties of Rocks 44

2.42 Effect of Pressure on F and *m* 45

2.43 Effect of Temperature on F and *m* 47

2.5 Effect of Experimental Techniques and its Condition on *n* 47

2.6 Porous Medium Modelling 49

CHAPTER 3

EXPERIMENTAL WORK 50

3.1 Introduction 50

3.2 Rock Testing System 51

3.21 Coreholder and Pressure Vessel 51

3.22 Electric circuits 53

3.23 Automatic Data System 57

3.3 Design of Experimental Program 58

3.31 Experimental Procedure 58

3.311 Rock Sample Selection 58

3.312 Sample Preparation and Basic Measurements 59

3.313 Sample Cleaning and Drying 59

3.314 Porosity and Permeability Measurements 61

3.315 Brine Preparation 63

3.4 Resistivity Measurements 64

3.41 Resistivity Measurements at Overburden Pressure 64

3.42 Resistivity Measurements by Porous Plate Method 65

3.43 Resistivity Measurements by Continuous Injection Technique

3.5 Capillary Pressure Measurements 67

3.6 Scanning Electronic Microscope 67

3.7 Results of Rock Characteristics 67

3.8 Porosity-Permeability Relationship 69

CHAPTER 4

EFFECT OF OVERBURDEN ON ARCHIE CEMENTATION FACTOR

4.1Introduction 71

4.2 The Overburden Pressure Effect 71

4.21 Effect of Overburden Pressure on F 71

4.22 Effect of Overburden Pressure on *m* 81

4.23 Effect of Overburden Pressure on *n* 89

4.3 Parametric Study 93

4.4 Conclusions 100

CHAPTER 5

EFFECT OF EXPERIMENTAL CONDITIONS ON ARCHIE SATURATION EXPONENT 103

- 5.1 Introduction 103
- 5.2 General Background 104
- 5.3 Flow Mechanism and Fluid characteristics 108
  - 5.31 Effect of Injection Rate 111
    - 5.311 Review 111
    - 5.312 Injection Rate Experiments 113
      - 5.3121 Experimental Results and Observation 117
      - 5.3122 Slow Injection vs. Fast Injection 125
      - 5.3123 Archie's assumptions and I_R/S_w relationships
    - 5.313 Summary 128
  - 5.32 Effect of Viscosity Ratio 129
    - 5.321 Review 129
    - 5.322 Viscosity Ratio Experiments 130
      - 5.3221 Experimental Results and Observation 131
      - 5.3222 High and Low Viscosity Ratio and I_R/S_w relationships 140
- 5.4 Parametric Study 142
  - 5.41 Injection Rate 143
  - 5.42 Viscosity Ratio 144
- 5.5 Conclusions 144

CHAPTER 6

ARCHIE'S PARAMETERS FOR CARBONATE ROCKS 147

6.1 Introduction 147

6.2 Porosity Types of Carbonates 149

    6.21 Intergranular-intercrystilline Porosity 149

    6.22 Vugular-Solution Porosity 150

    6.23 Fracture-matrix Porosity 150

6.3 Electrical Resistivity vs. Pore Geometry 151

6.4 Variations in the Archie Parameters 154

    6.41 Cementation Factor Variations 154

    6.42 Saturation Exponent Variations 155

6.5 Libyan Carbonate Reservoir Description 156

6.6 Archie Parameters Measurements 157

    6.61 Experimental Procedure 157

    6.62 Results and Discussion 159

6.7 Conclusions 168

CHAPTER 7

DISCUSSIONS AND CONCLUSIONS 170

7.1 Experimental Technique 171

7.2 Effect of Overburden Pressure on Electrical Properties of Rocks. 171

7.21 Effect of Overburden Pressure on Electrical Properties of Sandstones. 172

7.22 Effect of Overburden Pressure on Electrical Properties of Carbonates. 173

7.3 Hysteresis Effect 173

7.4 Effect of Experimental Conditions on I_R/S_w relationships 174

7.5 Non-linearity of I_R/S_w relationships 176

7.6 Archie's Parameters of Carbonate Rocks 176

7.61 Carbonate Reservoir Evaluation (Case Study) 176

7.62 Influence of Porosity Type on Archie parameters 177

7.7 Recommendations 180

7.71 Suggested Experimental Work 180

7.72 Suggested Physical and Mathematical Modelling 181

7.73 Sample Selection 182

REFERENCES AND BIBLIOGRAPHY 183

APPENDIX 202

LIST OF FIGURES

Figure	page
Fig. 2.1 Log F vs. Log ϕ for a particular rock	35
Fig. 2.2 Log I_R vs. Log S_w for Berea sandstone	42
Fig. 3.1 Schematic of the rock testing system	52
Fig. 3.2 Schematic of core sleeve with four-electrodes	54
Fig. 3.3 Four-wire resistivity measurements	56
Fig. 3.4 Schematic diagram of SPT saturator	62
Fig. 4.1 P vs. F of sandstone samples A1, A2	73
Fig. 4.2 P vs. F of sandstone samples A3 - A6	73
Fig. 4.3 P vs. F of sandstone samples A7, A8	74
Fig. 4.4 P vs. F of sandstone sample A9	74
Fig. 4.5 P vs. F of sandstone sample A10	75
Fig. 4.6 P vs. F of carbonate sample B6	75
Fig. 4.7 P vs. F of carbonate sample B9	76
Fig. 4.8 P vs. F of carbonate sample B12	76
Fig. 4.9 P vs. F of carbonate sample B2	77
Fig. 4.10 P vs. F of carbonate samples B3, B5, B6	77
Fig. 4.11 P vs. F of carbonate samples B7, B9, B10, B11	79
Fig. 4.12 P vs. F of carbonate samples B4, B8	79
Fig. 4.13 P vs. F of carbonate sample B12	80
Fig. 4.14 P vs. *m* of sandstone samples A1, A8, A9	83
Fig. 4.15 P vs. *m* of sandstone samples A3, A6	83
Fig. 4.16 P vs. *m* of sandstone samples A4, A5	84

Figure Page

Fig.4.17 P vs. *m* of sandstone samples A2, A7, A10 84

Fig. 4.18 P vs. *m* before and after ϕ correction (A2) 86

Fig. 4.19 P vs. *m* before and after ϕ correction (A3) 86

Fig. 4.20 P vs. *m* before and after ϕ correction (A10) 87

Fig. 4.21 P vs. *m* for carbonate samples B1, B3 and B5 87

Fig. 4.22 P vs. *m* of carbonate samples (B2, B10, B11) 88

Fig. 4.23 P vs. *m* of carbonate samples (B4, B6) 88

Fig. 4.24 P vs. *m* of carbonate samples (B7, B9) 90

Fig. 4.25 P vs. *m* of carbonate sample (B8) 90

Fig.4.26 P vs. *m* of carbonate sample (B12) 91

Fig. 4.27 P vs. *m* before and after ϕ correction (B2) 91

Fig. 4.28 P vs. *m* before and after ϕ correction (B4) 92

Fig. 4.29 P vs. *m* before and after ϕ correction (B9) 92

Fig. 4.32 ϕ_t vs. ϕ_e when P effect is ignored (A1) 94

Fig. 4.33 ϕ_t vs. ϕ_e when P effect is ignored (A2) 94

Fig. 4.34 ϕ_t vs. ϕ_e when P effect is ignored (A6) 95

Fig. 4.35 ϕ_t vs. ϕ_e when P effect is ignored (A10) 95

Fig. 4.36 ϕ_t vs. ϕ_e when P effect is ignored (B1) 96

Fig. 4.37 ϕ_t vs. ϕ_e when P effect is ignored (B2) 96

Fig. 4.38 ϕ_t vs. ϕ_e when P effect is ignored (B7) 97

Fig.4.39 ϕ_t vs. ϕ_e when P effect is ignored (B12) 97

Fig. 5.1 Flow zones during displacement process 109

Figure Page
Fig. 5.2 Layouts of continuous injection technique apparatus 114
Fig. 5.3 Multiple electrodes system 115
Fig. 5.4a I_R vs. S_w of sample C1 119
Fig. 5.4b P_c vs. S_w of sample C1 119
Fig. 5.4c PSD of sample C1 120
Fig. 5.5a I_R vs. S_w of sample C2 120
Fig. 5.5b P_c vs. S_w of sample C2 122
Fig. 5.5c PSD of sample C2 122
Fig. 5.6a I_R vs. S_w of sample C3 123
Fig. 5.6b P_c vs. S_w of sample C3 123
Fig. 5.6c PSD of sample C3 124
Fig. 5.7a I_R vs. S_w of sample C4 124
Fig. 5.7b P_c vs. S_w of sample C4 126
Fig. 5.7c PSD of sample C4 126
Fig. 5.8a I_R vs. S_w of sample D1 132
Fig. 5.8b P_c vs. S_w of sample D1 132
Fig. 5.8c PSD of sample D1 133
Fig. 5.9a I_R vs. S_w of sample D2 133
Fig. 5.9b P_c vs. S_w of sample D2 134
Fig. 5.10a I_R vs. S_w of sample D3 134
Fig. 5.10b P_c vs. S_w of sample D3 136
Fig. 5.10c PSD of sample D3 136
Fig. 5.11a I_R vs. S_w of sample D4 137

Figure	Page
Fig. 5.11b P_c vs. S_w of sample D4	137
Fig. 5.12a I_R vs. S_w of sample D5	138
Fig. 5.12b P_c vs. S_w of sample D5	138
Fig. 5.12c PSD of sample D5	139
Fig. 5.13a I_R vs. S_w of sample D6	139
Fig. 5.13b P_c vs. S_w of sample D6	141
Fig. 5.13c PSD of sample D6	141
Fig. 6.1 Schematic of electrical path through reservoirs	152
Fig. 6.2 Schematic of hydrocarbon affects the flow of electrical current	153
Fig. 6.3 F vs. ϕ of Libyan carbonate formation	160
Fig. 6.4 to Fig.(6.8) SEM photographs of carbonate samples	161-5
Fig. A1 Hassler cell for permeability measurements	207
Fig. A2 Schematic diagram of mercury injection experiment	209

LIST OF TABLES

Table Page

Table 2.1 *m* as function of rock type 34

Table 2.2 *m* values for different minerals 37

Table 2.3 Rock description vs. *m* values 38

Table 3.1 Physical properties of sandstones samples 68

Table 3.2 Physical properties of carbonate samples 68

Table 4.1 Comparison of ϕ_t, ϕ_e of sandstones 98

Table 4.2 Comparison of ϕ_t, ϕ_e of carbonates 99

Table 5.1 Petrophysical properties of the tested samples 105

Table 5.2 S_w calculations at different injection rates 143

Table 5.3 S_w calculations at different viscosity ratios 144

Table 6.1 Petrophysical data of Libyan carbonate samples 158

Table 6.2 Average values of *m* and *n* for each zone 166

Table 6.3 S_w calculation of each zone and % errors 167

ACKNOWLEDGEMENTS

Praise be to Allah, most beneficent, most merciful

The author would like to express his sincere thanks and appreciation to Dr. W. E. Mason, senior lecturer in the School of Mechanical and Offshore Engineering, The Robert Gordon University, for technical guidance and support in numerous ways. Dr. Mason's contribution to defining the scope of this study has helped to put this thesis in its final shape.

The author is greatly indebted to Mr. G. Sinclair, former general manager of Robertson Research, Aberdeen and to Mr. G. Buxtter, laboratory supervisor for many hours of hard work in setting up the experimental system and for their technical advice and moral support throughout this study.

The author wishes to express his sincere thanks to Mr. S. Duguid of Core Laboratories, Aberdeen for his assistance and help regarding the resistivity measurements by the continuous injection technique.

Also special thanks go to Dr. X. Jing of Imperial College, London for his advice and suggestions especially at the initial stage of this research programme.

Thanks are also due to Prof. Dr. M. Nasr of the Petroleum Department, Al-Fateh University, Tripoli, Libya, and to Dr. A. Adam and Mr. L. Power of the School of Mechanical and Offshore Engineering in The Robert Gordon University for their interest in this work, and for many useful comments and suggestions. Special thanks go to Dr. J. Rushton of Core Laboratories for his role in analysing the SEM images.

The assistance of Mr. M. Adris, Manager of Petroleum Research Centre, Tripoli, Libya and Mr. S. Anthony of Corex, Aberdeen UK is gratefully acknowledged for providing rock samples and the relevant information.

Special thanks go to Dr. E. Gobina of Robert Gordon University for his suggestions in the later stages of the research. Many thanks also to all friends and colleagues in The School of Mechanical and Offshore Engineering, 1995-1999, for their encouragement and friendship, including A. Bashir, Dr. C. Stewart, Dr. S. Jihan, A. Al-Ozire, S. Wan, and many more.

The author thanks sincerely the Ministry of Libyan Education for their sponsorship during his postgraduate studies.

Finally, the author would like to express his appreciation to his family for standing by him all these years, especially to his coolness of eyes, beloved and dear wife Zuhra Muammar Mehemmed whose understanding, patience and encouragement enabled him to complete this study.

NOMENCLATURE

Symbol	Units	Meaning
A	*cm²*	cross-sectional area
a		dimensionless constant (in Archie Equation)
C_o	s/*m*	rock conductance with 100% brine saturation
C_w	s/*m*	electrolyte solution conductance
Ct	s/*m*	conductance of rock partially saturated with brine
D_r	*m²*	pore size distribution function
F		formation resistivity factor
ϕ	*fraction or %*	porosity
I	*amperes*	current
I_R		resistivity index
K	*mD*	permeability
k_a	*mD*	air permeability
K_l	*mD*	liquid permeability
L	*cm*	length
m		cementation factor
μ	*cP*	viscosity
n		saturation exponent (in Archie Equation)
P	*psi*	pressure
P_c	*psi*	capillary pressure
Q	*cc/hr*	flow rate
r	*ohm*	resistance
R_o	*ohm/m*	resistivity of rock fully saturated with brine

R_w	*ohm/m*	resistivity of brine
R_t	*ohm/m*	resistivity of rock partially saturated with brine
T	$^oF/^oC$	temperature
V	cm^3	volume
V_p	cm^3	pore volume
V_b	cm^3	bulk volume

Conversion Factors:

Permeability:

1 Darcy = 1000 millidarcy (mD)

= 0.9869 µm

Length:

1 cm = 0.3937 inch

1 ft = 30.481 cm

1 µm = 10^{-6} m

Pressure:

1 psi = 6894.8 N/m^2 = 6.8948 kPa

1 atm = 14.696 psi

Temperature:

0 ^{0}C = 273.16 K

Volume:

1000 cm^3 = 1L = 0.2642 gallons (Imperial)

1 ft^3 = 0.02831 m^3 = 28.31 L

Viscosity:

1 P (poise) = 1 gm/cm . s

= 1 N-s/m^2

Surface Tension:

1 dyn/cm = 10^{-3} N/m

Conductivity:

s = 1/ohm (siemens)

Physical Constants:

g = 9.81 m/s^2

R (Gas Constant) = 8.3143 J/mol K

CHAPTER I

INTRODUCTION

For effective reservoir performance analysis and prediction of hydrocarbon production behaviour, comprehensive information is required about the *in situ* properties of the reservoir. To this end, the determination of petrophysical characteristics (porosity, saturation, electrical resistivity and permeability) play a vital role as these have a direct bearing on the evaluation of hydrocarbons in place and the prediction of oil/gas/water flow through the reservoir during production operations.

Laboratory core analysis and well logging are the two basic methods used to determine petrophysical properties. The quantitative interpretation of electrical log measurements is based on the fact that the formation water conducts electrical current and hydrocarbons do not. The variation of electrical resistivity with depth was first used by the Schlumberger brothers in 1927 to indicate the presence of oil and/or gas in rock formations. In 1942, Archie observed that the resistivity (R_o) of brine-saturated rock samples increased linearly with the brine resistivity (R_w). Archie's equation is

$$F = R_o / R_w = 1 / \phi^m, \qquad 1.1$$

where ϕ is the porosity, F is the formation resistivity factor, m is the Archie cementation factor, (representing the negative slope of an F versus ϕ double logarithmic plot). For partially saturated rock samples, Archie introduced a second equation

$$I_R = R_t / R_o , \qquad 1.2$$

where, I_R is the resistivity index and R_t is the resistivity of a rock sample partially saturated by brine. His experiments were performed on clean sands. Archie proposed the following relation

$$I_R = 1 / S_w^n , \qquad 1.3$$

where S_w is the water saturation and *n* is now called the saturation exponent, which must be determined experimentally. Relation (1.3) was based on experimental data reported in the literature (Martin *et al.*, 1938; Jackosky and Hopper, 1937; Wyckoff and Botset 1936; Leverett 1939).

Over the years, the oil industry has made extensive use of particular forms of the first Archie equation, e.g.

$$F = 0.62 / \phi^{2.15}$$

for sandstone formations, and

$$F = 1 / \phi^2$$

for carbonate formations. The use of $m = 2$ for carbonate formations has frequently led to significant errors in the determination of porosity and water saturation (Al-Mahtot *et al.* 1999). The current log interpretation of carbonate formation data is limited by the assumption that m is close to its value for sandstone formations regardless of the differences in petrophysical properties. Also, most of the previous work has been carried out on sandstone rock rather than carbonates in spite of the fact that carbonate reservoirs make up one-third of current hydrocarbon production and two-thirds of hydrocarbon reserves (Western Atlas 1992). In the best current field practice, the cementation factor is measured for a limited number of plug samples, ignoring the effects that pore type and structure may have on the value of m. However, because sandstone is considered as an ideal representative porous medium, and because of the common assumption that there is no major difference in electric current flow through either sandstones or carbonates, similar values of m and n are widely used for both types of formation.

Based on theoretical studies of electrical flow in carbonate rocks it appears that different porosity types would have different cementation factor values (Asquith, 1985), and this has been confirmed by the experimental measurements reported in the present work. Carbonate evaluation presents complex problems, and remains to be fully understood.

It has been common practice to measure the electrical properties of rock samples in the laboratory often without taking into account the effect of overburden pressure. Although a number of previous studies (Glanville 1959, Longeron et al. 1986, Mahmood *et al.,* 1988, Lewis *et al.,* 1988, Elashahab, 1993) have been carried out on this effect, more work is still needed to gain an insight into the mechanisms by which overburden pressure affects rock properties when one or more fluid phases are present.

The surface of the grains composing the solid matrix of sands, sandstones or clays is typically charged when it is in contact with an electrolyte. The counterions required to balance this charge form an electrical diffuse layer (EDL) (Revil and Glover 1997). Conduction through the EDL and also through any conductive solids present will contribute to the total conductance. The additional conductivity caused by the presence of conductive solids can be estimated from the equations of Waxman and Smith (1968). These effects are usually important for non-clean rocks but are insignificant for clean rocks as used in the present study.

Underlying Archie's equation is the key assumption that resistivity (R_t) depends only upon the porosity (ϕ) of a given rock, the water saturation (S_w) and water resistivity (R_w), i.e., R_t and S_w are the only variables in the equation. Therefore, the same value of saturation should give the same value of resistivity (R_t) whatever the fluid displacement method and the properties of the fluids also fluid/rock interactions. In order to examine the validity of this assumption, it is essential to investigate the influence of the fluid displacement mechanism and the fluid characteristics on the resistivity-saturation relationship and the Archie saturation exponent.

Research Objectives

The objectives of this research are to investigate experimentally the following:

1)- The effect of overburden pressure on the resistivity-porosity relationship of sandstone and carbonate rock samples (subjected to maximum pressures of 4500 psi and 10,000 psi respectively).

2)- The variation of the Archie parameters (*m* and *n*) for selected carbonate rock samples exhibiting various porosity types.

3)- The basic assumption of Archie's analysis that the saturation exponent is independent of fluid characteristics and the mechanism of the desaturation process. In particular, the influence of the viscosity ratio of the fluid phases and the injection rate of the displacing phase on the resistivity-saturation relationship were investigated.

Approaches

To achieve the above research objectives, the following experimental programme was undertaken:

1) Numerous sandstone (North Sea, UKCS) and carbonate (Sirte basin, Libya) rock samples were collected. These samples cover a wide range of petrophysical properties and represent different rock formation and reservoir qualities. The carbonate sample selection was made on the basis of different types of porosity, to permit thorough investigation of the effects of porosity type on the Archie's parameters.

2) An existing laboratory high pressure rock testing system was modified to meet the specific experimental requirements of the present research. The system can accommodate up to five rock samples of 1.5 inch diameter and 3.15 inch in length simultaneously, and the resistivity can be measured at various overburden pressure values.

3) Various established techniques were used to measure the electrical resistivity of fully and partially saturated samples. Different experimental conditions were selected in order to study their effects on the resistivity-saturation relationship. An experimental investigation of saturation exponent measurements was developed to study the effect of the nonwetting phase injection rate and the viscosity ratio of the displaced/displacing phases on the resistivity-saturation relationships, in order to examine the assumption that Archie's equation is not dependent on fluids characteristics or desaturation process.

Subsequently, the petrophysical implications of the results were examined by carrying out limited parametric studies to estimate the errors in hydrocarbon evaluation resulting from the influence of overburden pressure, porosity type, viscosity ratio and injection rate in typical situations. All experimental results were saved on floppy disks which attached to the thesis.

Arrangement of Thesis

In the next chapter, the theoretical background of electrical conduction in fully and partially saturated rock is presented, and Archie's equations and their application are reviewed in more detail. Chapter 3 describes the experimental techniques, procedures and apparatus used in this research. Chapter 4 presents and discusses the results of the study on the effect of overburden pressure on the resistivity of rocks, and especially on the Archie cementation factor. It also describes a parametric study. Chapter 5 deals with the effect of experimental conditions on the electrical properties of partially saturated rocks. This chapter reports a novel study of the influence of flow displacement mechanism and fluid characteristics on resistivity-saturation relationships and also includes a parametric study. Chapter 6 presents a case study for carbonate rocks. The Archie parameters of carbonate core samples were investigated, and it is shown that reliable formation evaluation for carbonates can be implemented taking into account the effects of porosity type on the Archie parameters. Chapter 7 is the final chapter which summarises the findings of this research and makes recommendations for further studies.

CHAPTER II

LITERATURE SURVEY

2.1 Introduction to Literature Review:

The principles of petrophysics deal with the study of the physical properties of porous media. For a rock formation to form a suitable reservoir, it must have a capacity for fluids (porosity), it must permit the flow of fluids (permeability), and it must contain sufficient quantities of hydrocarbons (saturation). Core analysis and well logging are the essential tools to characterise reservoir rocks (Cosse *et al.,* 1993).

Electrical conduction is defined as "the ability of a porous material to conduct electricity". The phenomenon of electrical conduction arises from the movement of electrons (metallic conduction) or ions (electrolytic and surface conduction) through the conducting system. In fluid-saturated porous rocks, electrical conduction results from the movement of ions through the fluid occupying the pores, and/or surface conductance at the fluid/grain interfaces under the influence of electrical fields. Most of the minerals present are insulators (dielectrics) and their charge carriers are ions rather than electrons. The contrast in conductivity between conductors and insulators results from two causes: there are fewer ionic charge carriers in dielectrics than there are conduction electrons in metals, and due to their larger volume and mass, the mobilities of the ions are much smaller. Ionic displacement occurs primarily by diffusion. (Gueguen and Palciauskas, 1994) . In porous media, oil and gas are non-conductors while water is a conductor when it contains dissolved salts. Under the influence of an electric field E, the movement of electrons or ions gives rise to an electric current I, defined as the rate of flow of charge. Ohm proposed that the current in a metallic wire is proportional to the potential difference between its ends. Ohm's law is expressed by the equation

$$E = I\,r\,, \tag{2.1}$$

where, E (volts) is the potential difference, which is related to I (amperes) by a constant called the resistance r (ohm). The resistance r of an electrical conductor is directly proportional to its length, and inversely proportional to its cross-sectional area. It changes with temperature and is dependent on the conducting material. Then

$$r = R\,L\,/\,A\,, \tag{2.2}$$

where R is the resistivity of the conductor material (ohm-meter) (i.e., the reciprocal of conductivity), L is the length of conductor material (meter), and A is its cross-sectional area (meter^2). The resistivity of an *in situ* rock depends on (Serra, 1984, Asquith 1985):

a) the resistivity of water in the pores (this varies with the nature and concentration of the dissolved salts);

b) the quantity of water present; i.e., the porosity and saturation;

c) the formation temperature;

d) pore geometry and porosity types.

As a consequence of the number of factors involved, any precise analytical relationship between electrical properties and petrophysical characteristics such as porosity, saturation and permeability is virtually impossible to achieve. However, many empirical equations have been established over the past six decades to permit the practical use of electrical logging data for interpretation of underground rock properties.

2.2 Electrical Resistivity in Porous Media:

In porous rocks without conductive solids, electrical conduction results from the movement of ions in the electrolyte solution (brine) in the pores. If a DC current is passed through the rock, electrolysis and polarisation occur which affect the proportionality between current and applied potential difference (Grattoni 1994). In order to avoid this, AC voltage (with frequency ~ 1-2 kHz) is used, so that insignificant accumulation of electrolysis products can occur at the electrodes.

In more porous rock with well cemented pores, the ions move easily and the resistivity will be low. For less porous rocks, with tortuous pore connectivity, ions follow long paths and the resistivity will be high. In both high and low porosity rocks, any hydrocarbons present restrict the movement of ions and the resistivity will be increased. For a particular rock sample, the more saline the brine is, the more conductive the rock becomes. A rock sample will have a higher resistivity if its conducting path is long and the cross-sectional area is small. If the clean core sample is partially saturated with oil, its resistivity will have a higher value, since the oil occupies part of the pore space, the area available for current flow becomes less and its flow path becomes longer (Elashahab *et. al,* 1995).

In core analysis, the resistivity is measured in the laboratory for different rock samples from a reservoir formation under different representative conditions to investigate the electrical properties which are essential for evaluating water/hydrocarbon saturations from the resistivity data obtained by wireline logging.

2.3 Archie's Equations:

Electrical well logs are used to characterise the rock-fluid system along the well bore and the interpretation of such logs is based on Archie's equations. Archie (1942) measured the electrical resistivity of a large number of cores collected from sandy formations. The samples were saturated with brine, and their resistivity measured. These samples had porosities ranging from 10% to 40% and the brine salinity was from 20,000 to 100,000 ppm NaCl. Archie correlated the observed formation resistivity factor (F) with porosity and permeability. He suggested that the correlation with porosity was more reliable. By plotting (F) versus (ϕ) on logarithmic co-ordinates, a simple relationship was found

$$F = R_o / R_w = a / \phi^m , \qquad 2.3$$

where F is defined as the formation resistivity factor of rock when fully saturated with brine, R_o is the brine-saturated rock resistivity, R_w is the brine resistivity and m (later called Archie's cementation factor) is the exponent representing the slope of the relationship on log-log graph paper, and *a* is a constant. Archie himself found m to lie between 1.8 and 2.0 for consolidated sandstones.

The relationships between the electrical properties and other physical properties of porous media are complex. They have been studied by Wyllie and Spangler (1952), who presented straight capillary-tube models of flow in porous media. Cornell and Katz (1953), developed inclined capillary-tube flow models, while Wyllie and Gardner (1958) and Winsauer *et. al.*, (1952) also worked along similar lines. The dependence of the resistivity factor on porosity was originally suggested by Sundberg (1932).

James Clerk Maxwell (reprinted 1954), in his famous *Treatise on Electricity and Magnetism,* derived the following expression for the electrical properties of a system of dispersed spheres

$$F = (3 - \phi) / 2\phi , \qquad 2.4$$

Slawinski (1926) subsequently developed the following theoretical expression for the same case

$$F = (1.3219 - 0.3219\phi)^2 / \phi , \qquad 2.5$$

Outstanding among the attempts to generalise the Maxwell equation is the work of Fricke (1924) who theoretically demonstrated that for a dispersed system of oblate and prolate spheroids,

$$F = [(x-1) - \phi] \; / \; x\phi \qquad 2.6$$

where x is a geometrical parameter.

One widely used modification of Archie's equation is the Humble equation. Winsauer *et al.*, 1952 showed that, in most cases, the value of the Archie constant *a* could be taken as unity with little loss in precision. While the Humble formula and its modifications (e.g. $F= 0.81/\phi^2$, Tixier,1951) is satisfactory for sucrosic rocks, better results are obtained using $F = 1/\phi^2$ in chalky rock and $F = 1/\phi^{2.2}$ to $1/\phi^{2.5}$ in compact or oolicastic rocks (Asquith 1982). The usual form of the Humble formula is

$$F = 0.62 \; / \; \phi^{2.15}, \qquad 2.7$$

Archie's equation has been studied widely and many forms of it have been proposed for different types of sandstones, carbonates and other rock types. Table 2.1 indicates different coefficient and exponents summarised by Asquith (1982).

Table 2.1 Values of *m* and *a* as function of rock type (Asquith, 1982)

$F = 1 / \phi^{2}$	for carbonates
$F = 0.81 / \phi^{2}$	for consolidated sandstones
$F = 0.62 / \phi^{2.15}$	for unconsolidated sands (Humble equation)
$F = 1.45 / \phi^{1.33}$	for 'average' sands
$F = 1.65 / \phi^{1.7}$	for calcareous
$F = 0.85 / \phi^{2.14}$	for carbonate
$F = 2.45 / \phi^{1.08}$	for pliocene sands (California)
$F = 1.97 / \phi^{1.29}$	for miocene sands (Gulf Coast)
$F = 1.0 / \phi^{(2.05\phi)}$	for clean granular formations

In general form Archie's equation can be written as

$$F = a / \phi^{m} \qquad 2.8$$

where *a* is an empirical constant, which appears to be function of pore geometry, and for which a value of 1 is often used (Lovell and Pezard, 1990, Maute *et al.*, 1992). *m* is the cementation factor as defined by Guyod (1944), which is the slope of a log F versus log ϕ plot as shown in Figure 2.1 (after Archer and Wall, 1992).

2.31 Variations in the Values of the Archie Parameters

Jackson *et al.*, (1978) carried out a series of laboratory experiments on sands with different particle shapes and sizes. Their results showed that each of these clean sand samples followed Archie's equation with a value of $a = 1$. The

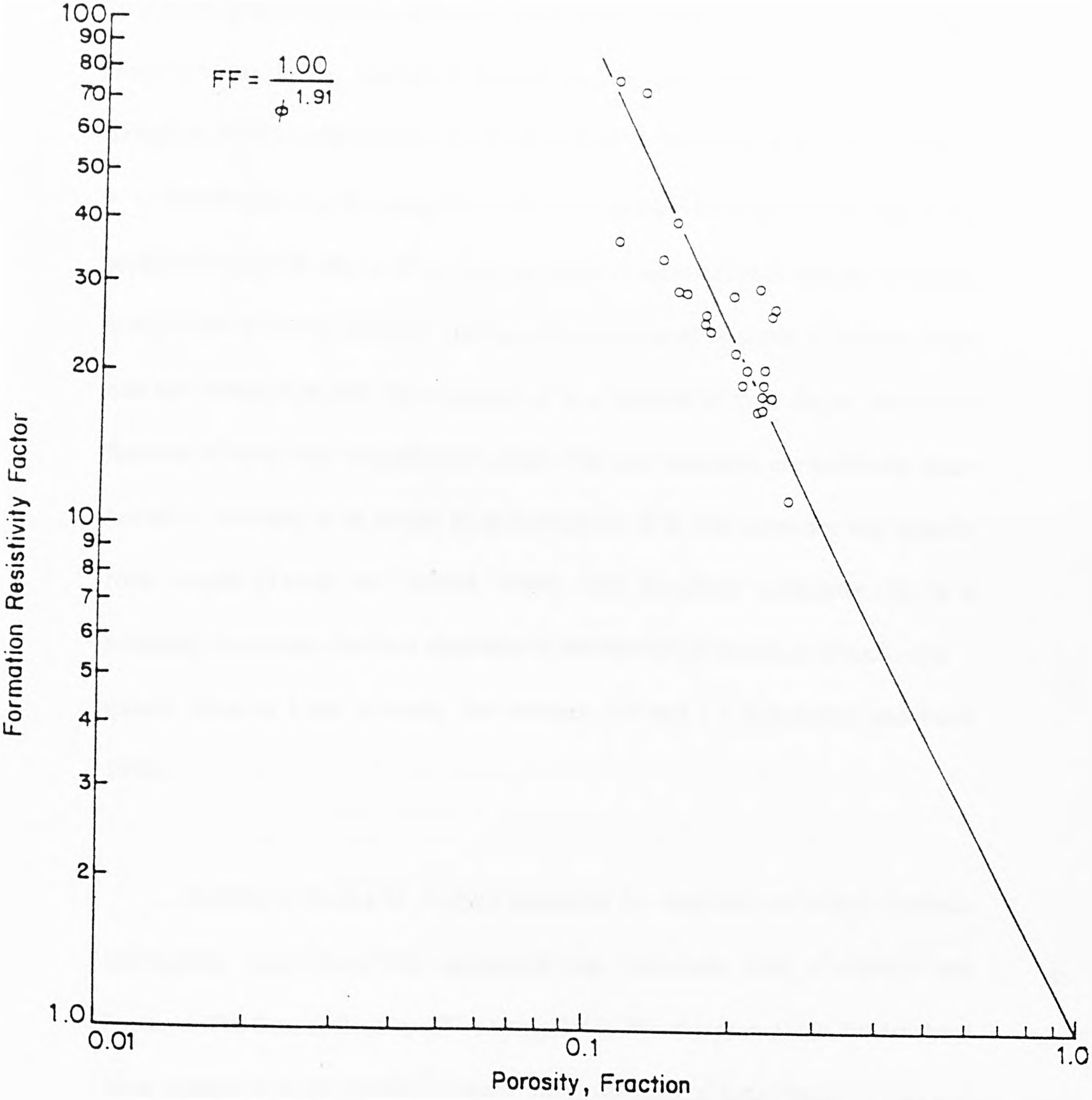

Fig. (2.1) Log F versus log ϕ plot (after Archer and Wall, 1992).

parameter *m* had a direct relation with particle shape. For spherical glass ballotini *m* was 1.4, increasing to 1.5-1.6 for rounded quartz sand and rising as high as 1.8 to 2.0 for platelet-shaped carbonate shell sands. Measurements on near-surface deep sea clay in the laboratory (Lovell and Pezard, 1990) showed that each sample followed a trend similar to that described by Winsauer et al. (1952) with $a \neq 1$. The deviation of the parameter *a* from unity was interpreted to be due to the surface conduction effects of the clay particles. Doveton (1986) concluded from a study of the porosity, electrical and fluid flow properties of sands of varying shape and size distribution that the exponent m is a function of pore shape, and *a* is a function of both pore size and pore shape. The two constants are inevitably inter-related; a decrease in *m* results in an increase in *a* or vice versa for any specific rock sample (Lovell and Pezard, 1990). The structural parameter (*a*) is a tortuosity factor and has been attributed to the interstitial structure of rock; it is usually close to 1 and normally lies between 0.5 and 1.5 (Unalmiser and Funk 1998).

Numerous studies of Archie's equations for reservoir rocks and synthetic sedimentary rocks have been conducted, e.g. Carothers 1986, Carothers and Porter, 1970, Gomes-Rivero, 1976, Lang, 1976, Worthington 1992. Whilst these have resulted in many specific formulae along the lines of both Archie (1942) and Winsauer *et al.*, (1952), as well as modifications thereof, there has been little progress in understanding the basic relationships. Helander and Camble (1966) produced a list of eight factors influencing the value of *m*, covering everything from the nature of the pore space to that of the matrix. Jackson *et al.*, (1978) suggested that data from a wide range of sources points increasingly to Archie's law relating not to particle shape but to pore morphology, a point originally hinted at by Archie (1942) and Winsauer et al. (1952). Lovell and Pezard (1990) concluded after their studies on the electrical properties of basalts that the constant a is dependent on the shape of the connected pores and the pore size. As a consequence *m* seems to increase with the complexity of the geometry, whilst *a* decreases, and they also concluded that *a* decreases with increasing numbers of fractures. Maute e*t al.*, (1992) improved the data-analysis method for determining Archie parameters from core data and they concluded that the constant a is a weak-fitting parameter with little physical significance, that can generally be set to unity. Typical values of *m* for various minerals and porous media as given by Hilchie (1964) are shown in Table 2.2. (It should be pointed that the value of *m* for a given mineral is strongly dependent on pore geometry).

Table 2.2 Cementation Factor values for different minerals(after Hilchie, 1984)

Minerals and solids	m	Minerals and solids	m
Na, montmorillonite	3.28	Carbonates	2.0
Ca, montmorillonite	2.7	Shell Fragments	1.9
Muscovite	2.46	Kaolinite	1.87
Attapulgite	2.46	Cemented sand	1.8
Mediterranean clays	2.4	Natural sand	1.6
Sandstones	2.15	Platy sand	1.52
Illite	2.11	Rounded quartz sand	1.4

Ransom (1984) concluded that the cementation factor is function of the shape and distribution of pores. Table 2.3 permits the selection of the approximate values of *m* from a lithologic description of the core of interest (Pirson, 1958).

Table 2.3 Rock description versus m values

Rock description	*m* values
Unconsolidated	1.3
Very slightly cemented	1.4 - 1.5
Slightly cemented	1.6 - 1.7
Moderately cemented	1.8 - 1.9
Highly cemented	2.0 - 2.2

Many researchers have tried to find a physical significance for both *a* and *m* in the above relations by interrelating ϕ and F to other factors such as permeability, grain shape, pore throat radius, and tortuosity. A background review of these relations can be found in Jing (1990).

2.32 Factors affecting the cementation factor

There are many factors that affect the values of Archie's parameters. These are summarised below (Winsauer, *et al.*, 1952, Serra, 1984, Elashahab, 1995):

1) Degree of cementation.

2) Shape, sorting and packing of particle system.

3) Types of pore system.

4) Presence of conductive solids.

5) Compaction due to overburden pressure.

6) Thermal expansion.

7) Measurement techniques.

Although the number of factors involved indicates the complexity of the problem, special attention in this research was given to the concept of porosity type and its effect on *m*, especially for carbonate rocks where the pore system is more complicated and needs further detailed study. Moreover, extensive attention was paid to the effect of the measurement techniques and experimental conditions on the value of saturation exponent, *n*.

2.33 Effect of porosity type:

Because of the unique pore structure of carbonate rocks and the various porosity types found in them, this study will concentrate on carbonate rocks. In general, carbonate reservoirs have complex pore structures, with different porosity types providing various electrical current paths. These different porosity types include intergranular, vuggy, fracture, etc. Also the pore sizes in carbonates vary from very large (megaporosity) to very small (microporosity). The different pore types and sizes result from diagenetic and depositional processes (Asquith, 1985).

Theoretically, the cementation factor may be equal to or close to unity if only fracture porosity exists, because fractures provide straight paths for current to flow. As the electrical path becomes more tortuous, the resistivity increases and *m* increases. In reservoirs containing primary porosity, water saturations calculated using Archie's formula have proved to be reliable in many cases. However, in the presence of different types of porosity or presence of secondary porosity, the evaluation of carbonates should be carried out with extra care. Previously, some workers adjusted the standard Archie's equation by modification of the parameter *m*, some suggested a single texture parameter (W), others used methods based on calculating log-derived parameters such as the productivity index ratio (PIR), (Asquith and Gibson, 1982, Nugent *et al.,* 1978, Guillotte *et al.*, 1979).

A selection of specific carbonate core samples was carefully made to enable the relation between theoretical aspects and experimental results to be studied, and to develop a systematic approach for carbonate evaluation. There are already a few valuable studies related to Archie's parameters for carbonates, such as the work of Sweeney and Jennings (1960) who suggested a scheme of carbonate classification based on pore size distribution, petrographic examination and wettability. Amin *et al*., (1987) concluded that in carbonate rocks with non-connecting vug porosity the standard Archie's equation often gives low water saturation values. This is because in such rocks *m* is usually higher than 2 as a result of the complex pore geometry.

2.34 The Second Archie's equation:

The second Archie's equation describes the effect of partial saturation. Archie's resistivity index is defined by

$$I_R = R_t \;/\; R_o \;, \qquad 2.9$$

where R_t is the resistivity of rock partially saturated with brine.

Archie used resistivity data for partially saturated rocks reported by other investigators (Martin *et al.*, 1938, Jackosky and Hopper, 1937, Wyckoff and Botest, 1936, Leverett, 1939). Plotting I_R versus S_w on double-logarithmic graph paper yields the relation (sometimes known as Archie's second equation)

$$I_R = S_w^{\ -n} \qquad 2.10$$

Where S_w is the brine saturation, and *n* is a constant known as the saturation exponent with a value of 2 for water-wet sandstone rocks. I_R versus S_w for a Berea sandstone sample is shown in Figure 2.2. The general form of Archie's equation can be written as

$$S_w \;=\; [\; 1/\phi^m \; R_w \,/\, R_t \;]^{1/n} \qquad 2.11$$

It should be stressed that all these equations are empirical in nature. Archie's equation applies for clean (clay-free) rock, while in shaly rocks additional electrical conductivity arises due to the presence of clay. The equation assumes that *n* is a constant for a given porous medium and that a uniform brine saturation exists along the core length.

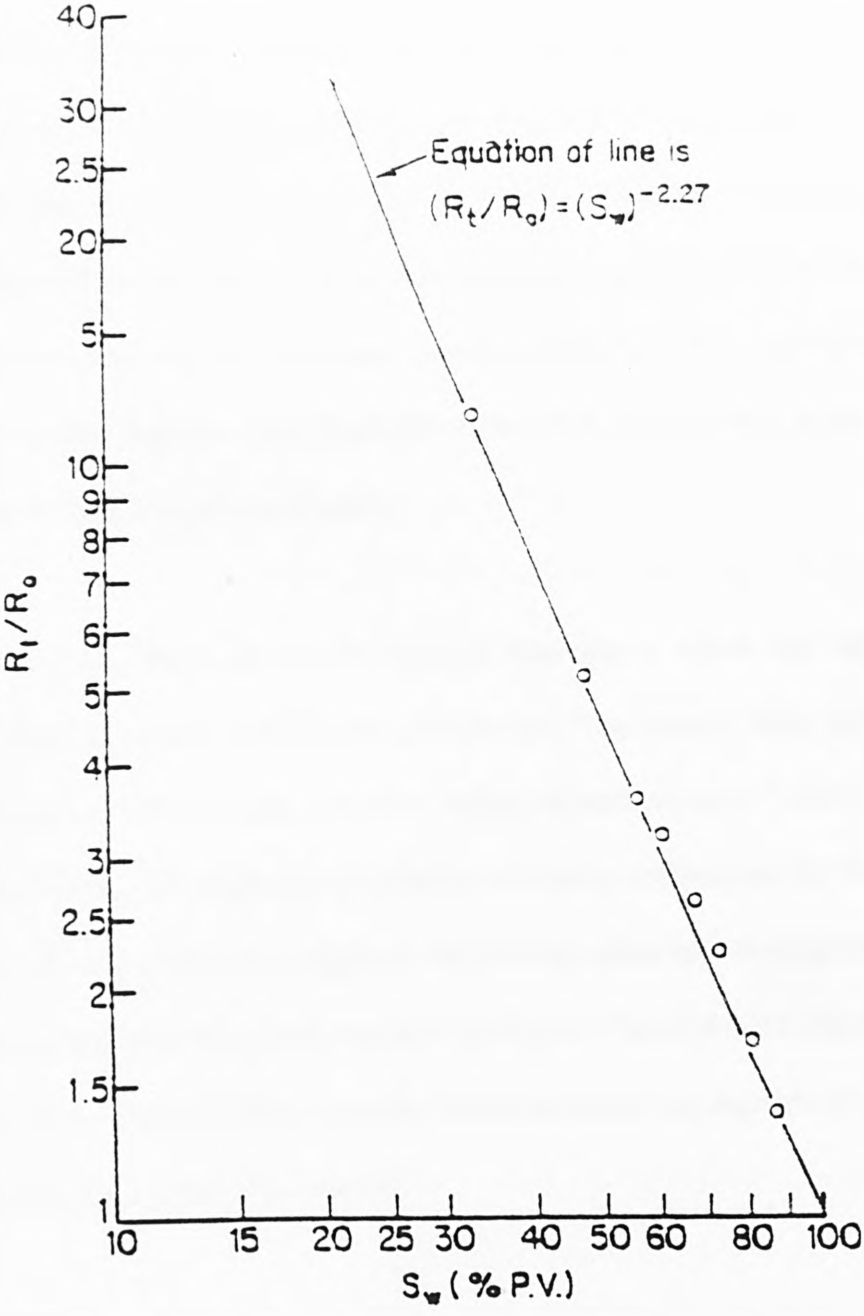

Fig. (2.2) I_R versus S_w for a Berea sandstone sample (after Archer and Wall, 1992).

Researchers following Archie, however, have shown that the increase in resistivity caused by hydrocarbons displacing brine depends on how the fluids are distributed in the pore space. The pore fluid distribution in turn is related to factors such as wettability, pore size distribution, and saturation history. The experimental techniques and conditions may also have an influence on the resistivity - saturation relationships and hence on n. Originally n was considered as constant and equal to 2 but values of *n* as low as 0.74 and as high as 10 have been reported (Elashahab *et al.*, 1995). Numerous researchers have investigated the influence of wettability on the saturation exponent (Amott, 1959, Anderson, 1986, Donaldson and Siddiqui 1987, Elashahab *et al.* 1995); however this point is not within the scope of the present research.

As early as 1948, researchers reported that the n value can vary significantly from 2. Guyod, 1948 reported Soviet data from several Baku fields and showed that n could vary with saturation, taking values between 1.7 and 4.3. Dunlap *et al.*, (1949) investigated the resistivity-saturation relationship for both consolidated and unconsolidated sandstones. They found values of n ranging from 1 to 2.5, which confirmed the results reported by Guyod. They indicated that the resistance of the core is not a unique function of the saturation but depends on the manner in which this saturation is achieved.

Experimental measurements of saturation exponent are based on core samples initially saturated with a wetting-phase which is displaced by a nonwetting phase; the resistivity and saturation readings are taken at suitable intervals. The most widely used techniques in the oil industry are the porous plate method and the continuous injection technique. (Rust 1952, Mahmood *et al.*, 1988, Worthington and Pallatt, 1992).

2.4 Effects of Pressure and Temperature

2.41 Effect of Pressure on the Physical Properties of Rocks

It has been common practice to measure the electrical and hydraulic properties of rock samples in the laboratory without taking into consideration the effects of pressure and temperature, in spite of the fact that the properties at reservoir conditions can differ significantly from those measured at laboratory conditions. Although a number of previous studies have been carried out to investigate the effect of pressure and temperature on these properties of rocks, more work is still needed to gain a better understanding of the mechanisms involved.

Reservoir rock, usually found at great depths, experiences considerable stress in its natural environment from three main sources. The burial depth induces stress by vertical loading from the weight of solid material above (typically estimated at ~1 psi/foot). The other type of stress is induced laterally as a result of geological deformation and lateral confinement. The fluids inside the pore space of rock also exert a hydrostatic force due their weight (typically estimated at approximately 0.45 psi/foot). The pore pressure inside the reservoir rock acts against the overburden pressure (due to the vertical weight of solid material) on the frame of the rock and so a net overburden pressure can be derived as the difference between these forces. In this thesis the term of overburden pressure will be used, which is defined as the total pressure applied on the rock sample (external confining pressure).

Reservoir rocks commonly show a time dependent elastic behaviour (Jaeger and Cook, 1977, Fjaer *et al.*, 1992). When reservoir core samples are brought to the surface at atmospheric pressure, the stress is released and the rock will begin to relax. This may cause changes in the pore structure and hence affect other rock characteristics such as porosity, permeability, capillary pressure and electrical properties. Complete recovery from the stress effect may not be reached and this is usually assigned to the stress hysteresis. Porosity generally decreases slightly with increasing stress. Electrical and hydraulic properties of rock samples measured at laboratory conditions can be significantly different from those measured at simulated reservoir conditions. This is attributed to compaction and thermal expansion effects, which may cause pore throats to close up and channels to narrow, and may also increase tortuousity which in turn will reduce permeability and increase resistivity.

2.42 Effect of Pressure on F and *m*

Many investigators have studied the effect of pressure on the formation resistivity factor and cementation factor for various rocks. Most of these studies were performed using sandstone rocks, although there are also a few experiments on carbonate rocks. Investigations by Fatt (1957) revealed that the formation factor increases with an increase in applied hydrostatic pressure and that the F-ϕ

relationship is pressure dependent. An increase in formation factor of up to 35% due to the effect of pressure (5000 psi) was reported by Fatt, which indicates that a formation factor measured *in situ* at great depth would differ significantly from one measured in laboratory, if the measurements are not conducted under the same pressure. Fatt (1957) also concluded that the pressure effect is more pronounced for clean sands than for shaley sands, and that laboratory measurements of formation resistivity factor, in which only external pressure is varied, are sufficient to study the effect of overburden pressure. Similar results were also reported by Wyble (1958) in a study of the effect of pressure on formation factor, permeability and porosity. An increase of Archie's cementation factor and formation factor with pressure was observed; this was attributed by Wyble to the closure of small crack-like pore spaces present in sandstone and crystalline rocks. Glanville (1959) observed an increase in formation factor with pressure; the effect being greater in less porous, less permeable rocks. On the contrary, Redmond (1962) reported a decrease in formation factor and cementation factor with pressure especially for high porosity sandstone rocks. Helander and Camble (1966) observed an increase in formation factor and cementation factor with pressure and attributed the change mostly to an increase in pore constriction. The reports of Brace et al. (1965), Brace and Orange (1968) and Timur et al. (1972) also confirmed a significant increase in formation factor with pressure. A review of the studies of electrical properties at high pressures was given by Parkhomenko (1982) showing that electrical resistivity at high pressures is related to other rock properties such as porosity, permeability, rock structure and pore geometry. In the few experiments performed on carbonate rocks, Longeron et al. (1986) noticed less variation in the formation factor and cementation factor with pressure compared with sandstone rocks. Mahmood *et al.* (1988) reported an increase in formation factor and cementation factor with pressure. They confirmed the conclusions of Fatt (1957) and King (1965) that the pressure influences the transport and elastic properties of rocks. Recently, Hausenblas (1995) showed that the cementation factor of carbonate rocks may decrease (rather than increasing) with increasing pressure, but no explanation was suggested.

2.43 Effect of temperature on F and *m*

Most of the previous work concluded that F and *m* change with temperature only slightly and some investigators reported that the temperature effect on F and *m* is negligible (Helander and Camble 1966, Sanyal *at al.,* 1972, Parkhomenko, 1982, Mahmood *et al.,* 1988, Sonden *et al.,* 1992). However the effect of temperature on Archie's parameters is not studied in the present work.

2.5 Effects of Experimental Techniques and Conditions on *n*

According to Archie's equation the resistivity will be independent of the method used to achieve the saturation variation, therefore several different experimental techniques can be used to obtain the saturation exponent, for instance capillary equilibrium, continuous injection, evaporation, etc. However there have been a considerable number of studies on the effect of different variables on the resistivity-saturation relationship (Argaud *et al.,* 1989, Arps, 1953, Baldwin and Yamanashi, 1989, Gray *et al.,* 1992, Jing *et al.,* 1993, Lewis *et al.*, 1986, Swanson, 1980, Worthington *et al.*, 1989, Wie and Lile 1992), which have demonstrated that the real situation is more complicated than Archie's equation assumes due to various factors are involved.

The resistivity will also vary with fluid distribution within the pore space and will be related in some way to aspects such as pore structure, fluid characteristics and fluid displacement mechanism which are not considered in Archie's equations. These aspects with their effects on the resistivity-saturation relationships were studied in this research in more detail in order to highlight this point which has not been given attention in previous work. The continuous injection technique is the most advanced technique currently used in the oil industry, having important advantages (de Wall *et al.*, 1991). In this technique, one phase (brine) is continuously displaced by another phase (oil) at a constant injection rate (Sprunt *et al.*, 1991, *Gray et al.*, 1992, Jing *et al.*, 1993a & b). As mentioned before it is assumed that Archie's equation is independent of fluid characteristics and of the fluid displacement mechanism. The effects of fluid characteristics such as viscosity, and the conditions of the fluid desaturation process (such as injection rate) on *n* have received much less attention in the past, probably on account of the time and cost involved in such experiments (Al-Mahtot *et al.*, 1998). The details of the backgrounds and the literature review of this issue are covered in chapter 5.

2.6 Porous Medium Modelling

Pore geometry is one of the important factors controlling the value of rock resistivity, and is very complex in terms of size, shape and connectivity. Macroscopic properties such as porosity, permeability and saturation are based on an average of the effects of many pores (Grattoni 1994). Because it is difficult to undertake direct observation of fluid distribution and pore shape/size distributions within the rock samples, therefore, various physical models have been suggested to represent the influence of pore structure on electrical resistivity, and mathematical network models have also been formulated in order to quantify the influence of pore structure on resistivity. (Slawinski, 1962, Maxwell, 1954, Dullien *et al.*, 1976, 1992, Yale, 1984, Jing, 1990, Dawe *et al.*, 1994, Grattoni and Dawe 1996). Generally, these models although have given some insight into the complex physical processes involved, and suggested further lines of enquiry. However, progress in this field has so far been quite limited on account of the extremely complex nature of the flow paths.

CHAPTER III

EXPERIMENTAL WORK

3.1 Introduction

It has been pointed out in Chapter 2 that extensive experimental data for rock samples covering a wide range of physical properties is essential for reliable prediction of the petrophysical properties of a reservoir formation at *in situ* conditions. The use of a few samples mostly representing one particular rock type or one specific pore structure cannot give reliable conclusions, therefore it is essential to examine the properties of many samples representing the different rock types present.

There is a serious lack of such comprehensive experimental data in the literature, as it is an expensive and time-consuming operation to examine the electrical properties of a large number of rock samples when only one sample can be dealt with at a time. To overcome this problem, an existing high pressure sample tester was modified and developed in order to speed up the process of obtaining the large amount of data required as the basis for general conclusions about a particular formation. This modified rock testing system has been built by Robertson Research at its premises in Aberdeen for the purpose of the present research. It permits up to five samples to be tested simultaneously under the same simulated overburden conditions of pressure. The design was based on a number of earlier experimental systems (Longeron *et al.* 1989 a & b, Jing and Archer, 1991, de Wall *et al.*, 1992, Jing, 1993 a & b).

3.2 Rock Testing System

This chapter presents the experimental apparatus and procedure and describes the rock testing system for electrical property measurements at overburden conditions of pressure. Figure 3.1 shows the schematic of the rock testing system, which can be divided into three main units as follows: (1) core holder and pressure vessel, (2) electrical circuits, and (3) the data acquisition system. All these units are described in detail below.

3.21 Coreholder and Pressure Vessel

The multiple core holder is made of high quality stainless steel along with the pressure vessel which is tested to withstand an applied pressure of more than 10,000 psi. Up to five core samples can be placed inside the pressure vessel simultaneously and subjected to selected overburden pressures for the electrical measurements. The selection of sleeve material is critical when the experiments are performed at overburden pressure as some materials gradually absorb the brine and become conductive. Therefore the rock samples were sleeved by specially designed four-electrode Viton sleeves. The current flows through five separate inlet and outlet stainless steel ports. These inlet and outlet ports are all insulated from top to bottom end closures of the vessel body. The electrode Viton sleeves inside the vessel are connected electrically to the outside of vessel through high pressure electrical feedthroughs. The core holder is mounted firmly on a frame. The electrical measurements can be made by the four electrodes which provide good contact with the samples. The pressure system consists of an air - oil pressure intensifier connected to the core holder. Pressures up to 10,000 psi can be applied to the core samples and this pressure is maintained ± 100 psi. In

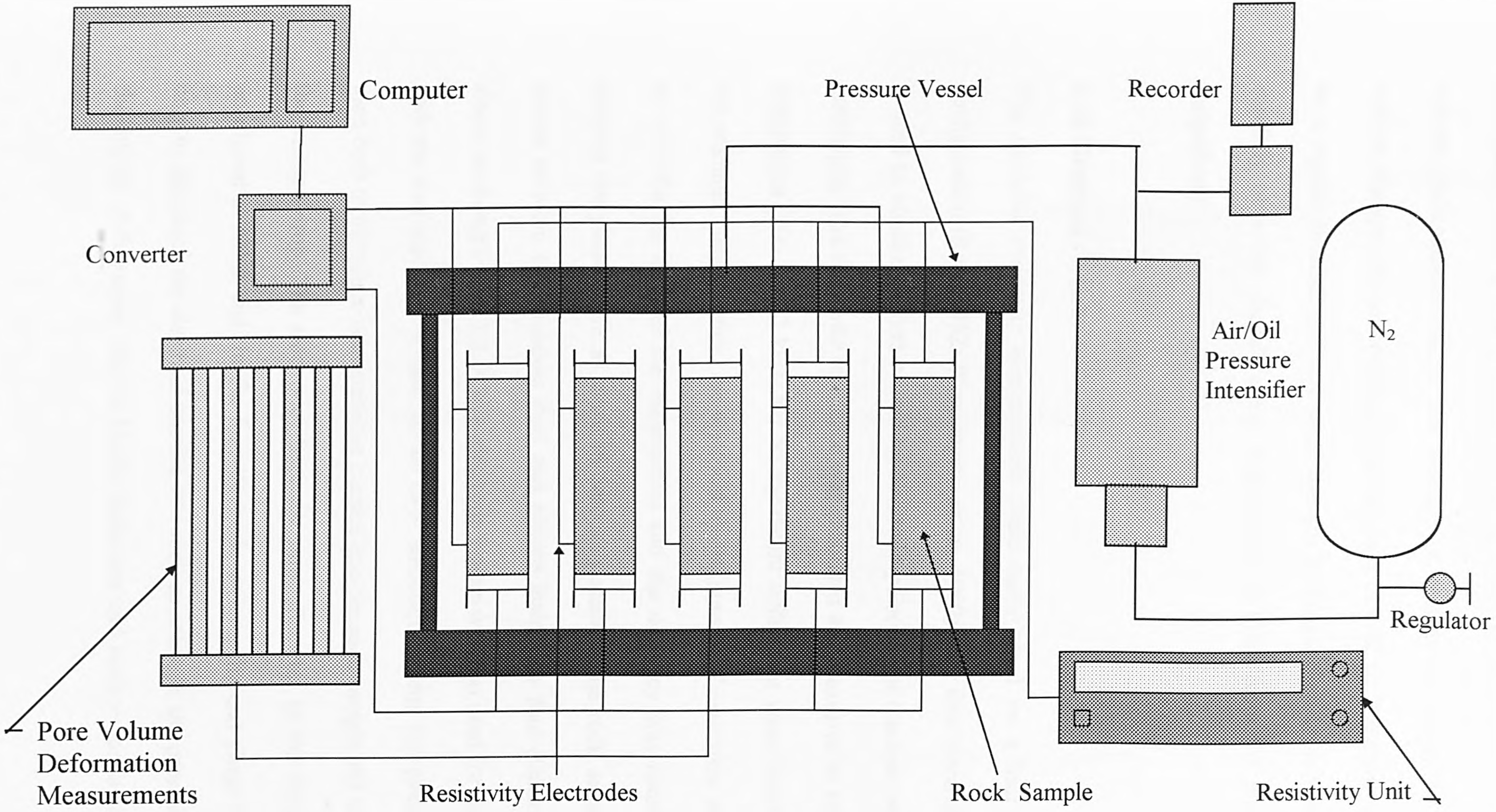

Fig. 3.1 Schematic diagram of the multiple rock testing system

the system there is also a hydraulic circuit which is used to record the pore volume deformations due to the changes of overburden pressure. The pore volume changes can be measured to an accuracy of 0.02 cc. Readings were taken on a regular schedule and any small changes in the expelled brine volume were carefully observed, therefore any evaporation of brine from the pipettes was insignificant.

3.22 Electrical Circuit:

The electrical resistivity measurements were made based on a four electrode configuration (Rust, 1952, Worthington *et al.,* 1990). The four electrode system is used to eliminate errors caused by electrode polarization reaction and contact resistances. The resistivity resistance was calibrated and measured at various low frequencies (200 Hz - 2 kHz) but no significant differences were found between the readings. Subsequently, the electrical measurements of resistivity were taken at 1-2 kHz for most of the experiments and the accuracy was maintained by keeping the phase angle as close to zero as possible. The rock samples were placed between two stainless steel end platens inside the four-electrode Viton sleeve as shown in Fig. 3.2. A two-electrode system was also used for comparison with the four-electrode system. In the two- electrode system, the electrodes are used both to introduce homogeneous current into the rock sample and to measure the voltage drop. The electrodes have the same diameter as the core and are positioned at either end. In the four-electrode system, the end plugs were used only to introduce the electrical current into rock samples. In the present research the effects of frequency, electro-kinetic behaviour and surface conductance were

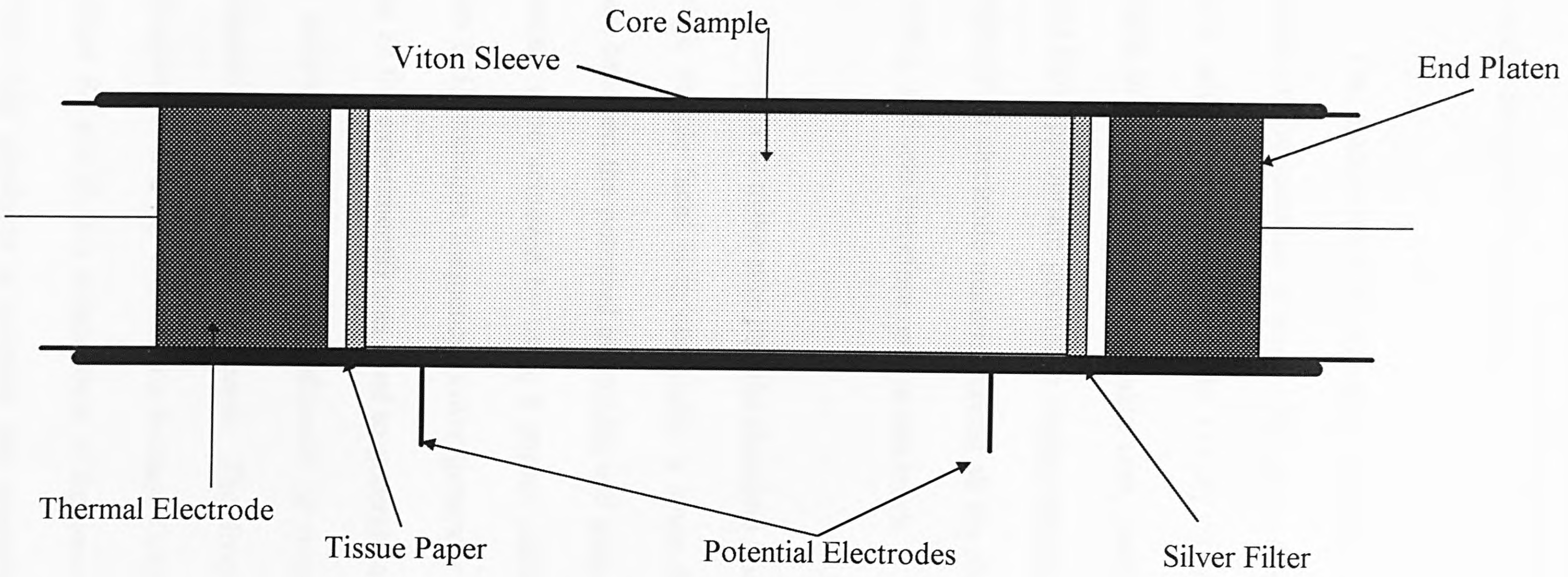

Fig. (3.2) Schematic of the core sleeve with 4-electrodes system not investigated. The potential difference was measured across the two potential electrodes along the Viton sleeve.

The electrochemical literature abounds with electrode descriptions and guidance on the selection of electrodes can be found in the work of Ives and Janz (1961), and Sawyer and Roberts (1974). The electrodes should be readily available in high purity at reasonable cost, easily renewable or replaced, easily formed into appropriate geometric configurations, and reusable. Silver is a good example of an electrode material having all the above properties (Worthington *et al.*, 1990), and was therefore used in this work.

In order to make sure that the electrical flow between the metal pieces and the rock sample faces is in continuity, a silver filter was used. Good capillary contact between the potential electrodes and pore fluids, and a high surface area of contact were achieved by using a porous stainless steel mesh. An alternating current (AC) multiple frequency power generator (maintained between 1-2 kHz during all the experiments) was used to generate a potential difference across the core samples (Fig. 3.3). The influence of frequency on resistivity was not investigated in the current reasearch. The frequency range selected for the experiments (1- 2 kHz) was chosen because Grattoni (1994) has shown that in this range R_w and R_o are independent of frequency, since the alternation of the electrical field produces a constant ion movement through the solution. As mentioned above, this was experimentally verified for the present apparatus. It is

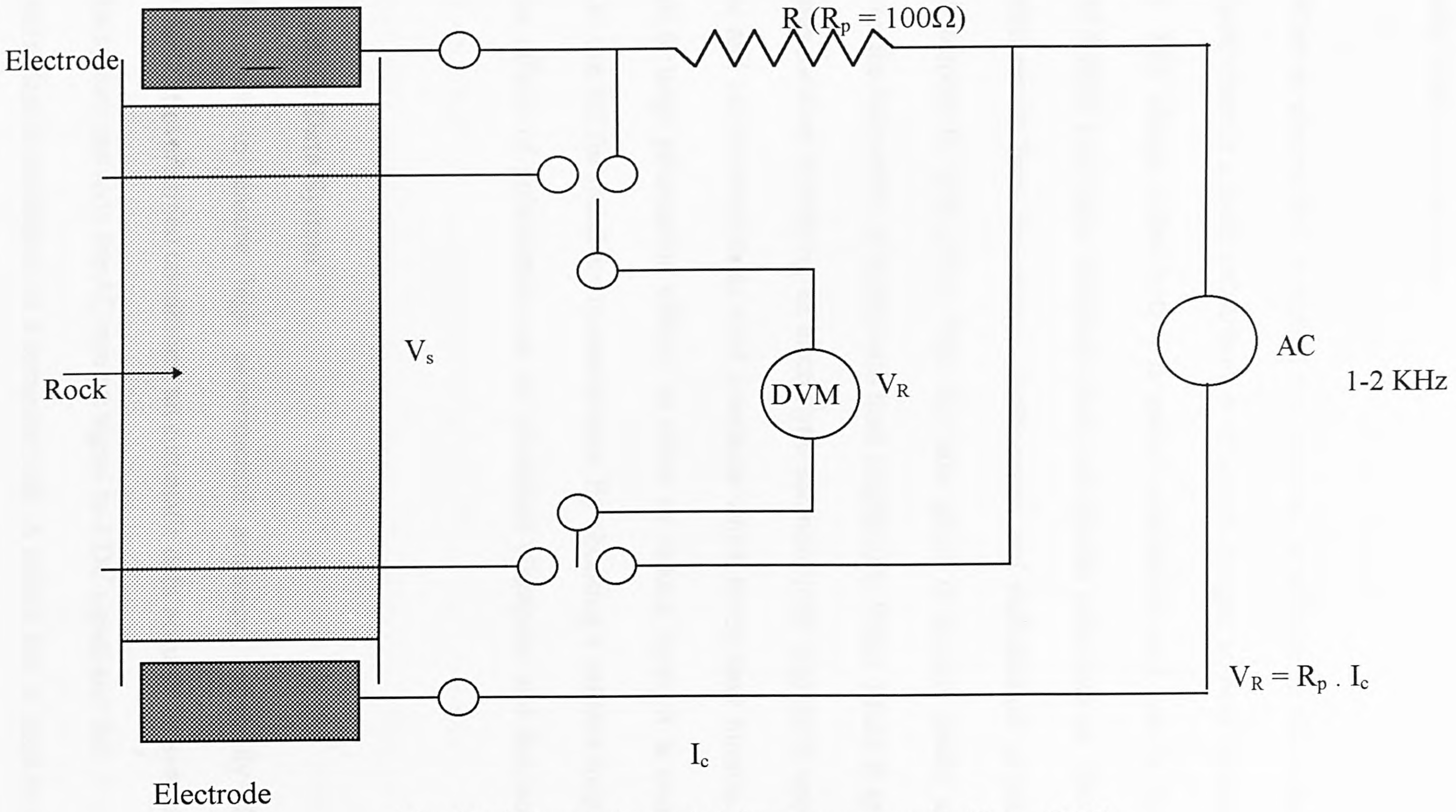

Fig. (3.3) Four-wire resistivity measurements (Rust, 1952) ssumed that the influence of surface conductivity and its contribution to total conductivity is less in clean rocks.

When an electric field is applied to a material, in addition to the current of free charges, there is a local redistribution of bound charges to new equilibrium positions. This charge redistribution is called polarisation and results from a number of distinct processes; electronic, ionic and dipolar polarisations. The ionic contribution results from the relative displacement and deformation of charged ions with respect to each other. This can take place in porous media and it depends on the interaction of atoms with their neighbours. When a field is applied to a porous medium containing an electrolytic solution, ions migrate in opposite directions and can accumulate at solid interfaces which block their motion. This can result in large polarisation effects. In order to reduce these, it is common practice to use AC for resistivity measurements. By choosing a suitable frequency range, the effects of polarization can be minimised (Gueguen and Palciauskas, 1994).

3.23 Automatic Data System

In order to ensure high experimental accuracy, especially during measurements at overburden conditions, an automatic data acquisition system was used. This system converts the AC current signal to a DC signal and the experimental data is transferred to a computer cell. A switch box is used to divert the measurements between the five rock samples. A pressure transducer is used to record the overburden pressures. All resistivity measurements were performed at ambient temperature (25°C). The variation of resistivity with temperature was taken into account.

3.3 Design of Experimental Program

3.31 Experimental Procedure

Over 100 rock samples covering a wide range of porosity and permeability values have been collected and selected for the purpose of this experimental investigation. Ten clean clay-free sandstone and twelve clean carbonate rock samples were chosen for measurements of their electrical properties at overburden pressure conditions using the modified rock testing system. Ten samples were used to study the effect of the experimental conditions (injection rate and viscosity ratio) on the resistivity-saturation relationships using the continuous injection developed recently (Chapter 5). Finally, 80 (with more than 20 core data) carbonate samples were selected in order to investigate the influence of porosity type on Archie's parameters using the porous plate method (Chapter 6). The experimental procedure for measuring formation factors and cementation factors at overburden pressure condition is divided into five main steps as follows

3.311 Rock Sample Selection

It is not uncommon that in core analysis tests, sample selection is carried out on semi-arbitrary basis which can lead to misleading formation evaluation. Sample selection in the present work was based on a wide range of petrophysical properties, different pore structures and porosity types and different oil-bearing provinces. Over 100 rock samples were collected from sandstone formations

(North Sea, UKCS) and carbonate formations (North-East Sirte Basin, Fasha formation, Libya) covering a wide range of porosity, permeability and grain density and having various pore structures and porosity types (interparticle, vuggy, etc.). These samples were collected from two different geological areas having different stratigraphic, structural and tectonic histories.

The core samples collected from the Sirte basin cutted parallel to the bed orientation with water-based mud and preserved quickly once they brought to the surface in order to prevent wettability alteration or grain loss, by wrapping in clingfilm, aluminium foil and strippable plastic. (The sample collection and wrapping was carried out by the Petroleum Research Centre, Tripoli, Libya).

3.312 Sample Preparation and Basic Measurements

In order to obtain reliable experimental results, the experimental system was calibrated before starting the experiments and this included checking the electrical insulation, testing the automatic data recording, etc. All samples were cut with precisely defined dimensions in length and diameter. All had the cylindrical shape commonly used in the oil industry with dimensions of 1.5 inch diameter and 3.15 inch length. A precision cut-off saw was used to trim the sample ends to ensure good contact with the current electrodes; no grinding was used.

3.313 Sample Cleaning and Drying

The core samples were cleaned to remove all traces of liquids, and to allow the original wettability to be restored. The method of core cleaning used in this study is described as "Flow-Through Core Cleaning" (Luffel and Randall 1960, Anderson 1986). This method involves cleaning sandstone samples by a series of solvent flows through the sample mounted in a Hassler cell. Initially, the flowing solvent is a mixture of 20% methanol and 80% chloroform, this is followed by 100% methanol. The mixture flows through the core sample until no further change in the colour of effluent is detectable, then the flow is interrupted for about half an hour to let the mixture soak. After this, the flow is resumed again. This cleaning process is repeated several times until no more residue can be displaced observed by eye (allowing sufficent time for the displacement to be completed). Methanol is then flowed through the sample to displace the solvent mixture and any brine that might still be present . Finally the sample is dried with air to displace the methanol and then placed in a humidity-controlled oven for two days at a temperature of 70°C (Elashahab, 1985).

For carbonate samples, 50% toluene and 50% methanol were used based on the work of Gant and Anderson (1988) and Grist *et al.*, (1975) to ensure that the rock stays in a water-wet condition. The samples were then placed in a high temperature furnace with the humidity was under automatic control. The firing process was carried out to ensure that the samples were rendered strongly water-wet. At the high temperatures used (600^0C), significant thermal cracking may take place, and this may change the internal rock structure, especially for quartz-bearing rocks (Glover *at al.*, 1994). To allow for this effect, the porosity and permeability of the samples were re-measured following the firing process. Wettability measurement data were not available and the rock samples were made preferentially water-wet (Amott, 1959, Donaldson *et al.*, 1969, Grist *et al.*, 1975 and Morrow 1990). For more details of core cleaning and drying, see Donaldson *et al.*, 1985, Wendl *et al.*, 1987, Anderson 1986.

The core sample dimensions were then measured precisely with callipers (multiple readings were taken for both length and diameter, and the mean values used in the final calculation) to determine the bulk volume, and the cores were weighed. (Archimedes method was not used in the current research). Before being placed in the pressure vessel for testing, the core plugs were fully saturated with brine solution. This was accomplished using a saturator as shown in Fig. 3.4. Core samples were placed in the pressure vessel under a vacuum for about 24 hours in order to remove air from the pores. The brine inlet valve was then opened, allowing de-aerated brine solution to enter the chamber, until the cores were completely submerged. Finally, an air-hydraulic pump was used to develop pressures up to 2000 psi inside the chamber to force the brine solution into the smallest pores. The samples were removed after 24 hours, at which point they were weighed. The porosities were then calculated from the difference between the dry weight and the wet weight. The difference between porosity obtained from this technique and that from the helium expansion method was generally less than 0.5% pore volume.

3.314 Porosity and Permeability Measurements

A helium gas expansion porosimeter was used for porosity measurements. This is based on Boyle's law, and helium is used due to its small molecular size which gives it the ability to penetrate all interconnected pores in a short time. For

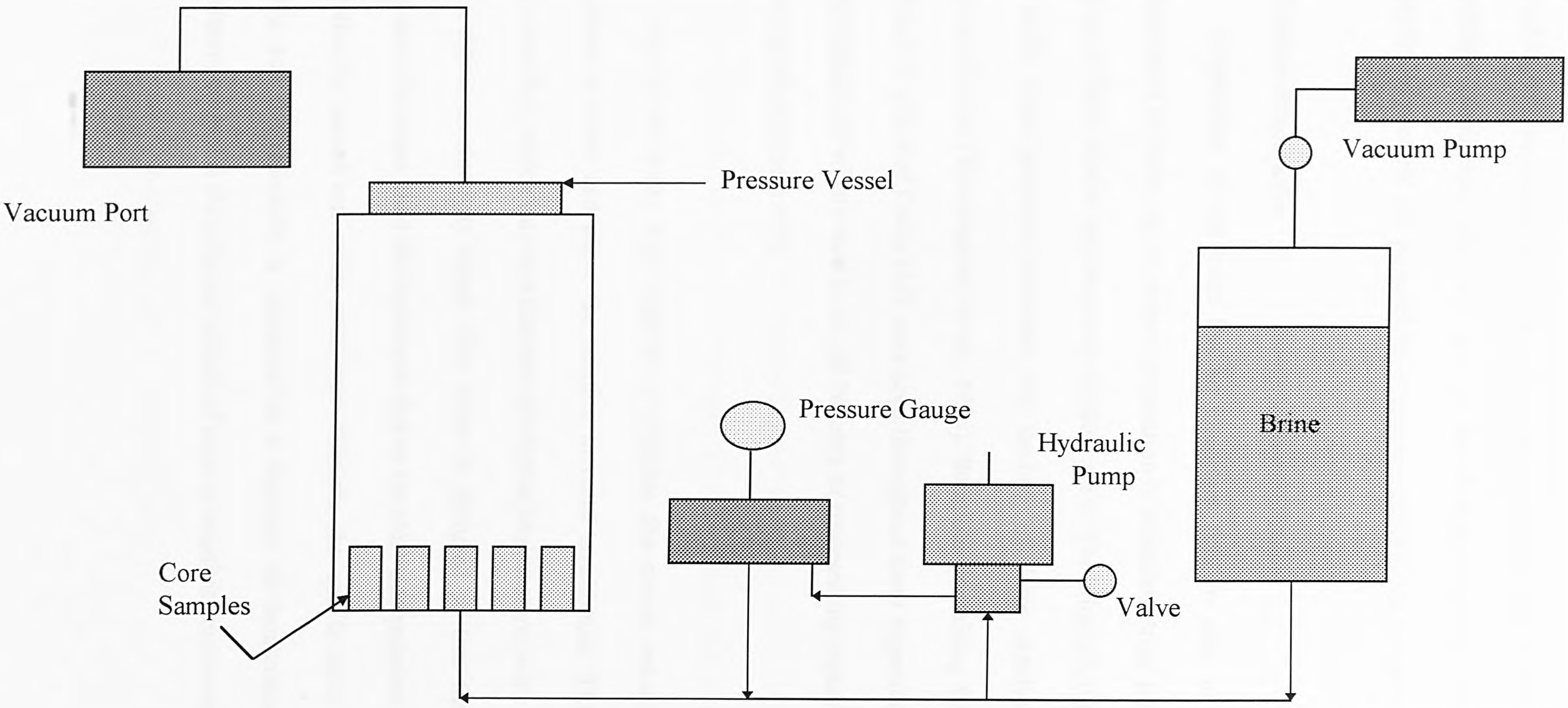

Fig. (3.4) Schematic Diagram of the SPT saturator permeability measurements a Hassler cell permeameter was used in the laboratory at ambient conditions, with dry gas as the flowing medium. The detailed description of porosity and permeability measurements is given in Appendix (A).

3.315 Brine Preparation

Preparation of the brine has an important role to play in resistivity measurements of rocks, so its proper preparation is essential. Brine solutions are made up of NaCl, $CaCl_2$ and deaerated distilled water. The brine solutions used in this study were prepared followed the Society of Core Analysts (SCA) recommendations (Worthington *et al.,* 1990). Solutions containing 80 g/litre of NaCl and 20 g/litre of $CaCl_2$ H_2O were used throughout these experiments; these concentrations are widely used in the oil industry as representing typical reservoir conditions (Robertson 1995).

Up to 48 hours was required to dissolve the coarse solute particles completely in water and allow the solution to reach equilibrium. The solution resistivities (R_w), which vary as a function of solution temperature, were measured with a digital conductivity meter. This meter is designed so that the solution resistance is far larger than the impedance due to the electrode polarization. After calibration is carried out using potassium chloride, the cell is filled with the solution and the resistivity is measured as a function of temperature. (Poor temperature control is the principal source of error in resistivity measurements).

The accuracy of these measurements was tested by comparing the results with other experimental methods (e.g. Hilchie (1982), and with empirical equations (Arps, 1953) and no significant differences were found.. For carbonate rocks, the electrical resistivity R_w was measured after the reconstituted brines had been kept for one week at 40°C in the presence of crushed rock (Longeron *et al.* 1986).

3.4 Resistivity Measurements

3.41 Resistivity Measurements at Overburden Pressures

The resistivity measurements at overburden pressure began with the placement of the brine-saturated samples inside the Viton sleeves. The plug sample was inserted into the sleeve under the brine solution to prevent air bubbles being trapped inside the core. Two plattens which also serve as current electrodes were inserted into the sleeve so that both ends of the core were tightly against the platens. The core holder was wrapped carefully and assembled onto the bottom end closure with the flow tube passing smoothly through the electrical feedthrough in the bottom end closure. The same procedure was repeated for each sample. Before the bottom end closure with all five core holders assembled on it was loaded into the pressure vessel, the electrical connections of all the potential electrodes were made and the electrical insulation of the current leads was checked. After the bottom end closure was installed and fixed with a screwed ring, the vessel was filled with oil. The top end closure was then loaded with all the flow process tubes going through the feedthroughs.

The electrical insulation of all current and potential electrodes was finally checked, and both screwed rings were tightened. The oil from the pressure intensifier was pumped through the overburden pressure lines to prevent any air bubbles being trapped inside. An initial overburden pressure of about 200 psi was applied to ensure that all the sleeves sealed onto the core plugs and platens. Then the automatic data logging system was connected.

For each stable pressure, readings were taken when the brine level in the calibrated glass burette stopped rising and the voltage stabilised (3 - 12 hours). The pressure increments were 500 psi and 1000 psi for sandstone and carbonate samples respectively.

3.42 Resistivity Measurements by the Porous Plate Method

In this method, the resistivity measurements and the desaturation processes are performed separately. All the samples are first saturated with brine, R_o and R_w are measured, then the samples are placed in the porous plate apparatus and desaturated simultaneously by applying a gradually increasing gas pressure. The gas enters the sample from all directions except the bottom face, which is in capillary contact with the porous plate. Despite the relatively long duration of the test, this method was chosen because it results in a semi-uniform distribution of water saturation, beginning from the achievement of the first capillary equilibrium (Longeron *et al.*, 1986).

The major advantage of this method is that it eliminates the capillary end effect by containing the end effect zone within the porous plate, which has pore sizes much too small to allow the nonwetting phase to enter. The saturation gradient in the rock is generally negligible when the system reaches equilibrium at any given capillary pressure. A capillary bridge is needed between the sample and the porous plate in order to ensure the continuity of the brine phase and a cellulose filter was used for this purpose in the current research. Oil can be used as an alternative to gas as the nonwetting phase; the use of gas simplifies and increases the accuracy of saturation measurements by the gravimetric technique. One of the disadvantages of this method is the possible loss of sample grains during core removal from the porous plate which may introduce significant errors in saturation determination. This method can be used both with and without confining pressure (Maerefat *et al.*, 1990).

3.43 Resistivity Measurements by the Continuous Injection Technique

This is a rapid and accurate technique, and it is considered today as the most rigorous method in oil industry use. Fully brine saturated core samples are mounted in a core holder and subjected to constant stress. Oil is injected at one end of the sample and brine is expelled at other end through a semi-permeable membrane. This technique was used in the present study to investigate the effects of experimental conditions (injection rate and viscosity ratio) on the resistivity-saturation relationships. Details are presented in Chapter 5.

3.5 Capillary Pressure Measurements

The pore size distribution in a given rock type, which has been shown to influence initial saturation distribution, permeability and electrical resistivity, can be determined using capillary pressure measurements. There are four basic methods available for the experimental determination of the capillary pressure characteristics of rock samples. In the present work, the mercury injection method was used (Appendix A).

The basis of this method is to inject mercury into the test samples at incremental pressures and derive the mercury injection versus capillary pressure relations. These tests are used for a quantitative description of pore size distribution (PSD). Mercury injection tests were carried out for selected samples to investigate the effect of the pore size distribution on the form of the resistivity index versus water saturation plots (see Chapter 5).

3.6 Scanning Electronic Microscopic (SEM) Experiments

Scanning electronic microscopy is used to study reservoir rocks by obtaining qualitative information about their grain pore geometry. It provides several unique advantages for geologists and engineers when compared with optical microscopes (Pittman and Thomson 1979). In the current research SEM was used to study carbonate rock samples in order to differenate between the different porosity types and to study their correlation with *m* (See chapter 6).

3.7 Results of Rock Characteristics

Table 3.1 lists the results of measurements of core grain density (ρ_g), porosity (ϕ), air permeability (k) and grain density (G. D.) for the 10 sandstone samples studied. Table 3.2 lists the corresponding data for carbonate samples.

Table 3.1 Sandstone Sample Properties

Sample	ϕ %	GD, g/cm^3	k_a, mD*	Sample	ϕ %	k_a,mD*	GD,g/cm^3
A1	30.47	2.68	143.8	A6	15.43	45.2	2.65
A2	28.83	2.66	133.9	A7	13.88	22.7	2.68
A3	19.34	2.67	77.6	A8	9.92	9.98	2.66
A4	17.73	2.71	82.6	A9	6.18	15.5	2.68
A5	16.27	2.68	78.2	A10	3.45	11.9	2.64

Table 3.2 Carbonate Sample Properties

Sample	ϕ, %	k_a ,mD*	GD, g/cm^3	Sample	ϕ, %	k_a, mD	GD, g/cm^3
B1	9.73	0.5	2.84	B7	20.39	6.2	2.84
B2	10.63	0.01	2.83	B8	23.36	0.1	2.8
B3	10.84	0.2	2.84	B9	13.0	1.72	2.84
B4	11.3	3.1	2.84	B10	30.19	2.01	2.85
B5	11.84	2.8	2.86	B11	32.44	26.14	2.84
B6	13.85	0.4	2.86	B12	36.48	53.4	2.85

* confining pressure = 400 psi

* Mean pressure = 1 - 1.2 atm

Gas Type: Nitrogen

3.8 Porosity-Permeability Relationship:

The relationship of permeability and porosity for sandstones and carbonate samples are shown in Figures 3.5 and 3.6 respectively. The correlation between ϕ and k is much stronger for the sandstone samples than for the carbonate samples.

Fig. (3.5) Permeability vs. Porosity for sandstone samples

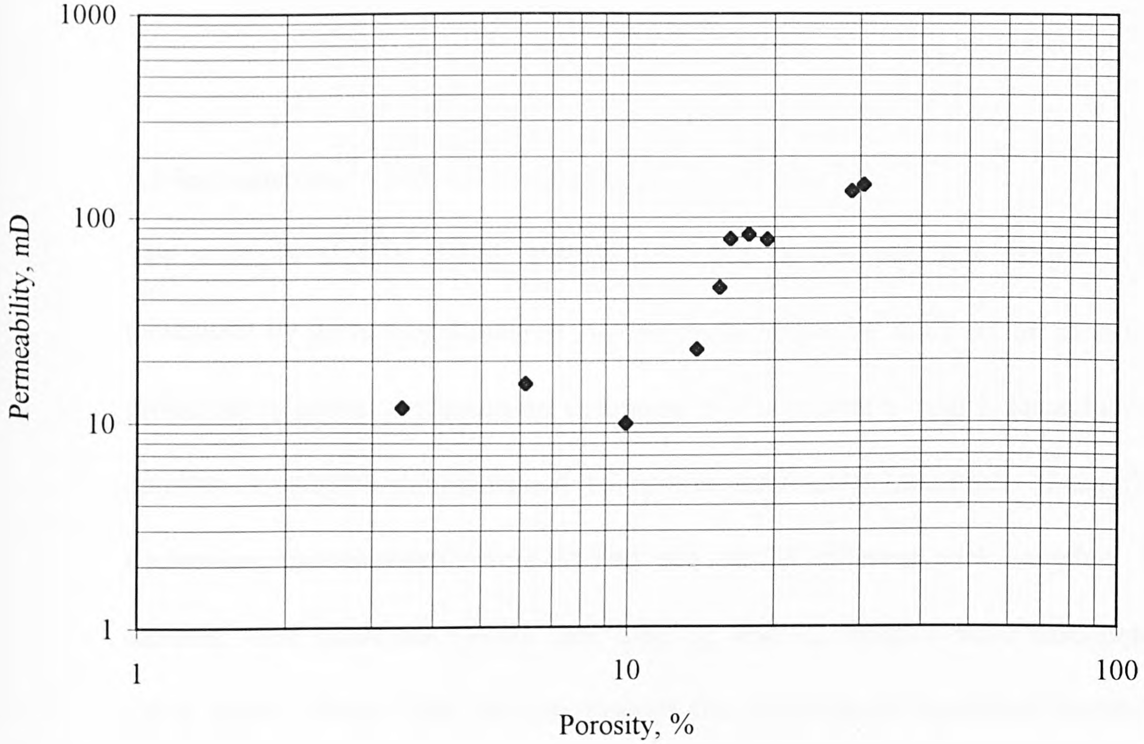

Fig. (3.6) Permeability vs. Porosity for carbonate samples

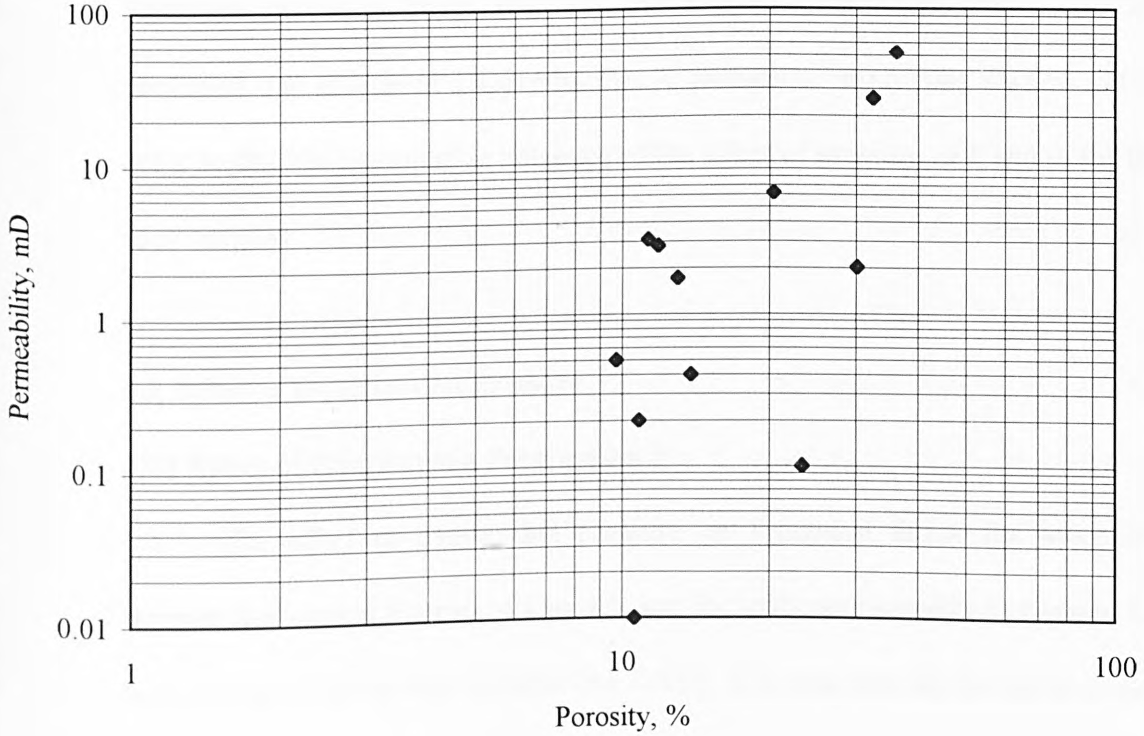

CHAPTER 4

EFFECT OF OVERBURDEN PRESSURE ON ARCHIE CEMENTATION FACTOR

4.1 Introduction

The multiple sample testing system described in the previous chapter was developed by Robertson Research in order to facilitate the study of the electrical properties of rocks. An important advantage of this system is that it can subject a number of samples simultaneously to various overburden pressures. Using this equipment, measurements were carried out on 22 different rock samples; 10 samples were sandstone (North Sea, UKCS), and 12 samples were carbonates (Sirte Basin, Libya). This chapter presents the experimental results of electrical resistivity measurements on these sandstone and carbonate samples at simulated reservoir conditions of overburden pressure. The effect of overburden pressure on formation resistivity factor (F), and the Archie's cementation factor (m) are presented and discussed (Appendix B). A parametric study was carried out in order to find the quantitative influence of the effect of pressure of F and *m* for the rock samples.

4.2 Effect of Overburden Pressure

4.21 Effect of Overburden Pressure on F

The effect of overburden pressure on formation factor for sandstone samples is shown in Figures 4.1 to 4.5, and for carbonate samples in Figures 4.9 to 4.13. For the sandstone samples (A1 - A10), it is seen that the formation factor increases with overburden pressure over the range of 0 - 4500 psig. This increase in F was more pronounced for the less porous samples (A9 and A10). However the rate of increase of F is generally greater at lower pressures (0 - 2000 psi) than at higher pressures for most of the samples. The effect of overburden pressure on F is greater for samples A8, A9 and A10 (Figures 4.3, 4.4 and 4.5) than for samples A1, A2, and A3 (Figures 4.1, and 4.2), which are more porous and permeable. For the carbonate samples, there is a hysteresis effect, since F values measured as pressure is increasing are always smaller than those measured when pressure is decreasing (samples B6, B9 and B12 in Figures 4.6, 4.7 and 4.8. No hysteresis effects were seen with the sandstone samples .

The effects of overburden pressure on formation factor for carbonate samples are shown in Figures 4.9 to 4.13. It was observed that F increases as overburden pressure increases over the range 0 - 10,000 psig, and this increase is noticeable for samples B2, B4 and B8 which have porosity values of 10.63%, 11.3% and 23.36% respectively. It is also noticeable that F increases only slightly with increasing pressure for medium to low porosity samples. Sample B11 (Fig. 4.11) shows different behaviour where F decreased markedly with pressure (>1000 psig), and a similar result (though less marked) was obtained for sample B3 (Fig. 4.10). This effect, which agrees with the observations of Hausenbles (1995), may be the result of grain crushing or re-arrangement of grain packing taking place at high pressure (Glover *et al.* 1994). However, F for the majority of these samples increased more steeply at lower pressures than at higher pressures. As pressure increases, the formation factor values eventually become almost

Fig.(4.1) Formation Factor vs. Pressure for Sandstones

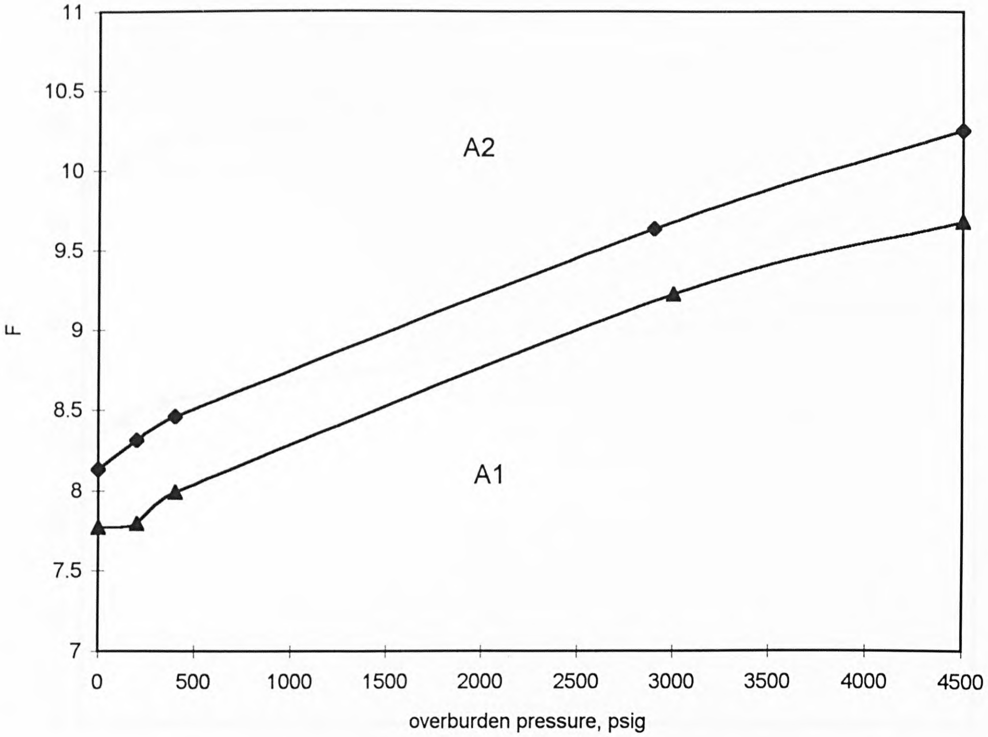

Fig.(4.2) Pressure vs. Formation Factor for Sandstones

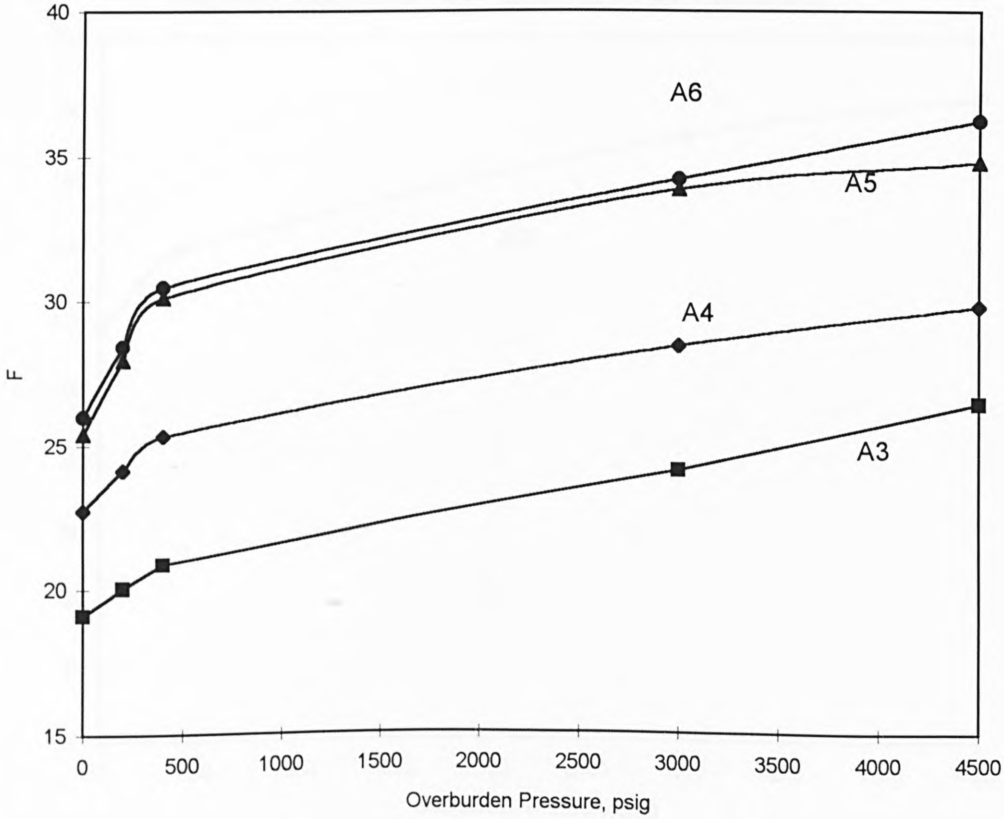

Fig.(4.3) Pressure vs. Formation Factor for Sandstones

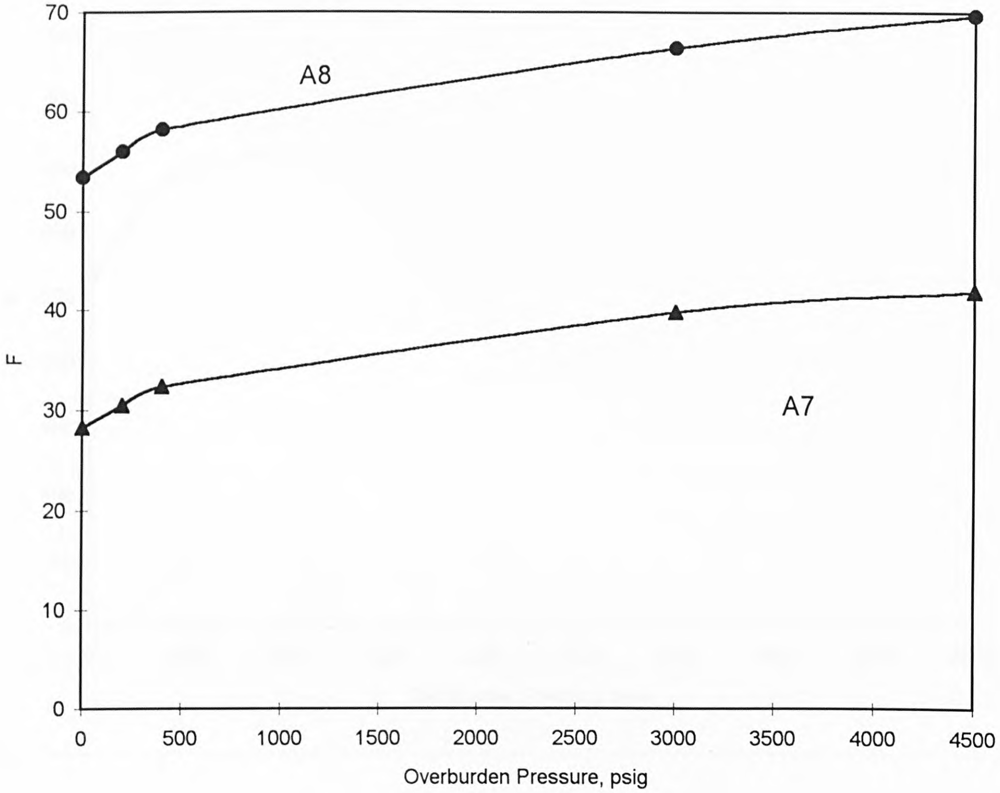

Fig.(4.4) Pressure vs. Formation Factor for Sandstones

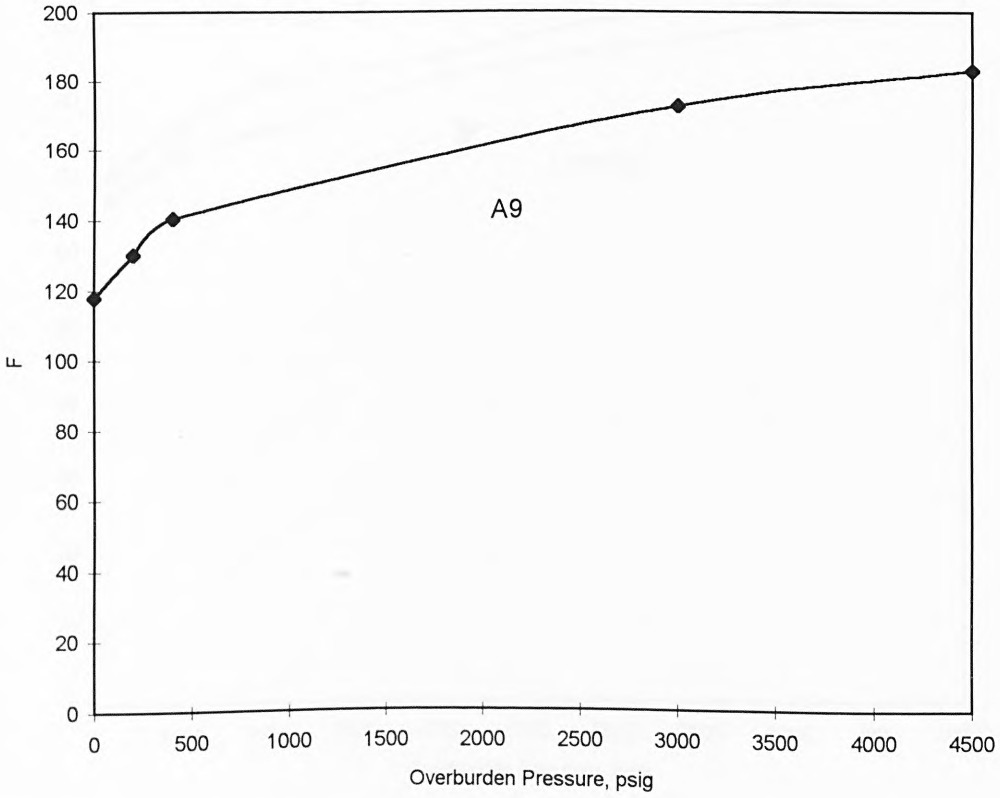

Fig.(4.5) Pressure vs. Formation Factor for Sandstones

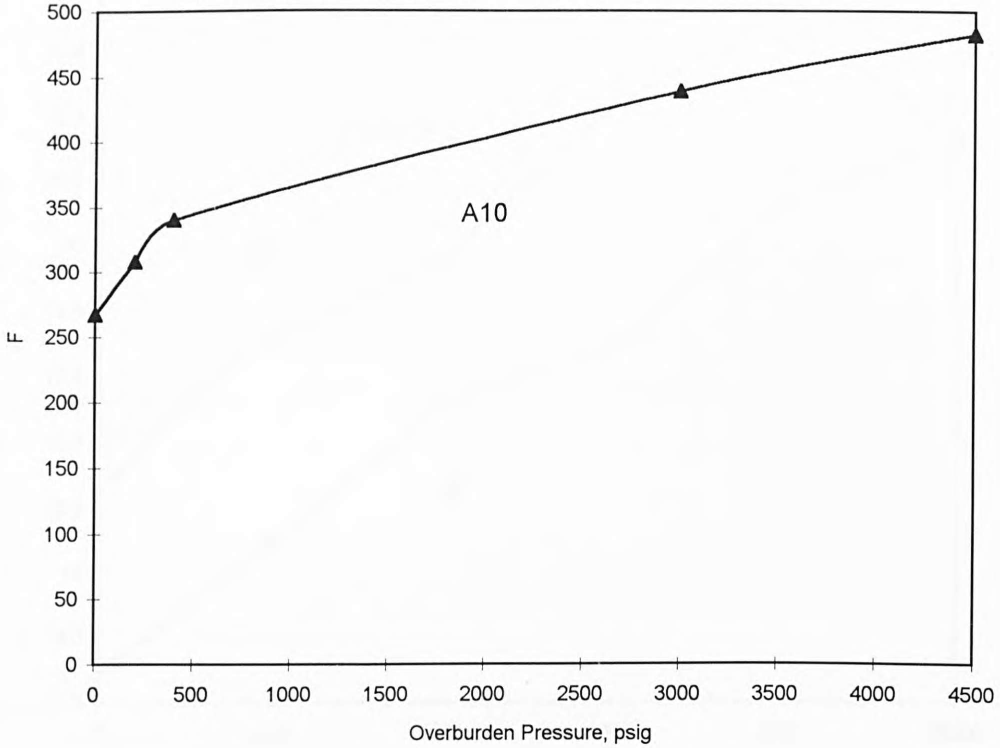

Fig.(4.6) Formation Factor vs. Overburden Pressure (sample B6)

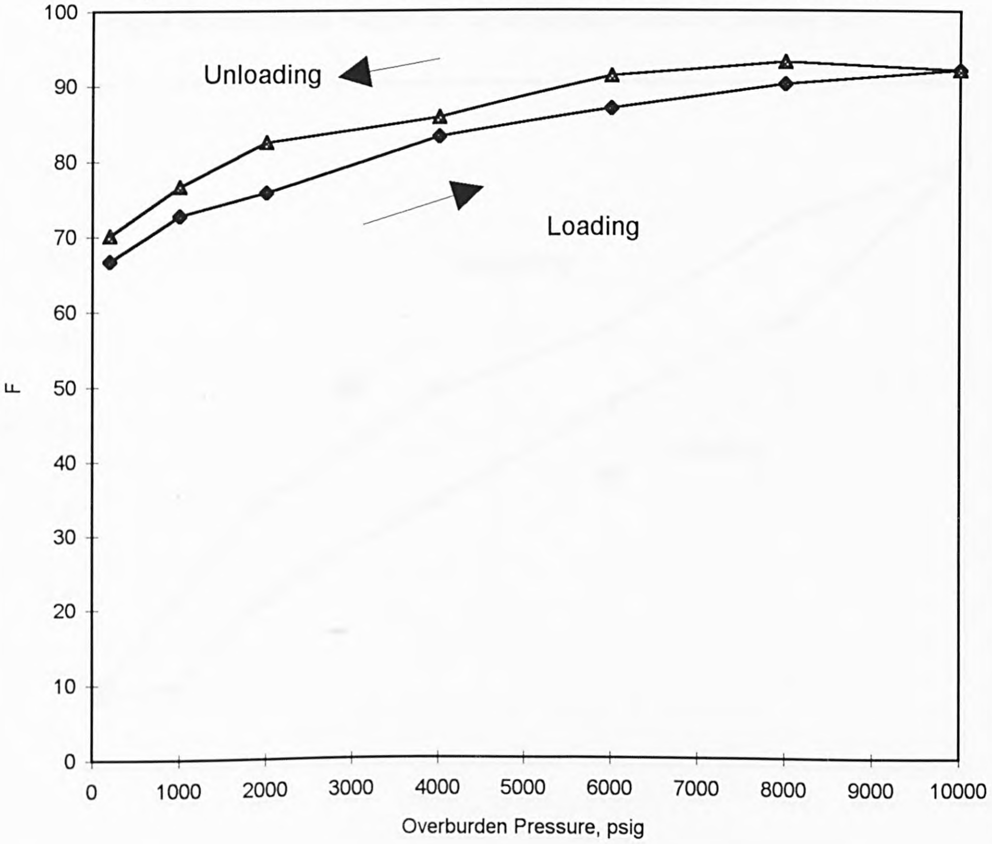

Fig.(4.7) Formation Factor vs. Overburden pressure (B9)

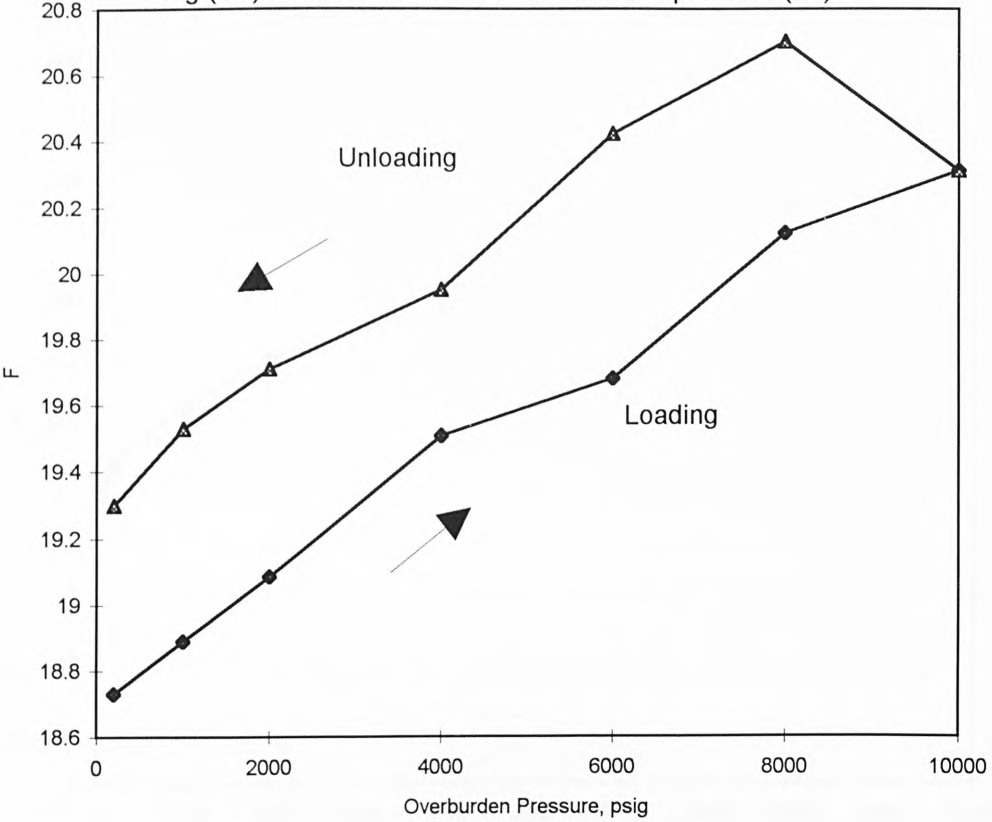

Fig.(4.8) Formation Factor vs. Overburden Pressure (sample B12)

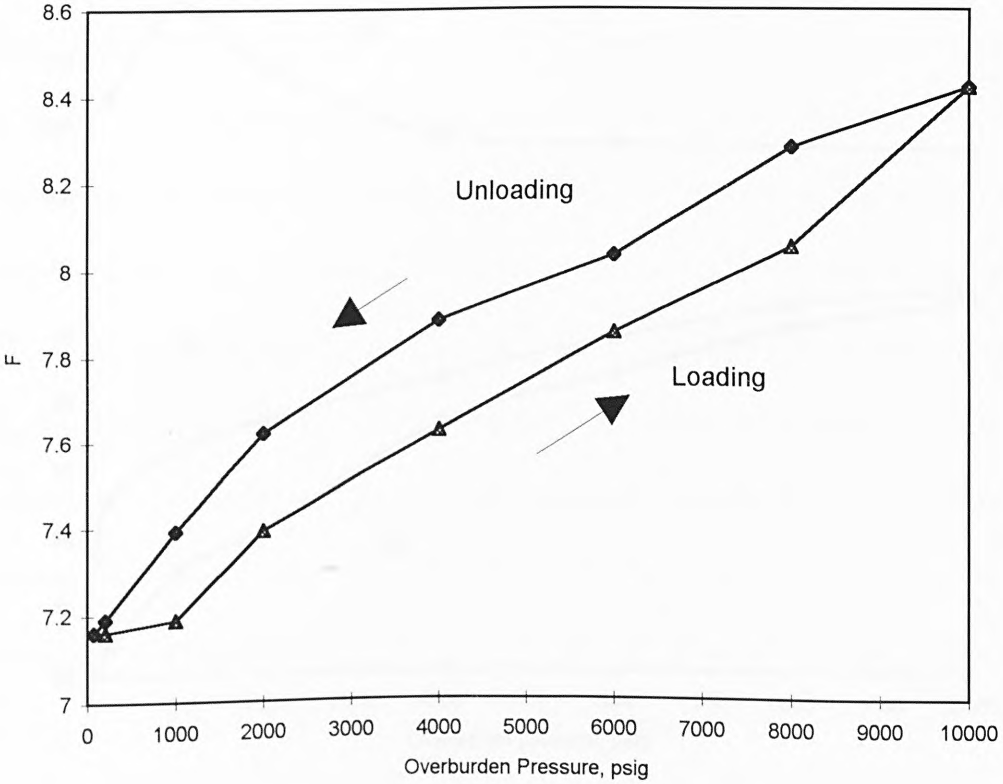

Fig(4.9) Formation Factor vs. Overburden Pressure (sample B2)

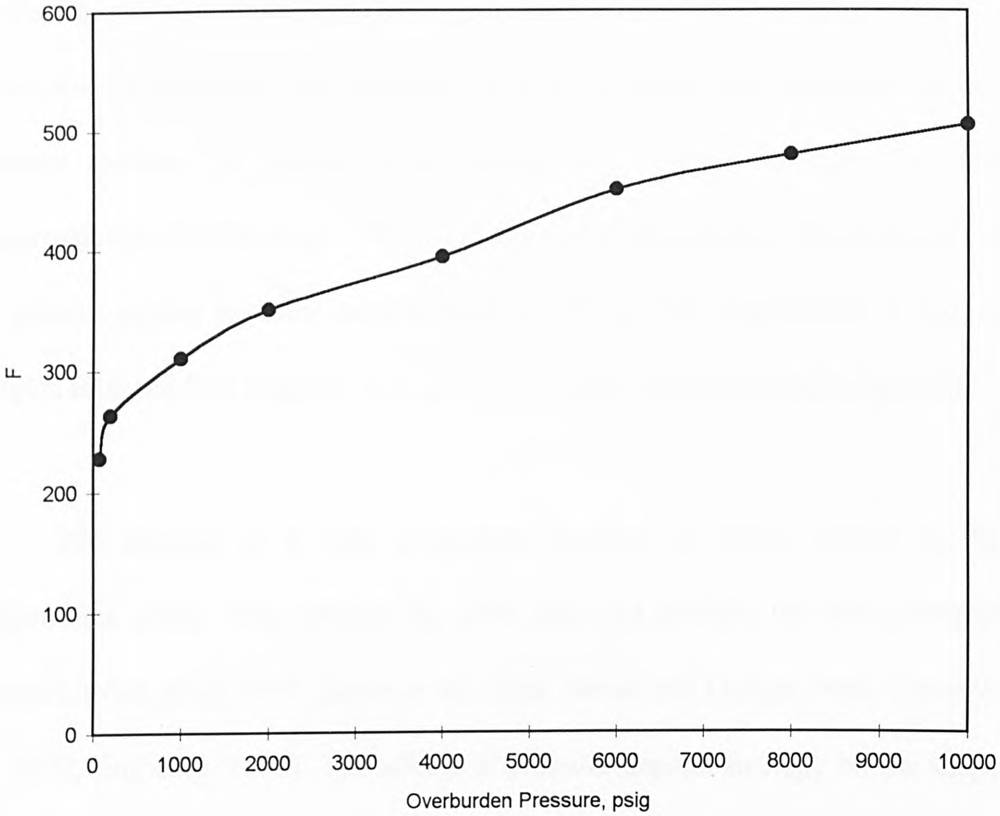

Fig.(4.10) Formation Factor vs. Pressure (Carbonates)

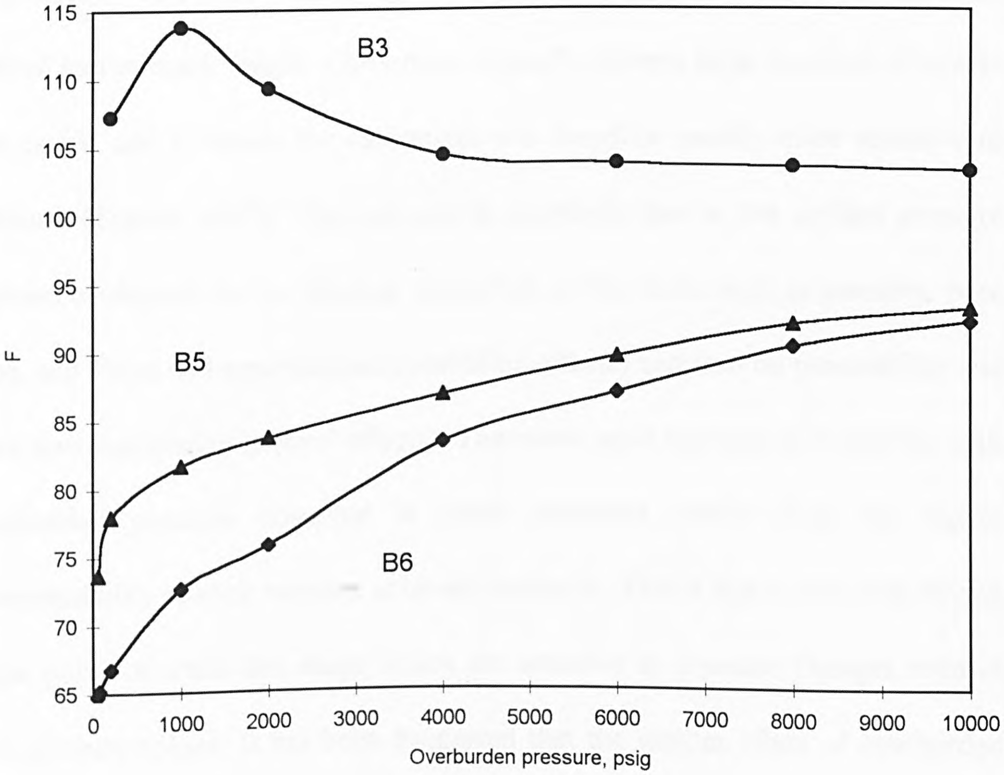

constant (small $\Delta F/\Delta P$) due to the effective closure of the smaller pores. In other words, the increase in resistivity with additional increase in pressure is small; this arises when compaction has occurred to such an extent that asperities on the adjacent surfaces of mineral grains comes into contact reducing the rock compressibility (Glover *at al.,* 1994). For the carbonate samples, the changes in F are greater in low porosity samples such as B5 and B6 (Figure 4.10) than in samples B10 and B12 (Figures 4.11 and 4.13) which have much higher porosity.

The increase of F with overburden pressure is simply related to the compression effect. This reduces the pore sizes and changes the flow paths of electric current (Fatt, 1957, Brace *et al.,* 1965, Brace and Orange 1968, Timur *et al.,* 1972, Jing et al. 1990). The effects of pressure depend strongly on the shape of the pore cross-section. Equant pores are generally not sensitive to closure due to pressure while thin crack-like pores will close readily if the applied stress acts normal to the crack length. Carbonates typically contain large numbers of crack-like pores, and F values for carbonates are therefore usually quite sensitive to pressure (Doyen, 1987). The increase in resistivity due to the applied pressure appears to depend on the physical properties of the rocks such as porosity, pore type, and shape and cementation (controlling effects) and also on permeability and pore size distribution (coeval effects). The more rapid increase of resistivity with overburden pressure observed at lower pressures results from the higher compressibility of rock samples at lower pressures. This is due to the rock having some pores of crack-like shape which are sensitive to pressure changes even at low pressure values. It has been suggested that the greater effect of overburden

Fig.(4.11) Formation Factor vs. Overburden Pressure (Carbonates)

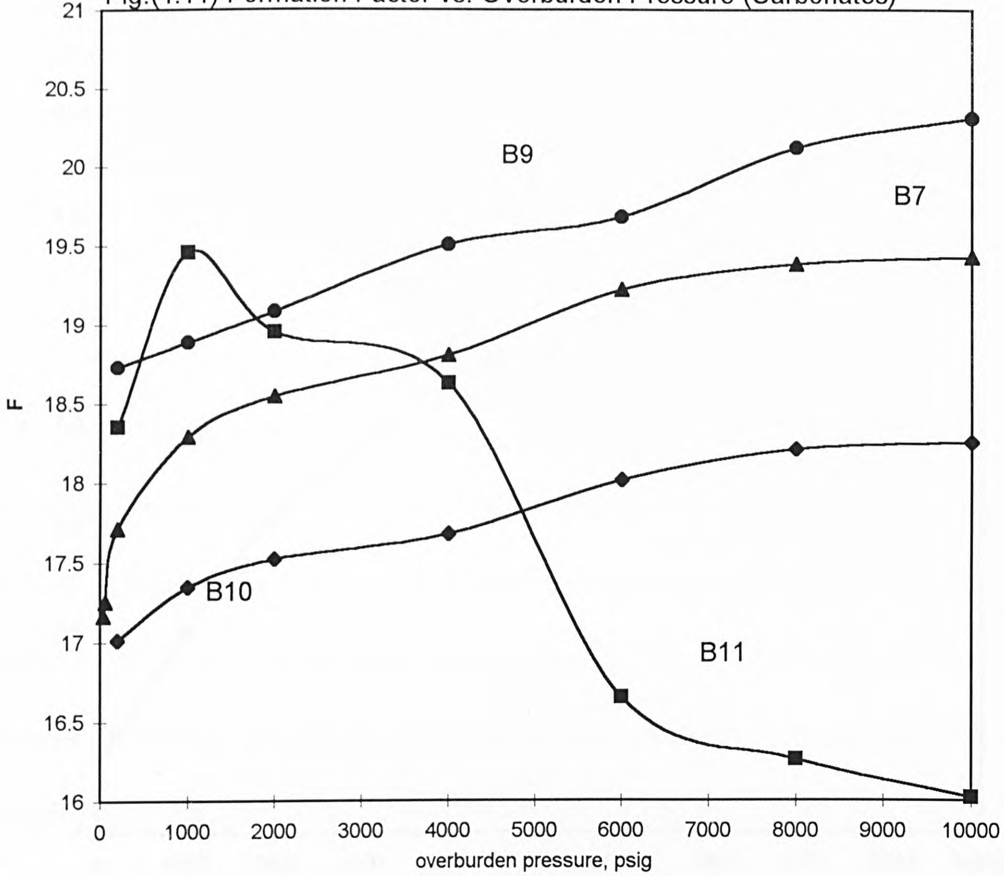

Fig.(4.12) Formation Factor vs. Overburden Pressure (Carbonates)

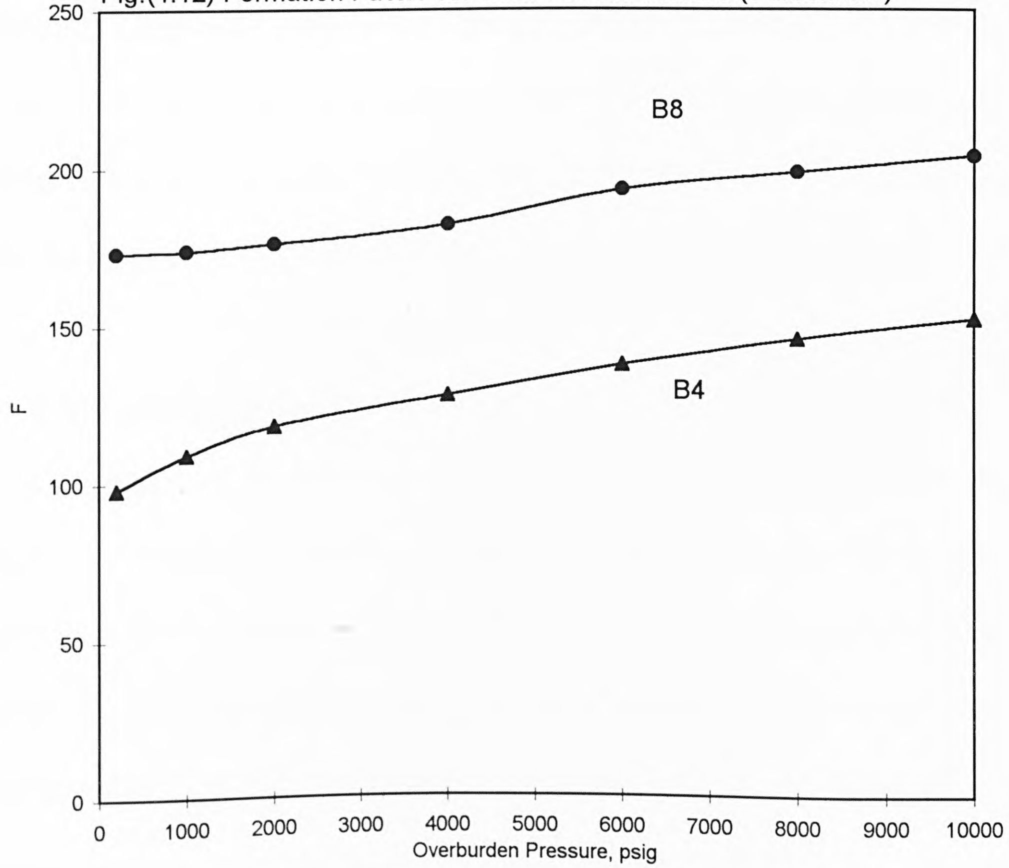

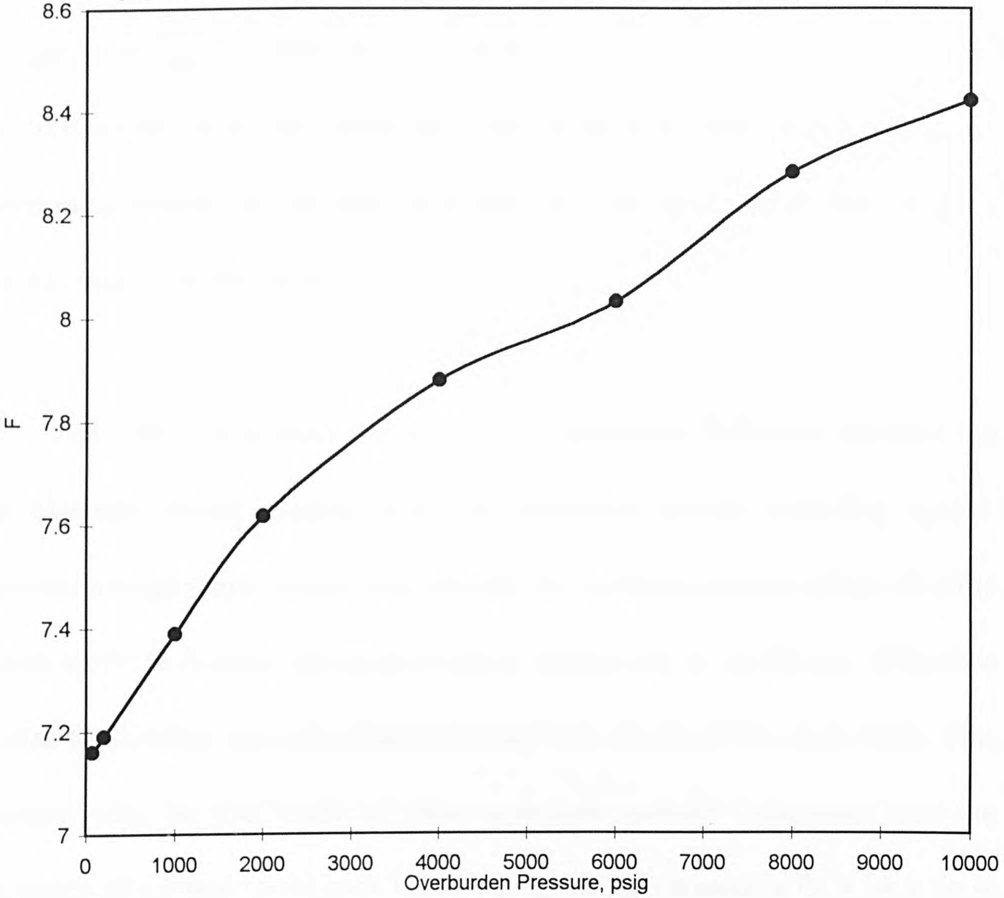

Fig.(4.13) Formation Factor vs. Overburden Pressure (Sample B12) pressure on F in less porous samples (especially the sandstones) can be related to the high percentage of small pores which are more compressible than the larger pores (Glanville, 1959), but others have concluded as a result of theoretical and experimental studies that the small pores are not more compressible than the large ones (Gueguen and Palciauskas 1994).

Fatt (1957) suggested that there is no significant difference between the data obtained during loading and that measured during unloading cycles. However, a longer time interval was allowed for equilibrium to be achieved in the present work (2-3 days for each pressure point) and a significant difference between the loading and unloading properties was observed for each cycle. This hysteresis may be the result of time-dependent inelastic behaviour, i.e. the occurrence of damage to the rock when it is left at high pressures for a long time; this effect is especially pronounced in sensitive cements and clays (Glover *et al.*, 1994). For a given rock, the hysteresis depends on the magnitude, the duration and the increment of pressure. The hysteresis is generally found to be reproducible when the loading cycles are repeated (Jing, 1990, Jaeger and Cook 1977).

4.22 Effect of Overburden Pressure on *m*

Figures 4.14 to 4.17 show the effect of overburden pressure on the cementation factor for sandstone samples A1 to A10, and figures 4.21 to 4.26 show this effect for carbonate samples B1 to B12. The Archie cementation factor ($m = -\log F / \log \phi$) for sandstone increases significantly with pressure (e.g. samples A9 and A10, which are less porous and permeable than samples A1 and

A2). For medium porosity samples such as A5 and A7 (Figures 4.16 and 4.17), the rate of increase in cementation factor with pressure is much greater than for samples with high porosity. Gueguen and Palciauskas, (1994) showed by a theoretical analysis that for an anisotropic stress field the energy reaches a minimum when the pore cross section is changing from a circular shape to an elliptical shape.

For sandstone samples, the effect of overburden pressure on m was investigated over the pressure range of 200 to 4500 psig. It can be seen that m increases with pressure and this effect is more pronounced for medium and low porosity samples (except sample A8) than high porosity samples. It is found that after a specific pressure value is reached, (approximately 3000 psig), the change of m with pressure becomes smaller. For highly porous samples such as A1 and A2 (Figures 4.14 and 4.17) the increase in cementation factor with overburden pressure becomes smaller at pressures above 3000 psig, and for low porosity samples such as A8 and A9, this increase in m become smaller at >4000 psig. For medium porosity samples, the effect was variable.

The experimental values of the Archie cementation factor *m* for sandstone samples at various overburden pressures before correction for porosity changes caused by overburden pressure (i.e. ignoring the porosity changes during the calculation of *m* at various pressures) show that m apparently increases dramatically with pressure. After correction, however, the changes in m resulting from increasing pressure become relatively smaller although still significant.

Fig.(4.14)Cementation Factor vs. Overburden Pressure (Sandstones)

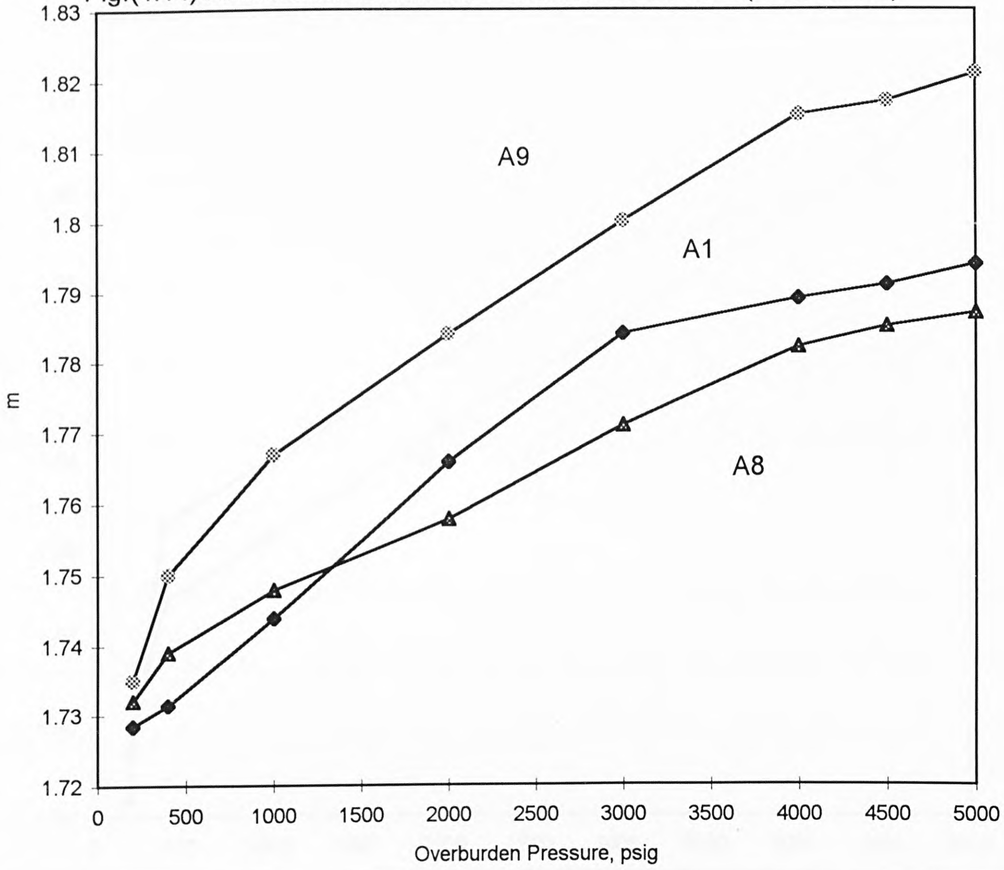

Fig. (4.15) Cementation Factor vs. Overburden Pressure (Sandstone)

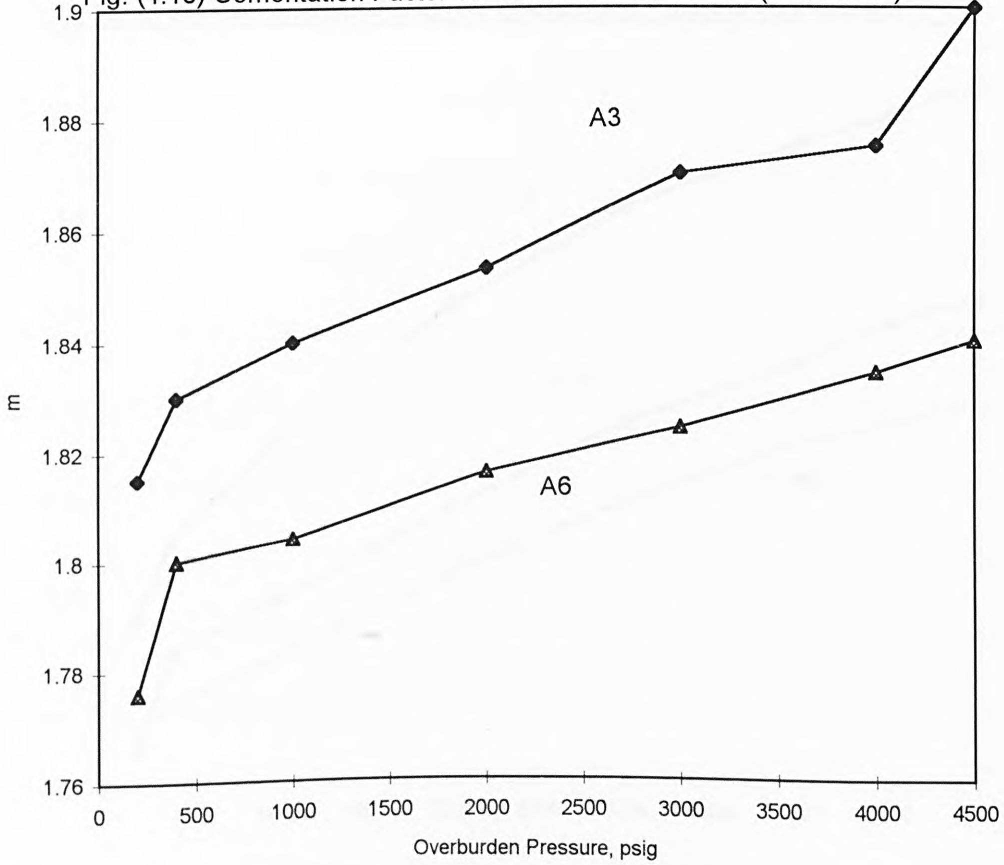

Fig.(4.16) Cementation Factor vs. Overburden Pressure (Sandstone)

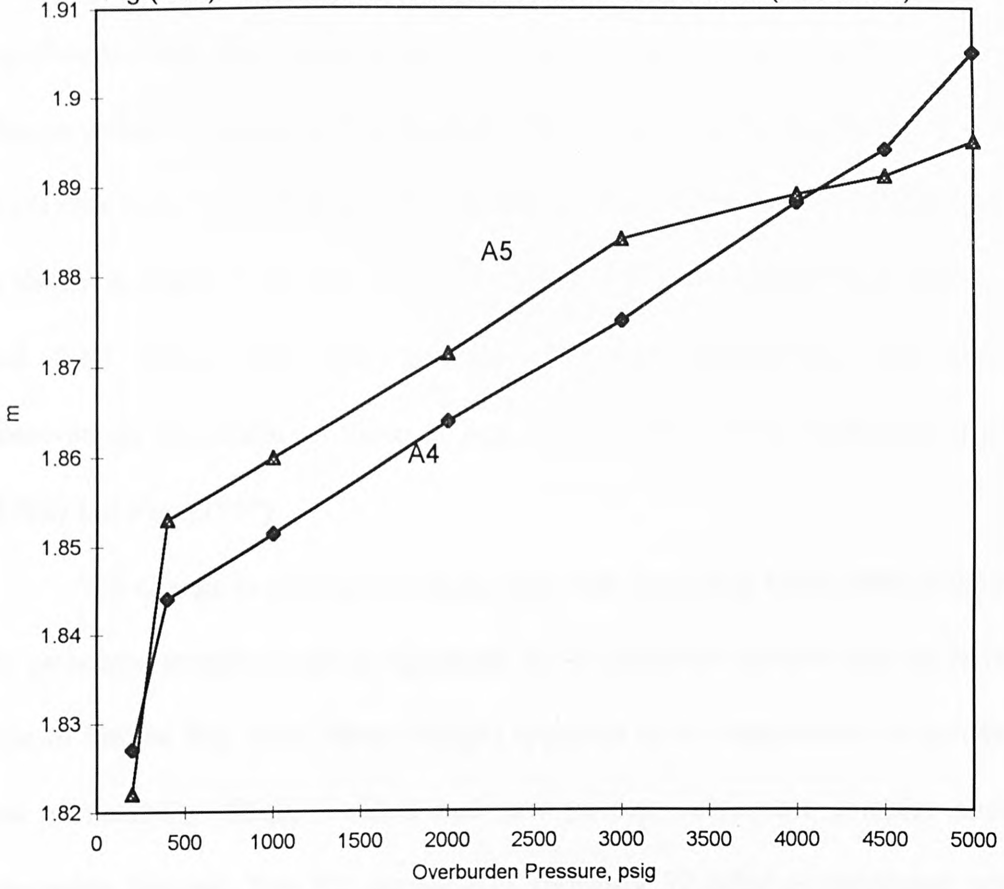

Fig.(4.17) Cementation Factor vs. Overburden Pressure (Sandstone)

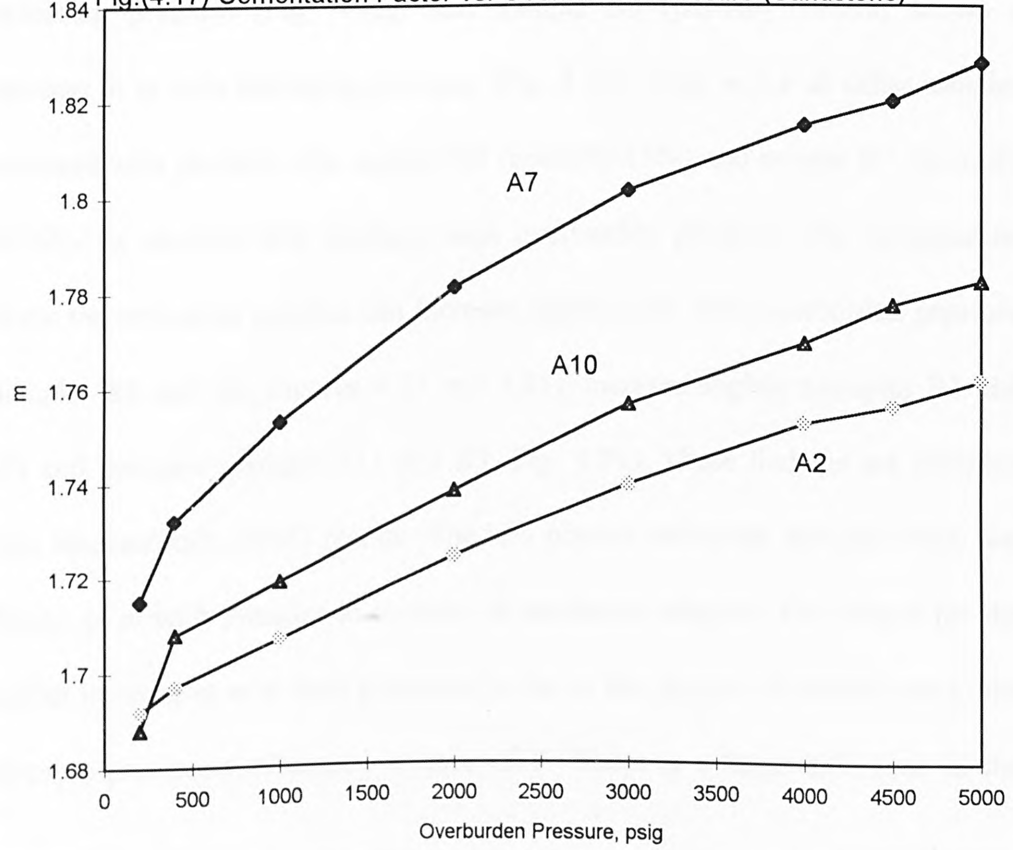

The cementation factor for sandstone samples appears to increase significantly with overburden pressure before taking into account the porosity change caused by pressure. For example, the change in m for sample A2 (Figure 4.18) was 0.19, while after porosity correction, the change was 0.07. Sample A3 is shown in Figure 4.19. For sample A10 (Fig. 4.20), the change in *m* was 0.18 and 0.12 before and after porosity correction respectively. The above observations are similar to those of Jing *et al.*, (1991; 1992), Mahmood *et al.*, (1988) and Fatt (1957).

The change in cementation factor *(m)* with increasing overburden pressure for carbonate samples is not as significant as for sandstone samples (except in the case of sample B2). Also, these changes appeared to be independent of porosity and permeability. High, medium and low porosity carbonate samples show interesting features. For the sample B11 (porosity 32.44%) *m* decreased with increasing pressure (Fig. 4.22); also Sample B3 (porosity 10.9%) shows a decrease in *m* with increasing pressure (Fig. 4.21), while *m* for all other samples increased with pressure. For sample B9 (porosity 13%) and sample B7 (porosity 20.39%) *m* showed little increase with overburden pressure. The cementation factor for carbonate samples can increase significantly with overburden pressure (samples B2 and B4, Figures 4.22 and 4.23), increase slightly (samples B1 and B5) and decrease (sample B11 and B3, Fig. 4.21). These findings are different from Hausenbles's (1995) results. The less porous carbonate samples show less change of *m* with pressure in contrast to sandstone samples. The reason for the smaller increase in *m* at high pressures is due to the closure of narrow crack-like pores as previously discussed in case of F. There is a large difference in the

Fig(4.18) Cementation Factor vs.Overburden Pressure (Sample A2)

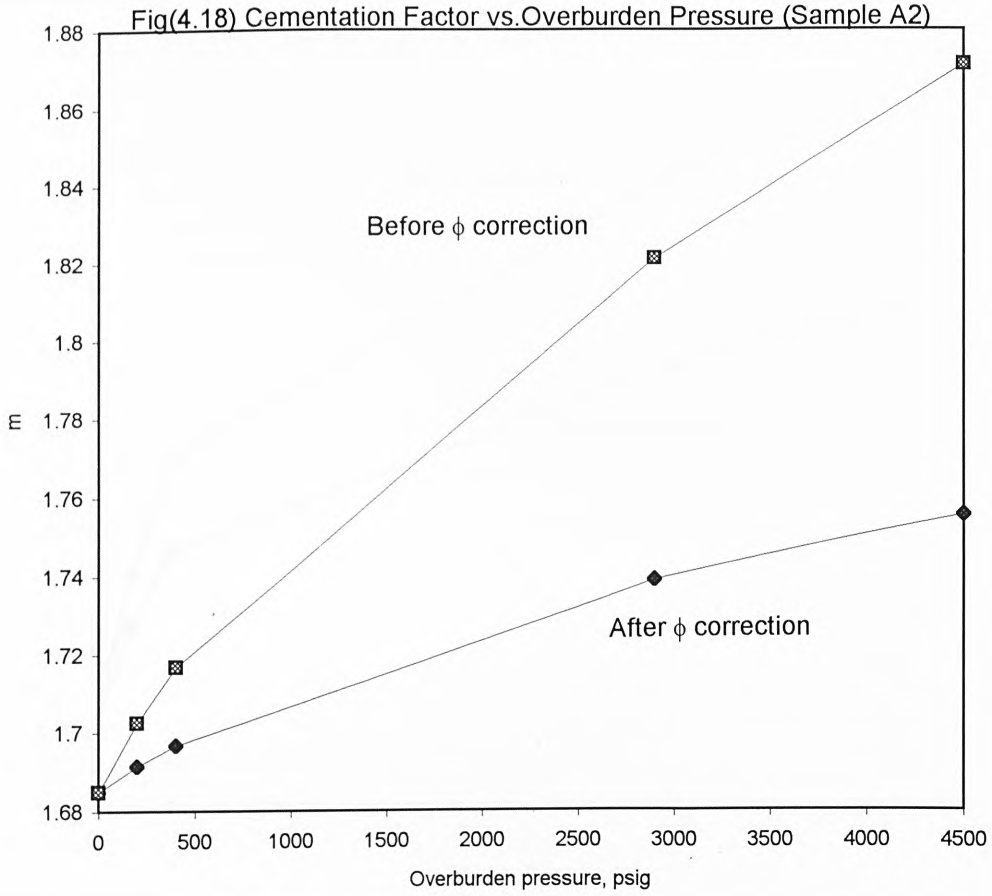

Fig.(4.19) Cementation Factor vs. Overburden Pressure (sample A3)

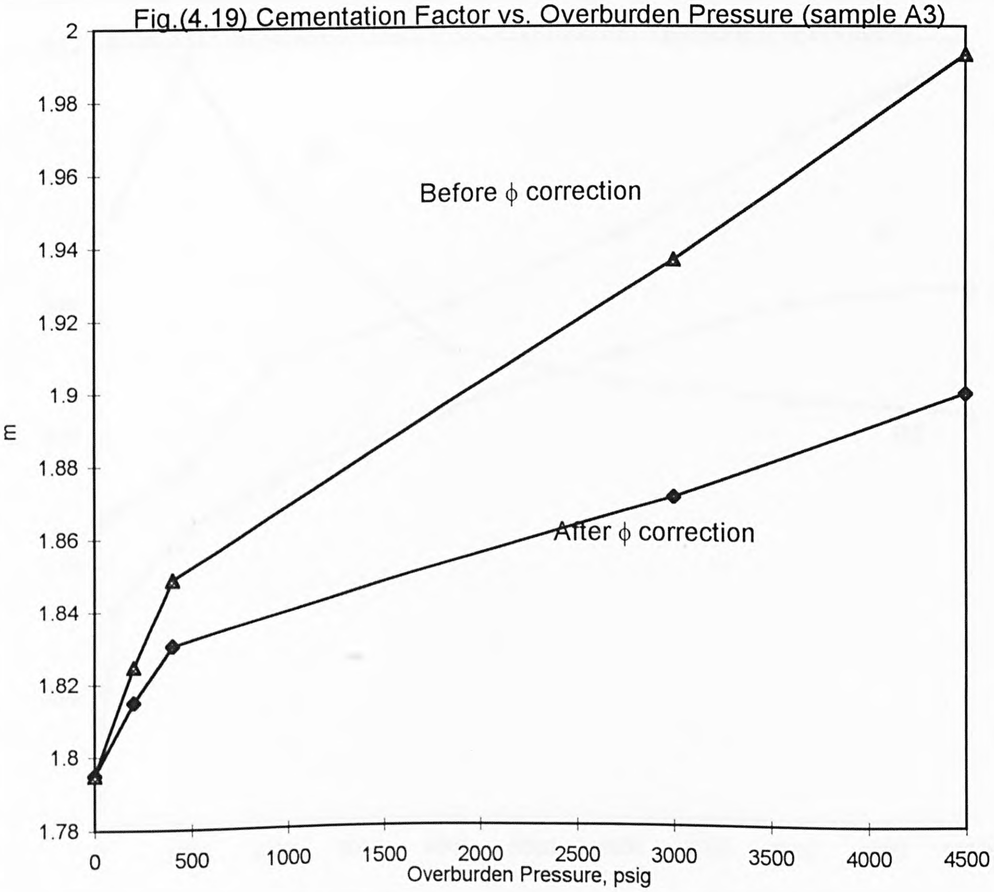

Fig.(4.20) Cementation factor vs. Overburden pressure (sample A10)

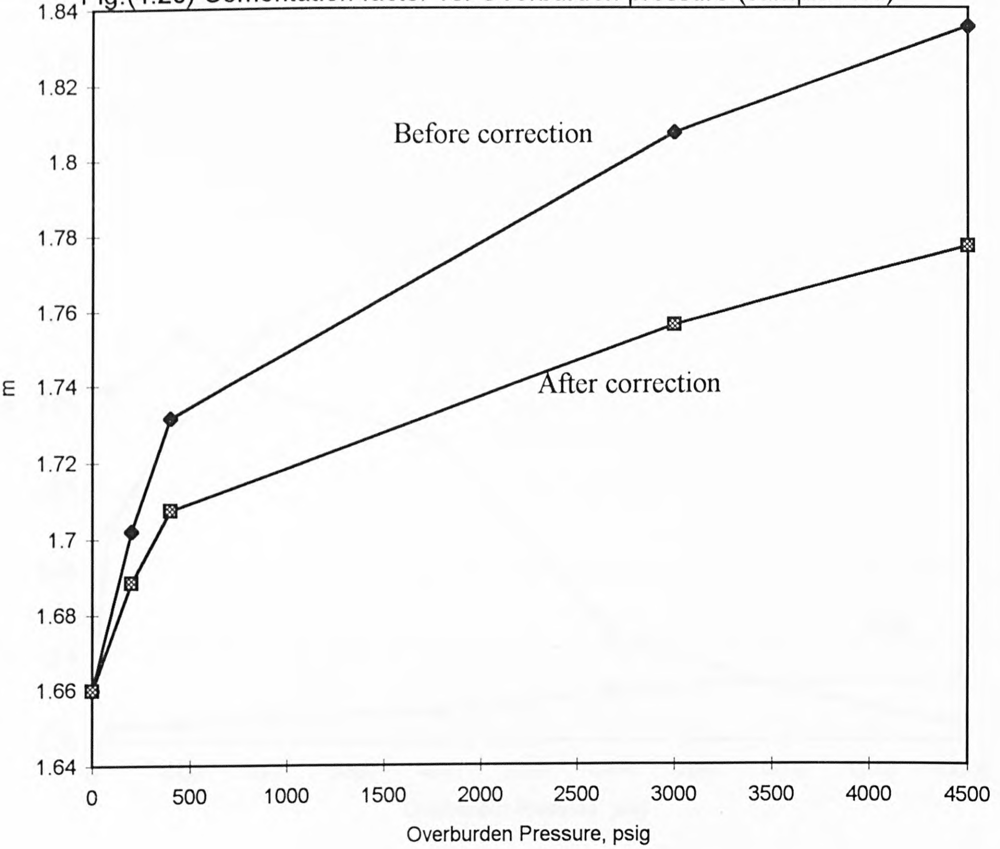

Fig.(4.21) Cementation Factor vs. Overburden Pressure (Carbonates)

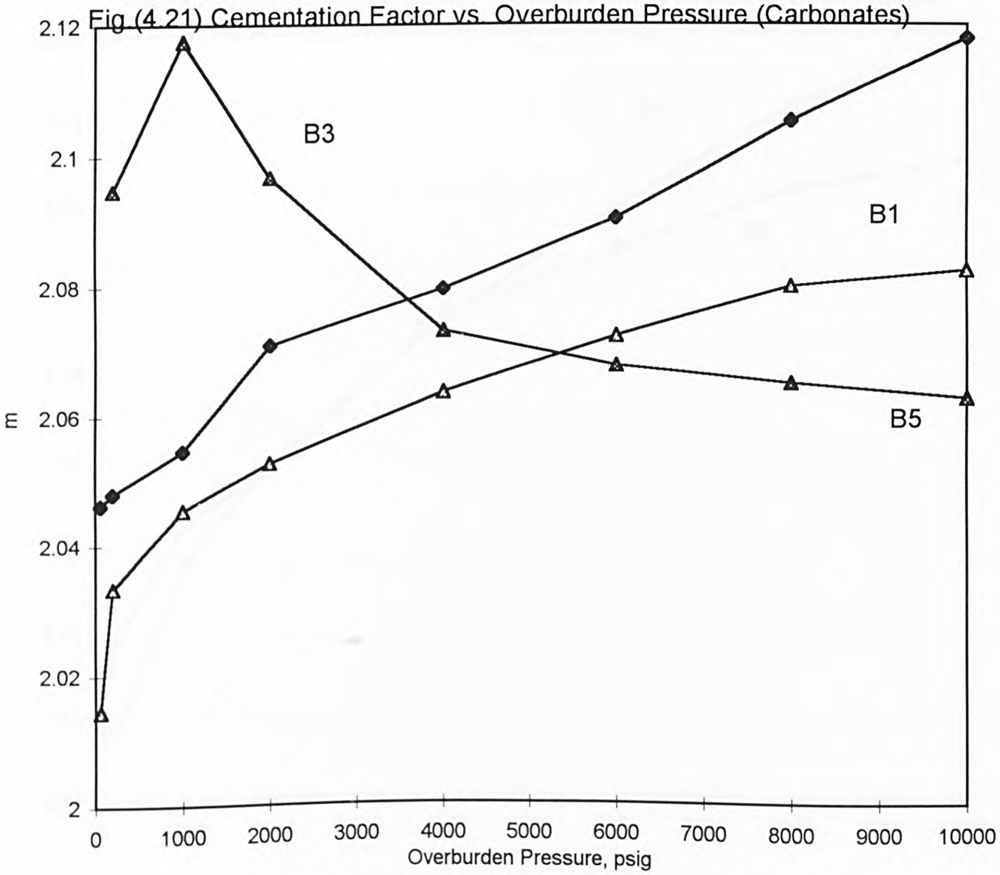

Fig. (4.22) Cementation Factor vs. Overburden Pressure (Carbonates)

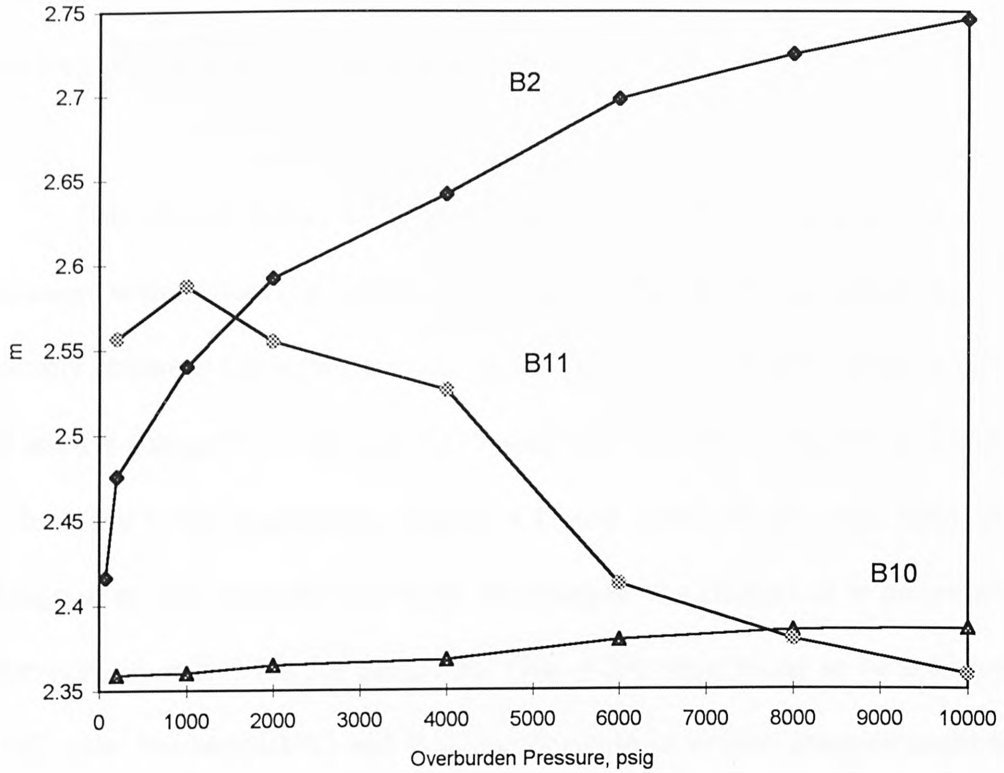

Fig.(4.23) Cementation Factor vs. Overburden Pressure (Carbonates)

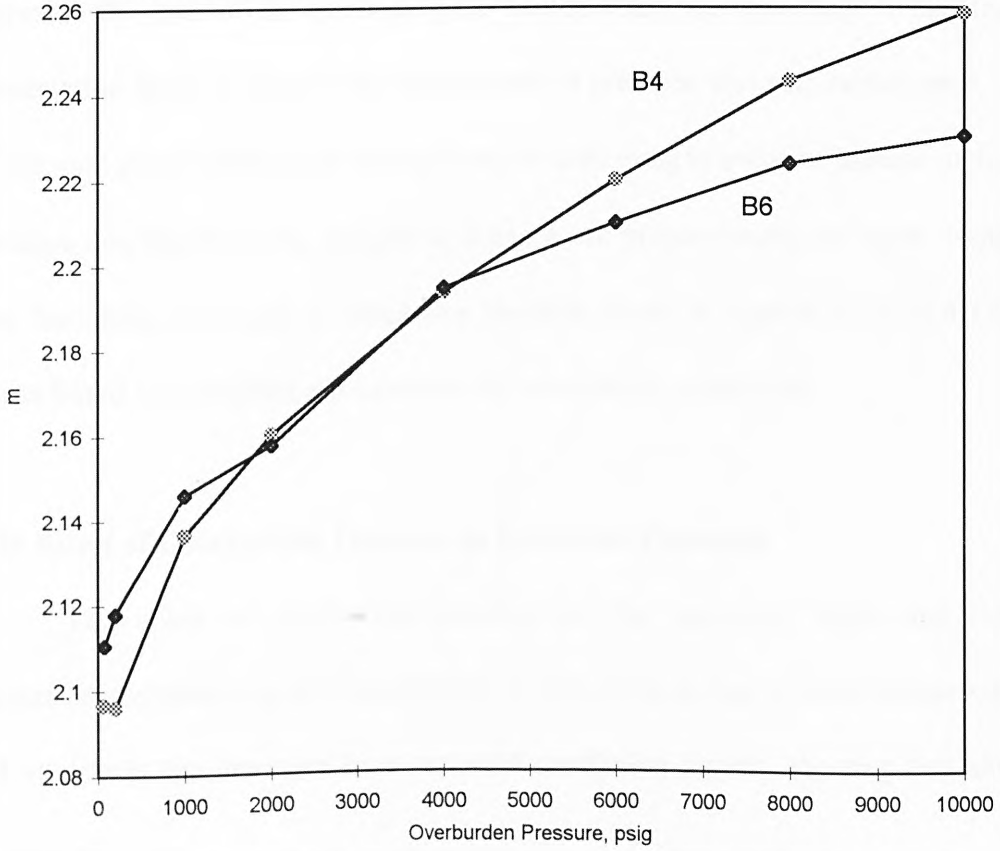

change of *m* with pressure for the low porosity samples, e.g. for sample B2 *m* changes by 0.33 while in sample B1, it changes only by 0.07, in spite of the fact that their porosities are low and similar in value (10.63% and 9.73% respectively).

Cementation factors for carbonate samples can show both large and small increases with increase in overburden pressure before the correction due to porosity change is taken into account. Before porosity correction, *m* for samples B2 and B4 changed by 0.355 and 0.205 while after porosity correction it changed by 0.33 and 0.162 respectively, (figures 4.27 and 4.28). On the other hand, the change in m with pressure was small; for example, the changes in *m* before and after porosity correction for sample B9 (Fig. 4.29) were found to be 0.04 and 0.022 only. For samples B3 and B11, the decrease in *m* with pressure could be explained by the increase of porosity due to collapse of cementing materials which increases the area of the electrical path and decrease the resistivity. When the cementation factor is found to be independent of pressure, this may be the result of the rock pores (uniform or nonuniform) all deforming in a similar manner under pressure and therefore the changes in F and ϕ are proportionally the same. Note that the values of m used in calculating the data shown in Figures (4.14 to 4.17) are all based on porosities are corrected for overburden conditions.

4.23 Effect of Overburden Pressure on Sauration Exponent

The effect of overburden pressure on the resistivity index and the saturation exponent was not investigated in this research due to time limitations, but studies in the literature have reported conflicting results, showing that the

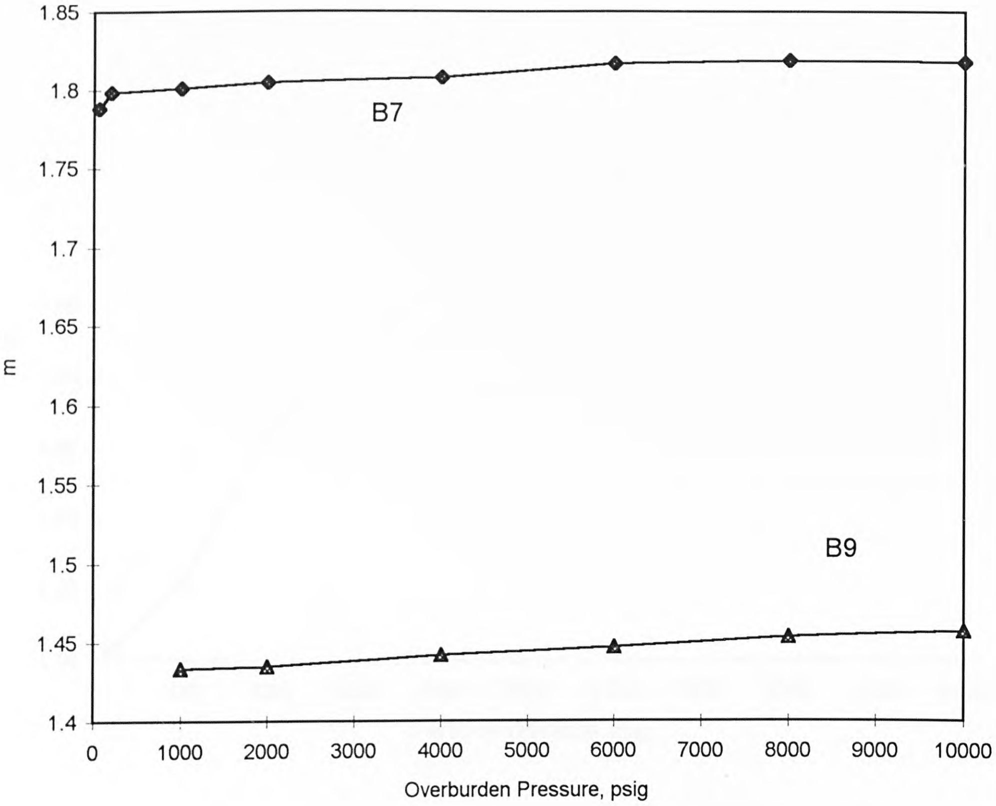

Fig.(4.24) Cementation Factorvs. Overburden Pressure

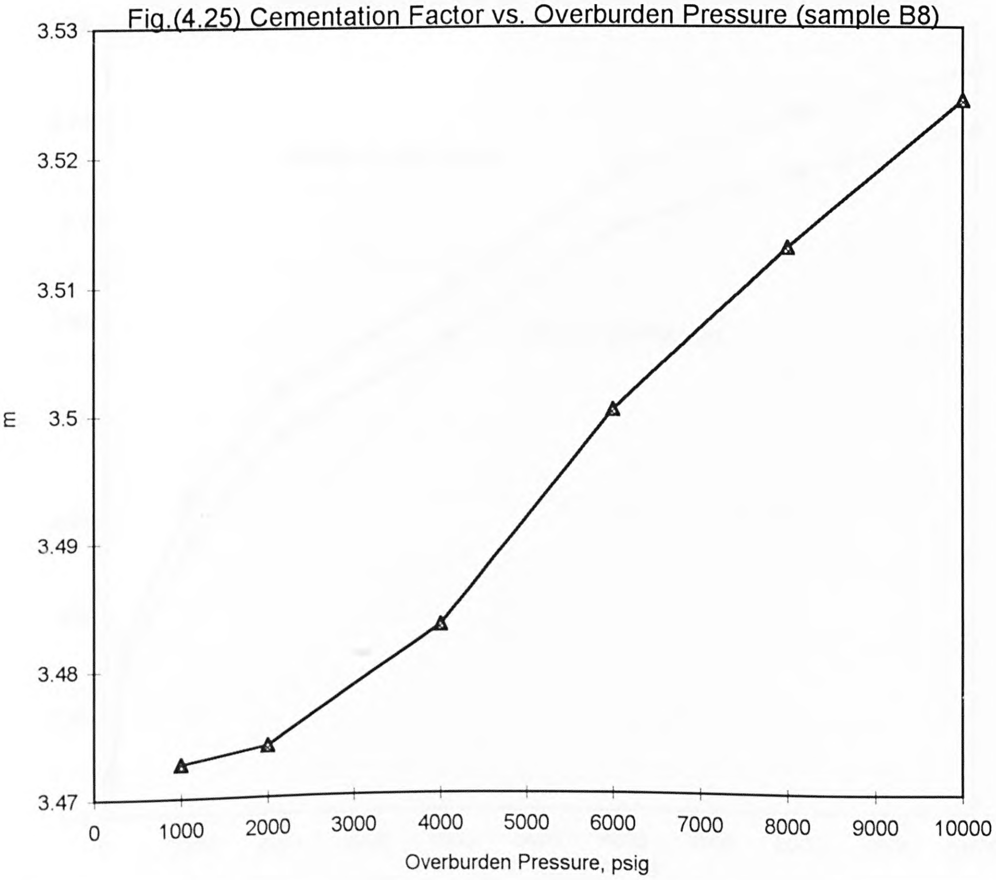

Fig.(4.25) Cementation Factor vs. Overburden Pressure (sample B8)

Fig.(4.26) Cementation Factor vs. Overburden Pressure (sample B12)

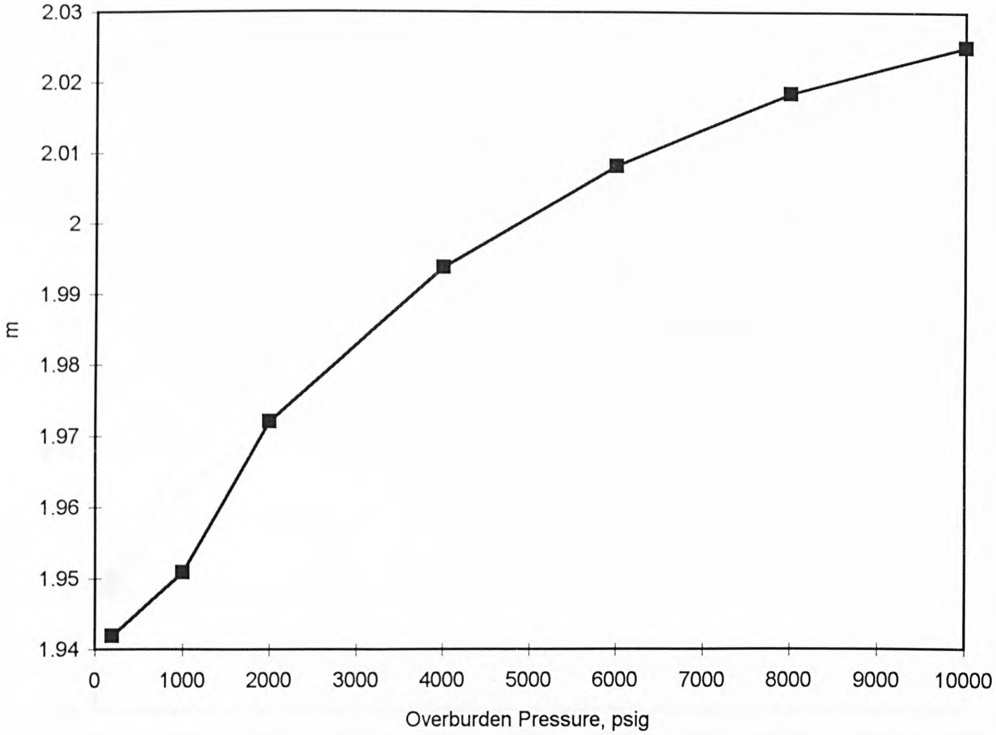

Fig.(4.27) Cementation Factor vs. Overburden Pressure (sample B2)

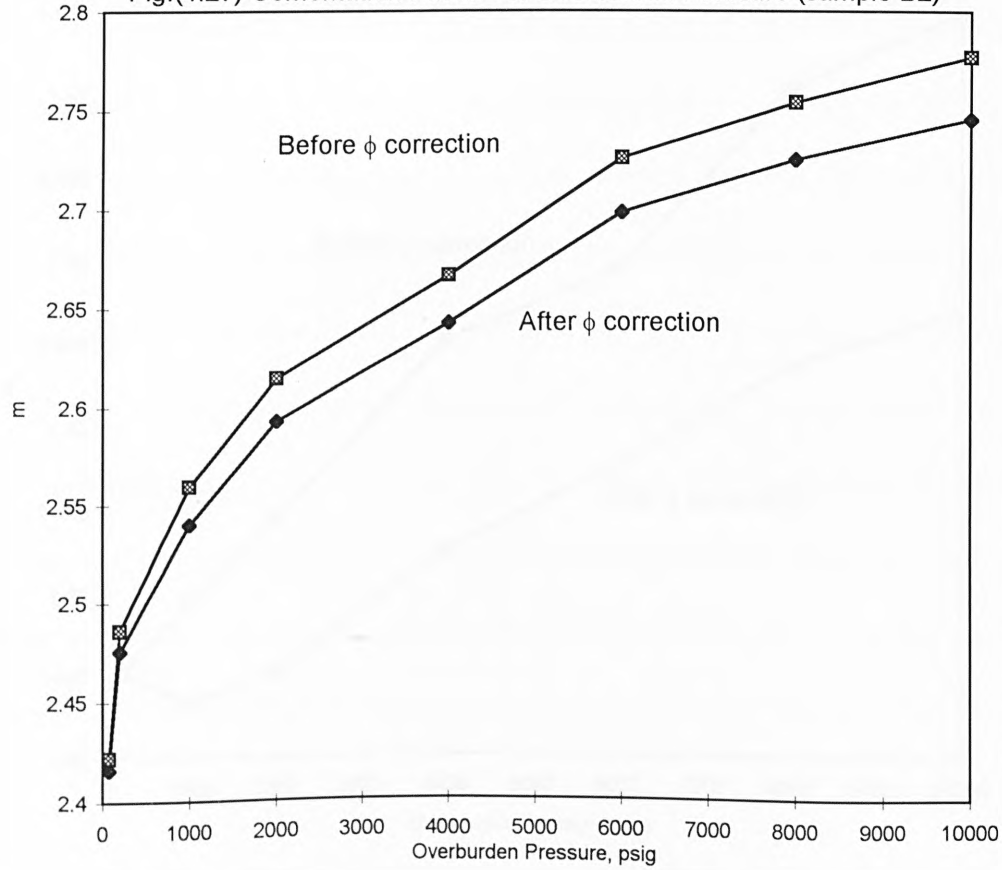

Fig.(4.28) Cementation Factor vs. Overburden Pressure (sample B4)

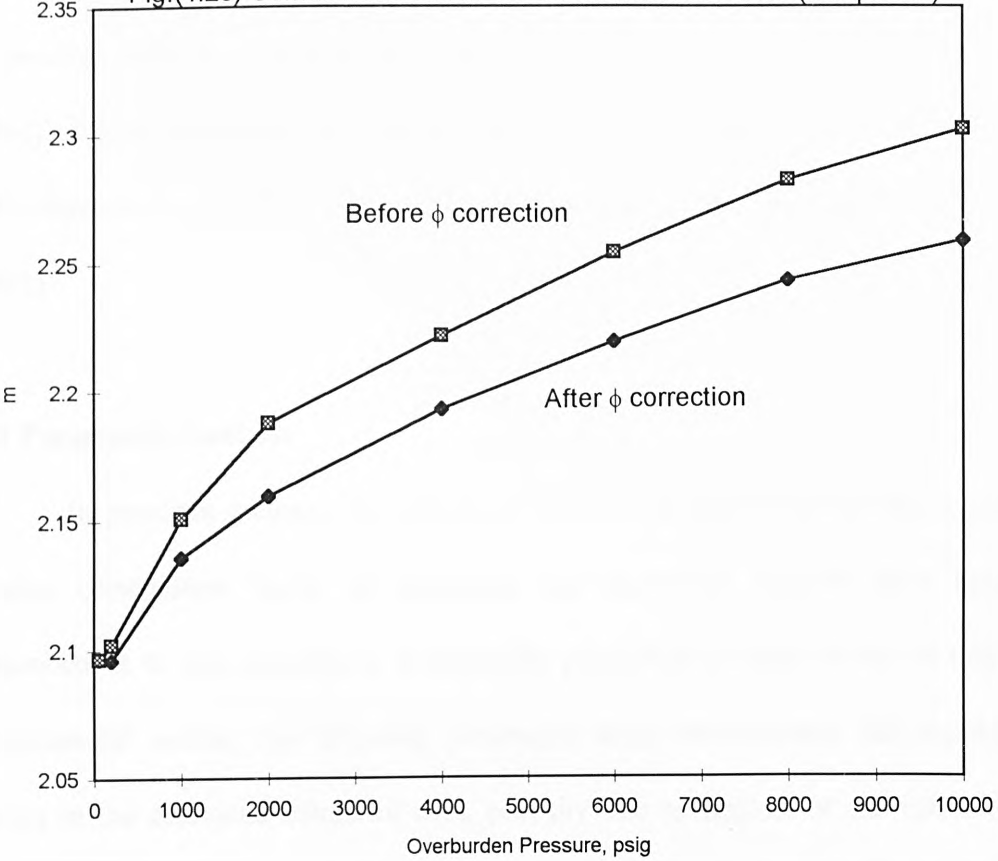

Fig.(4.29) Cementation Factor vs. Overburden Pressure (sample B9)

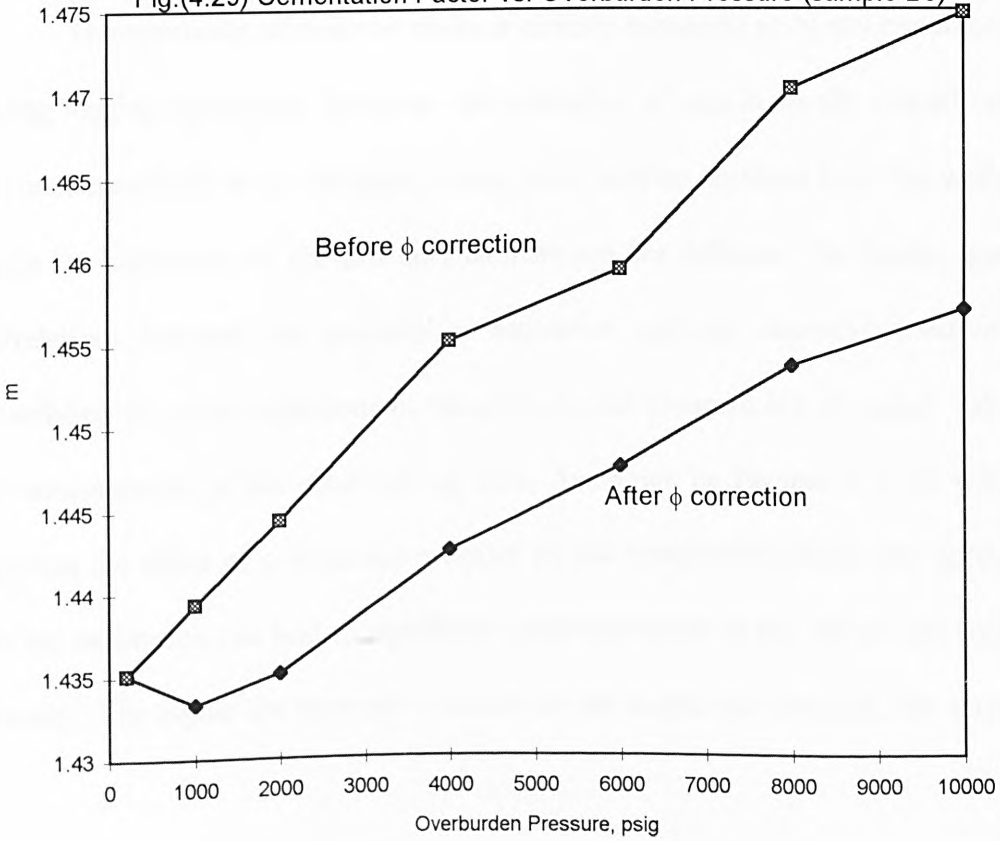

saturation exponent may either increase or decrease with increase in pressure (Glanville, 1959, Longeron *et al.*, 1986, Lewies *et al.*, 1988, Elashahab *et al.*, 1994). These variations in results may be due to experimental difficulties (Worthington *et al.*, 1986, Moore 1958, Worthington *et al.*, 1990, de Wall *et al.*, 1991).

4.3 Parametric Analysis

In previous sections, the effects of pressure on the formation factor and Archie cementation factor of sandstone and carbonate samples have been described. It is now possible to examine the petrophysical implications of these experimental results. The following parametric study demonstrates the possible errors in the estimated values of rock porosity due to neglect of the effect of pressure.

The resistivity of reservoir rocks is directly measured at *in situ* conditions during logging operations. However the calibration of logs is usually carried out at room conditions in the laboratory using core samples obtained from the wells. Since the conditions of pressure and temperature are different, the Archie type correlations between the porosity or saturation and the electrical resistivity established for room conditions of temperature and pressure are no longer valid for interpretation of the electrical log data. As shown by Figures 4.32 to 4.39, ignoring the effect of overburden pressure on the cementation factor (m) during the log calibration can lead to significant underestimation of the real *in situ* rock porosity. The higher the reservoir pressure or the deeper the reservoir, the more

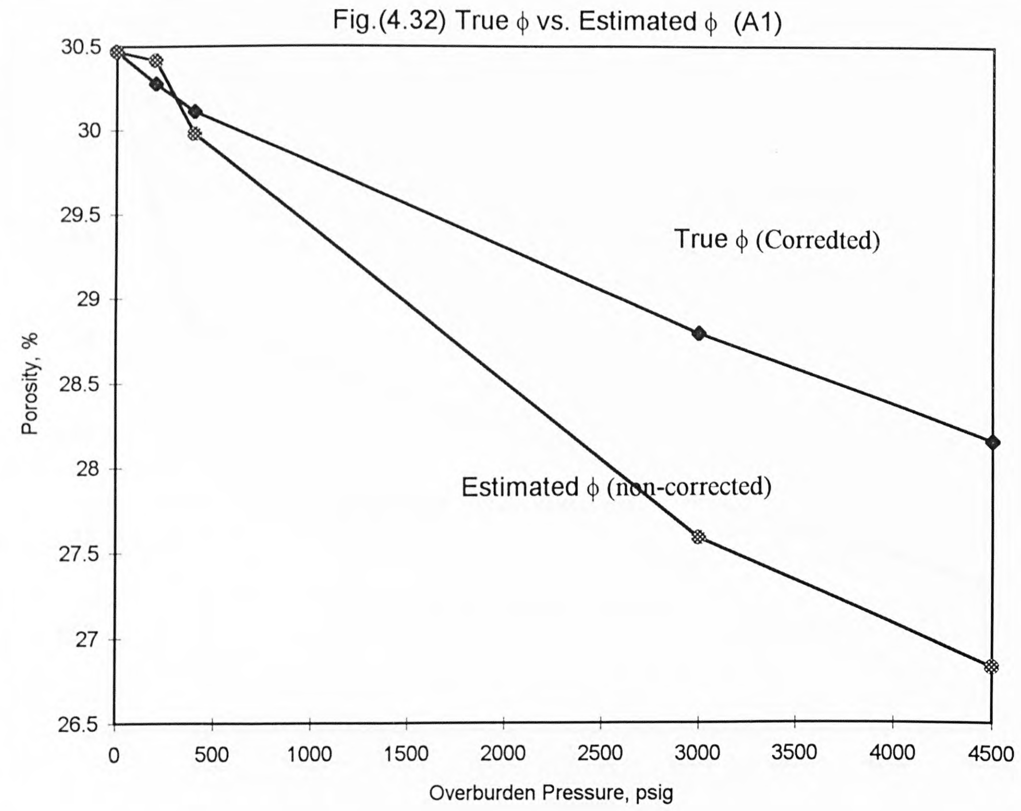
Fig.(4.32) True ϕ vs. Estimated ϕ (A1)
Porosity, %
30.5
30
29.5
29
28.5
28
27.5
27
26.5
True ϕ (Corredted)
Estimated ϕ (non-corrected)
0
500
1000
1500
2000
2500
3000
3500
4000
4500
Overburden Pressure, psig

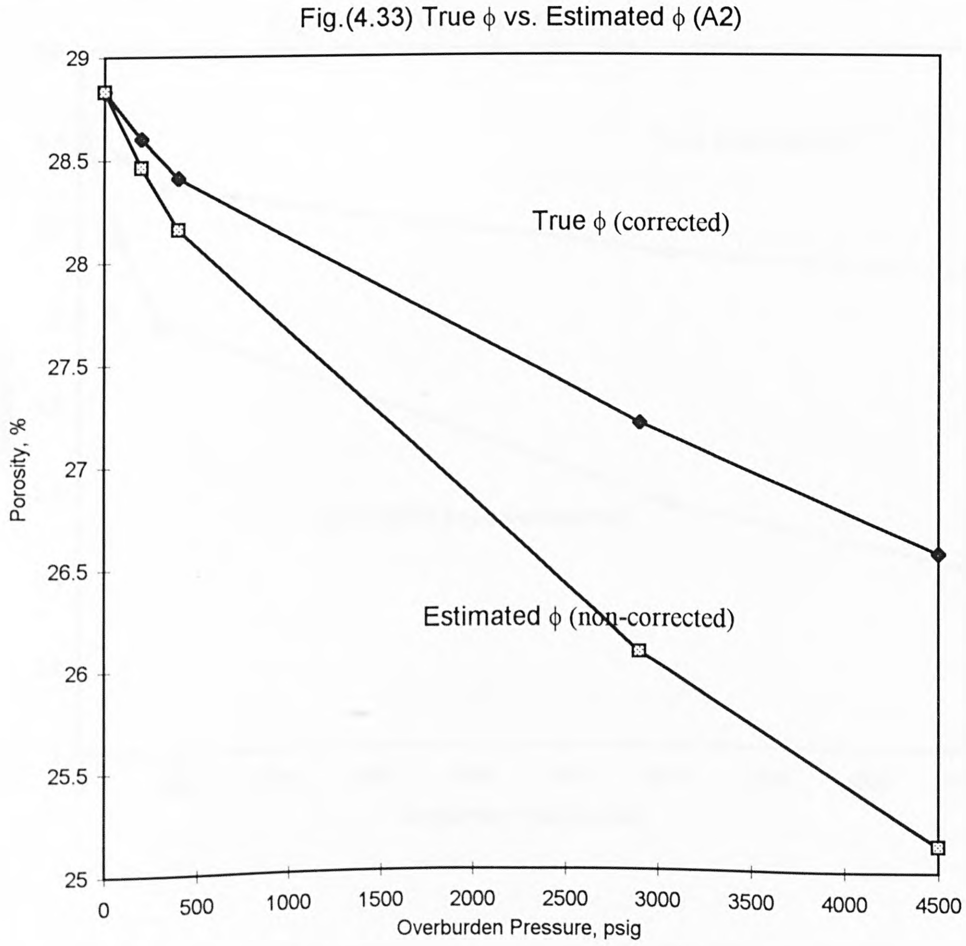
Fig.(4.33) True ϕ vs. Estimated ϕ (A2)
Porosity, %
29
28.5
28
27.5
27
26.5
26
25.5
25
True ϕ (corrected)
Estimated ϕ (non-corrected)
0
500
1000
1500
2000
2500
3000
3500
4000
4500
Overburden Pressure, psig

Fig.(4.34) True ϕ vs. Estimated ϕ (A6)

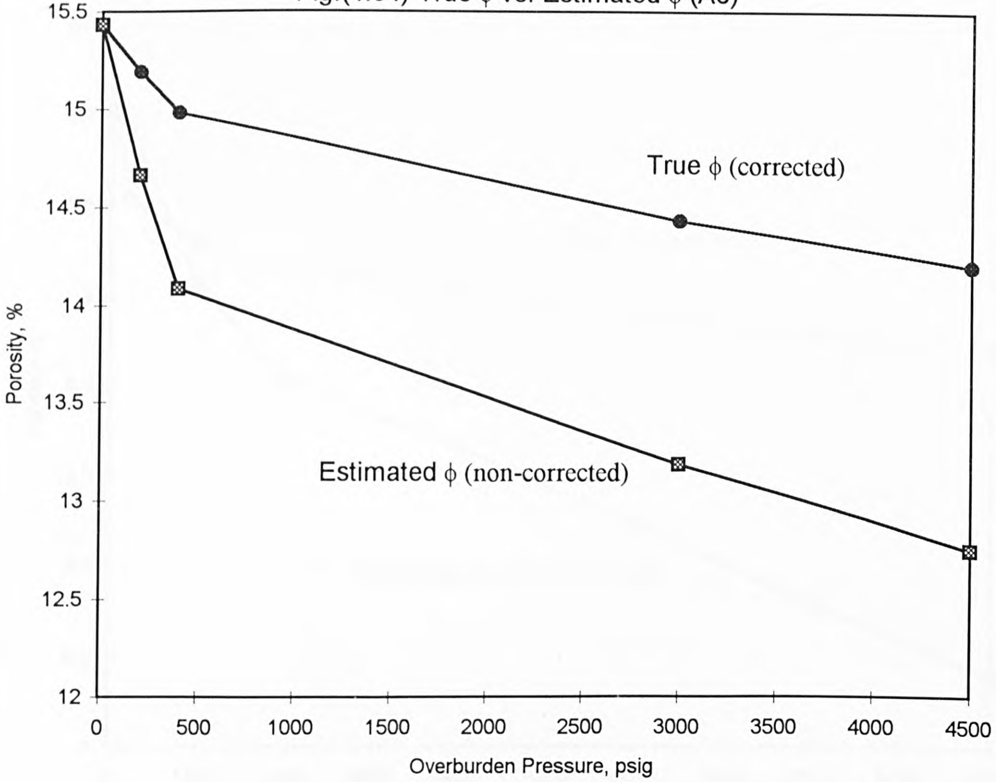

Fig.(4.35) True ϕ vs. Estimated ϕ (A10)

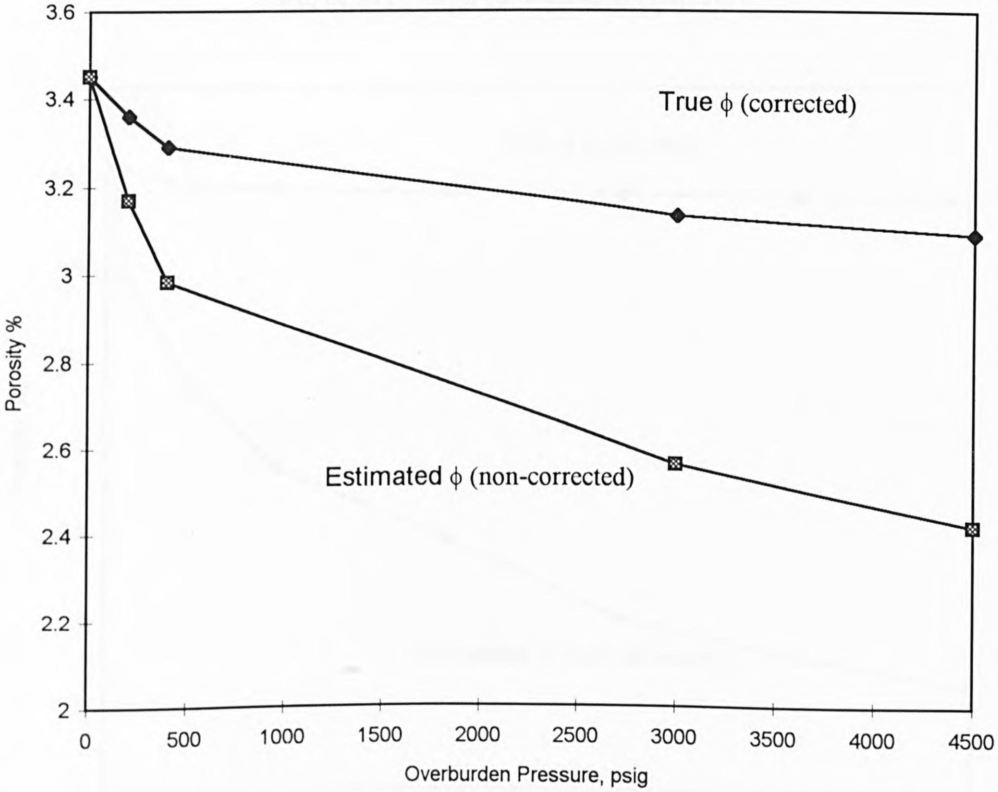

Fig.(4.36) True ϕ vs. Estimated ϕ (B1)

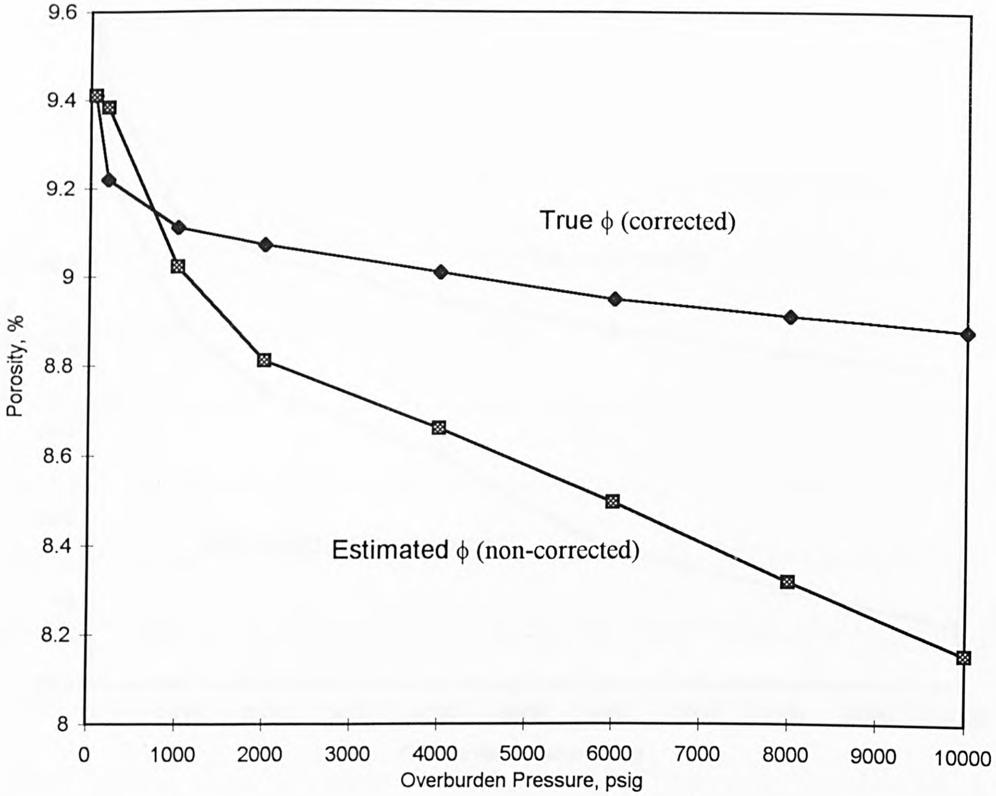

Fig.(4.37) True ϕ vs. Estimated ϕ (B2)

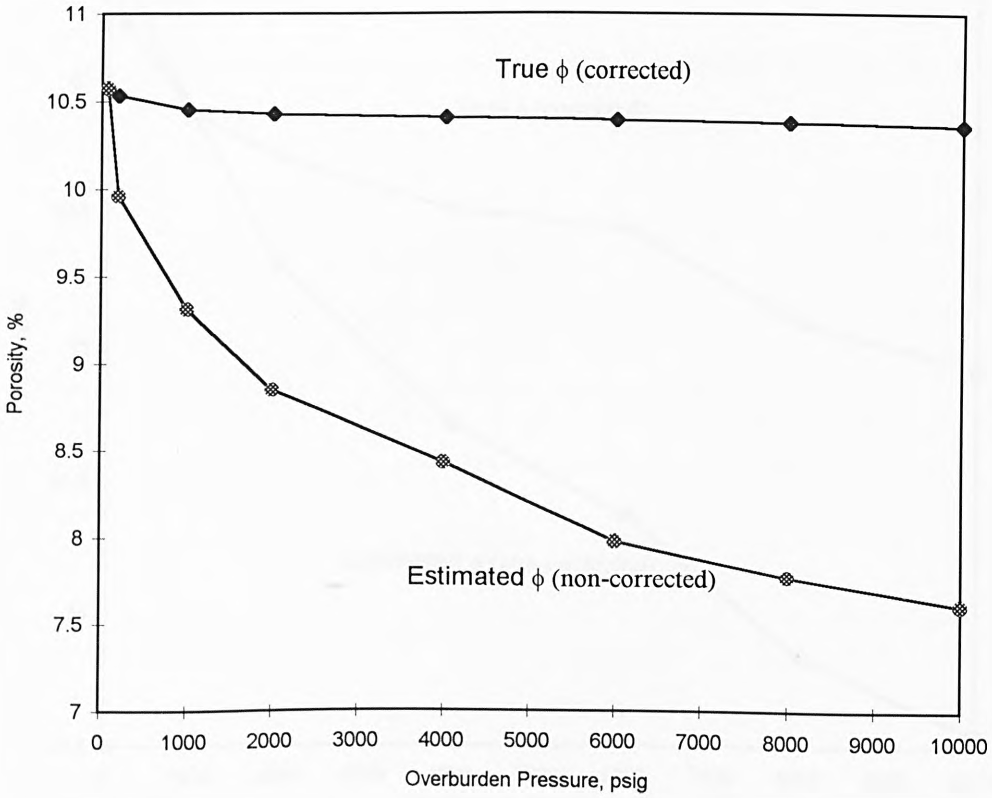

Fig. (4.38) True ϕ vs. Estimated ϕ (B7)

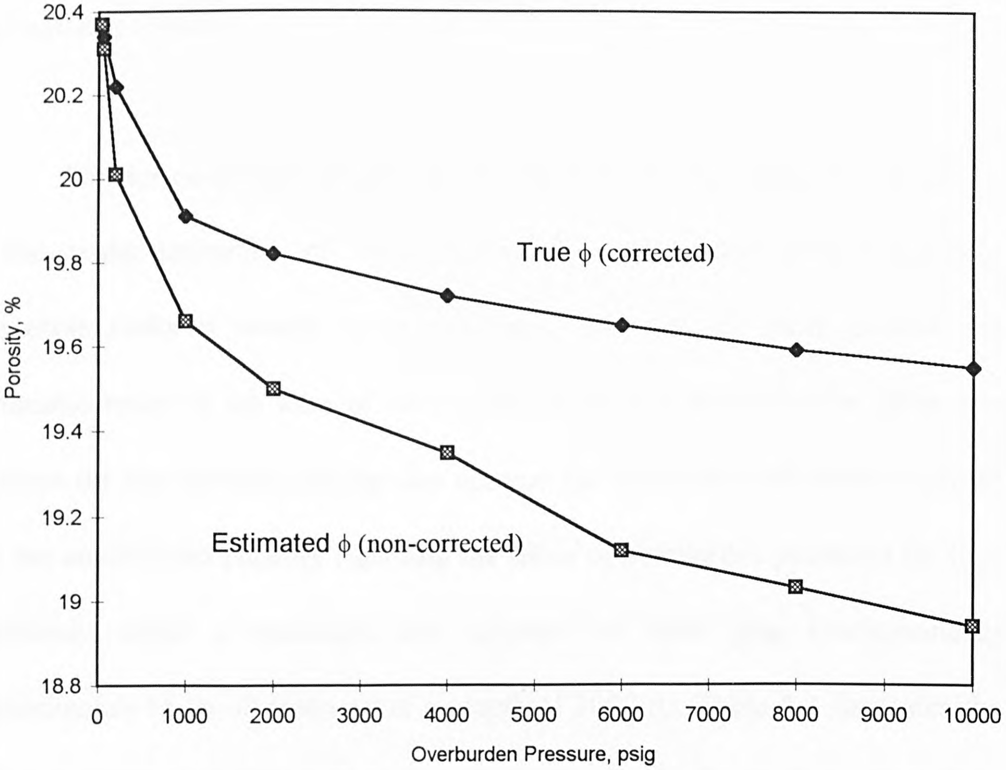

Fig.(4.39) True ϕ vs. Estimated ϕ (B12)

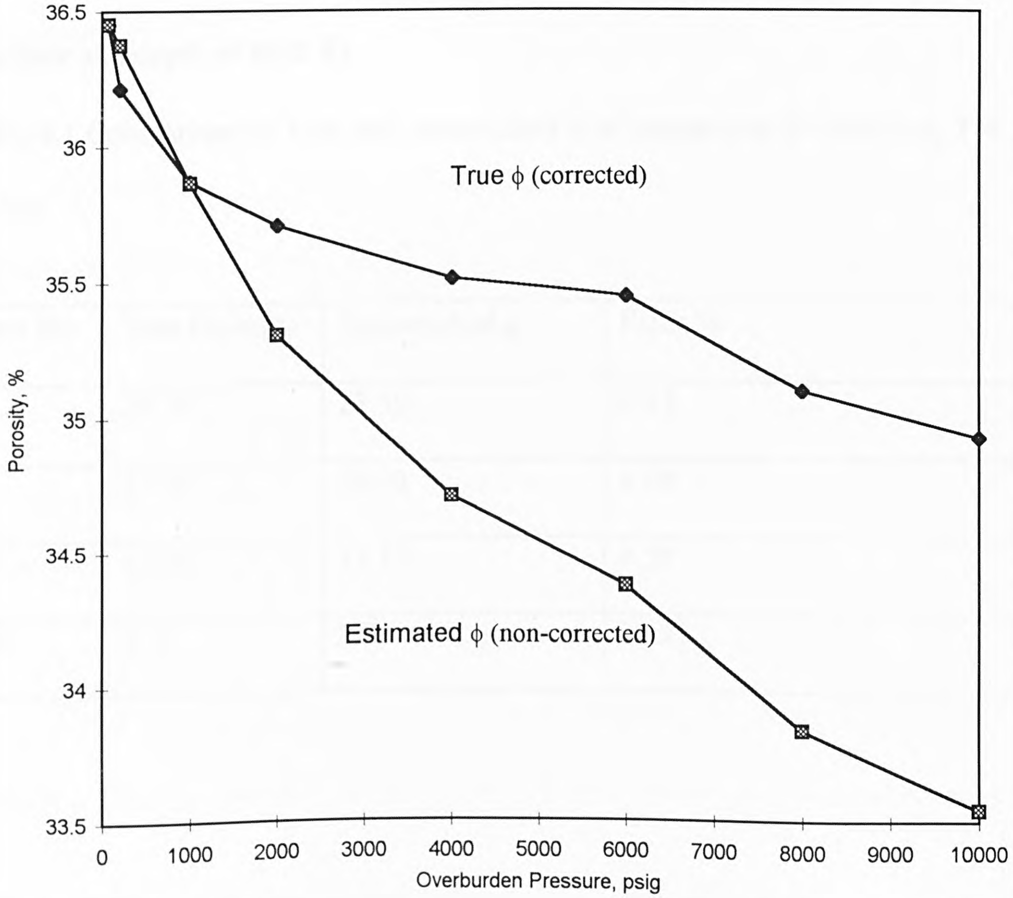

significant the difference between the real porosity and the uncorredted (estimated) porosity.

Another conclusion which may be drawn from these experimental results is that under-estimation of the porosity of relatively less porous and less permeable rocks is usually more significant than that for more porous and permeable rocks in the case of sandstones. Table 4.1 illustrates the difference between the true porosity (taking into account the effect of overburden pressure) and the uncorrected porosity (ignoring the effect of overburden pressure) for four sandstones under a maximum test pressure of 3000 psig (corresponding approximately to an oil reservoir at a depth of 3000 ft). Table 4.2 illustrates the difference between the true and uncorrected porosities for four carbonates under a maximum test pressure of 4000 psig (corresponding approximately to an oil reservoir at a depth of 4000 ft).

Table 4.1 Comparison of True and uncorredted ϕ of Sandstones (P=3000 psi, T = 20 ^{0}C)

Core No.	True Porosity	Uncorredted ϕ	Error %
A1	28.79	27.59	4.17
A2	27.19	26.08	4.08
A6	14.43	13.19	8.59
A10	3.13	2.56	18.21

Table 4.2 Comparison of True and uncorredted ϕ of Carbonates (P=4000 psi, T = 20 ^{0}C)

Core No.	True Porosity	Uncorrected ϕ	Error %
B1	9.01	8.72	3.22
B2	10.41	8.48	18.54
B7	19.72	19.35	1.88
B12	35.51	34.7	2.28

As listed in Table 4.1, up to 18.21% under-estimation in the rock porosity resulted for sample A10, which is the least porous of the four samples listed. On the other hand only 4.08% error arises between the real and estimated porosity for sample A1 which is one of the most porous among the four samples listed. The results of other samples (A2 and A6) lie in between the above two extreme cases as predicted.

For carbonates, as listed in Table 4.2, up to 18.54% under-estimation in the rock porosity was observed for sample B2, which has a low porosity value, however, an error as low as 1.88% is obtained for sample B7 which is a more porous sample. The highly porous sample B12 has a relativelly higher error percentage in porosity (2.28%). The results of the other sample (B1) lie in between the two extreme cases.

There appears to be a general trend between the error in estimated porosity (Ignoring the effect of pressure) and the actual rock porosity (Taking pressure effect into account). This suggests that with more comprehensive experimental data some simple empirical correlations between the uncorredted porosity and the real *in situ* porosity could be derived to allow for the pressure effect without measuring each individual rock.

4.4 Conclusions

a. Significant increases in formation factor and cementation factor with overburden pressure were observed for the sandstone samples studied, while this increase was not significant for carbonate samples over some ranges of pressure. This is related to the the changes in pore shape and re-arregments of grains packing under the effect of pressure as well as due to types of minerals present and their response to the applied pressure. The changes in the electrical properties of these clay-free samples with pressure are attributed to the changes in porosity and pore constrictions caused by rock deformation.

b. A marked feature of the results is that the changes in F and *m* observed with increasing pressure are much greater for low porosity samples than for high porosity samples. The reasons for this have been discussed above in sections (4.21) and (4.22). The changes for high porosity samples will not in general lead to significant errors in water saturation calculations, since the changes in m and F are proportionally smaller for these samples.

c. Ignoring the effect of pressure on the Archie cementation factor during log calibration leads to errors of porosity estimation up to 18.21% for sandstones and up to 18.54% for carbonate samples tested. The effect of pressure on the error is found to be much more pronounced for the less porous samples.

d. The hysteresis occurring during the pressure experiments suggest that not only the reservoir pressure conditions but also the history of changes of pressure can influence the resistivity of rock samples.

e. Increases in resistivity formation factor and cementation factor (*m*) with overburden pressure were observed for the majority of carbonate samples, while decreases in F and *m* were noticed in some cases. It is important to note that processes such as dissolution, precipitation and cementation which affect the behaviour of *m* with pressure operate very slowly in comparison with the time scale of laboratory experiments. Hence the laboratory samples do not have time to reach equilibrium with respect to these processes and behaviour may differ from that of *in situ* rocks. The changes in electrical properties of carbonates could not be correlated with the porosity and permeability of the samples. However, the change in F is more pronounced at low pressures than higher ones. Generally the changes in F and *m* for the carbonates tested in this work are less significant than for tested sandstones.

CHAPTER 5

EFFECT OF EXPERIMENTAL CONDITIONS ON SATURATION EXPONENT

5.1 Introduction

Electrical resistivity is used to estimate the water saturation in hydrocarbon reservoirs and so to evaluate the initial oil/gas in place. For clean rocks (where electrical conduction is only due to the ions in the brine) the interpretation methods are based on Archie's equation

$$S_w = (\phi^{-m} R_w / R_t)^{1/n} . \qquad 5.1$$

The saturation exponent *n* is determined in the laboratory for core samples initially saturated with brine which is displaced by another phase (gas or oil), and the resistivity is measured during the desaturation process. The electrical resistivity of fluid-saturated rocks depends on many factors such as rock composition and structure, degree of saturation of each phase, applied stress, temperature. Within the porous medium, the displacement of one fluid by another is a complex process. The desaturation process can be either drainage (decrease in the wetting phase saturation) or imbibition (decrease in the nonwetting phase saturation). However in the present research only the drainage process is considered. When desaturation occurs, the flow mechanism affects the fluid distribution within the porous medium, and so influences the electrical resistivity, and also the form of the resistivity-saturation relationship. This is due to the fact that the electrical resistivity depends not only on brine saturation but also on the fluid distribution which is controlled by capillary and viscous forces (Grattoni and Dawe 1996). However this chapter describes novel studies examining the effect of the flow displacement mechanism (injection rate) and fluids characteristics (viscosity ratio) on resistivity index versus water saturation relationships. In principle, Archie's equation assumes that whatever fluids characteristics and flow displacement are used, a fixed value of saturation should give the same value of resistivity (i.e., the saturation exponent is independent of these factors) because S_w and R_t are only the variables in the equation.

The effect of factors such as wettability, pore structure, pore size distribution, stress, temperature, etc. have been investigated extensively (Elashahab *et al.,* 1993, Morrow 1990, Lewis *et al.,* 1988a, Longeron *et al.,* 1986 & 89, Koerperich 1975, Wei and Lile 1992), but the influence of the experimental conditions (such as the brine and oil physical properties, the interfacial tension between the phases and the rate of phase displacement in the desaturation process) has received much less attention in the past, probably on account of the time and cost involved in such experimental studies.

5.2 General Background

Archie's equation makes the important assumption that the fluids saturating the core sample are distributed uniformly; on this basis the equation implies that the saturation exponent is constant over the entire saturation range.

Ten clay-free samples (carbonate plugs with different porosity types collected from Sirte Basin, Libya) were used to study resistivity changes under different experimental conditions. Four of these samples were used to examine the effect of injection rate, while the other six were used to study the effect of the viscosity ratio. The petrophysical properties (including pore volume (PV), diameter (d) and length (L)) of these sample are shown in Table 5.1.

Table 5.1 Petrophysical properties of the tested samples

Sample No.	ϕ (%)	k (mD)*	P.V. (cm^3)	d (cm)	L (cm)
C1	34.5	25.1	15.475	3.801	3.97
C2	17.7	8.5	9.184	3.804	4.63
C3	33.1	23.2	18.81	3.795	5.05
C4	15.1	2.4	9.21	3.784	5.433
D1	11.61	2.1	7.67	3.73	4.5
D2	18.50	3.1	8.86	3.81	4.02
D3	15.21	1.9	7.12	3.815	4.27
D4	16.30	1.2	6.81	3.72	4
D5	32.60	66	20.86	3.815	4.18
D6	16.13	8.0	7.51	3.808	4.92

* Confining pressure = 400 psi
* Mean pressure = 1 - 1.2 atm

In this research the resistivity index measurements were carried out at high and low viscosity ratios as well as at high and low injection rates. The continuous injection technique used is believed to be powerful and accurate and has the advantage that it provides continuous I_R/S_w curves rather than a limited number of points (de Wall *et al.*, 1991). In this technique, the brine is usually continuously displaced by oil at both fixed rate and at fixed viscosity ratio and under effective reservoir stress.

The selection of the experimental conditions, including the injection rate of the displacing phase and the viscosity ratio of the brine and the oil may have an important influence on the non-linearity of the I_R/S_w relationship; this has been encountered in many studies (Jing *et al.*, 1993b, Lyle and Mills 1989, de Wall *et al.*, 1991). The laboratory evaluation of the saturation exponent can result in large errors in hydrocarbon calculations as described by de Wall *et al.*, 1991. In order to apply Archie's equation, a uniform saturation distribution should be achieved along the core samples and the I_R/S_w curves obtained should represent steady-state conditions. However, if unsuitable experimental conditions are used to measure resistivity index a nonuniform distribution may prevail and invalid I_R/S_w curves will be produced, hence erroneous values of the saturation exponent will be obtained.

According to Archie's equation (5.1) the resistivity index should be independent of the method used to achieve the different saturation conditions and therefore several different experimental methods can be used to obtain the saturation exponent, for example the porous plate method, the continuous injection technique, evaporation, etc. Most of the previous workers in both experimental and theoretical investigations have demonstrated that the real situation is more complicated than that assumed by Archie's equation.

Moreover, according to Archie's equation (5.1) the value of rock resistivity will only change when different oil-water proportions develop within the porous media (Grattoni and Dawe 1996). The resistivity will also vary with the fluid distribution and will be related in some way to aspects such as pore structure, wettability and fluid characteristics which are not considered in Archie's equation. Some of these aspects are considered in this chapter. As pointed out before, the electrical resistivity is affected by the brine saturation but also depends on the distribution of the fluids within the porous medium, which is controlled by capillary, gravitational and viscous forces as the fluids move through reservoir.

During reservoir formation, oil migrates from the source rock through permeable and water filled strata, so oil is always associated with water in different proportions and properties in the reservoir. The appropriate fluid distribution that represents the reservoir conditions and hydrocarbon production process should be reproduced for realistic laboratory resistivity experiments, and these experiments should be conducted using appropriate fluid characteristics which represent those existing in the reservoir. The results of the experiments on the effects of fluid properties and flow rate are analysed and finally, the implications for core experiments are discussed.

5.3 Flow Mechanism and Fluid Characteristics

The objectives of the work reported in this chapter were to carry out an investigation of the effects of fluids displacement on electrical resistivity and therefore on resistivity-saturation relationships, and also to identify any additional variables that influence the electrical resistivity. The electric current is transported by the ions in the water so the water distribution will influence the resistivity and this will affect the I_R/S_w relationships. To develop this argument an experimental investigation was carried out in order to study the effect of phase distribution caused by different displacement process and different fluids characteristics.

However, an analysis of the resistivity-saturation relationship and how it behaves in terms of uniformity/nonuniformity is affected by viscosity, and fluid velocity in the drainage process can indicate the way in which laboratory resistivity experiments should be conducted, especially in generating fluid distributions to represent actual reservoir conditions.

When the flow displacement starts the nonwetting phase displaces the wetting phase, setting up a front which can be described as series of heads and neck menisci (Figure 5.1, Hawes *et al.*, 1996). The fluids physical properties and the pore structure affect the shape of the displacing front (transition zone) which in turn modifies the fluid distribution behind it, and hence influences the resistivity value and I_R/S_w relationships.

An oil reservoir can contain up to three fluids (oil, water and gas) saturating a porous solid phase. The fluids, if immiscible, are separated by interfaces. The properties of these interfaces are important in understanding the

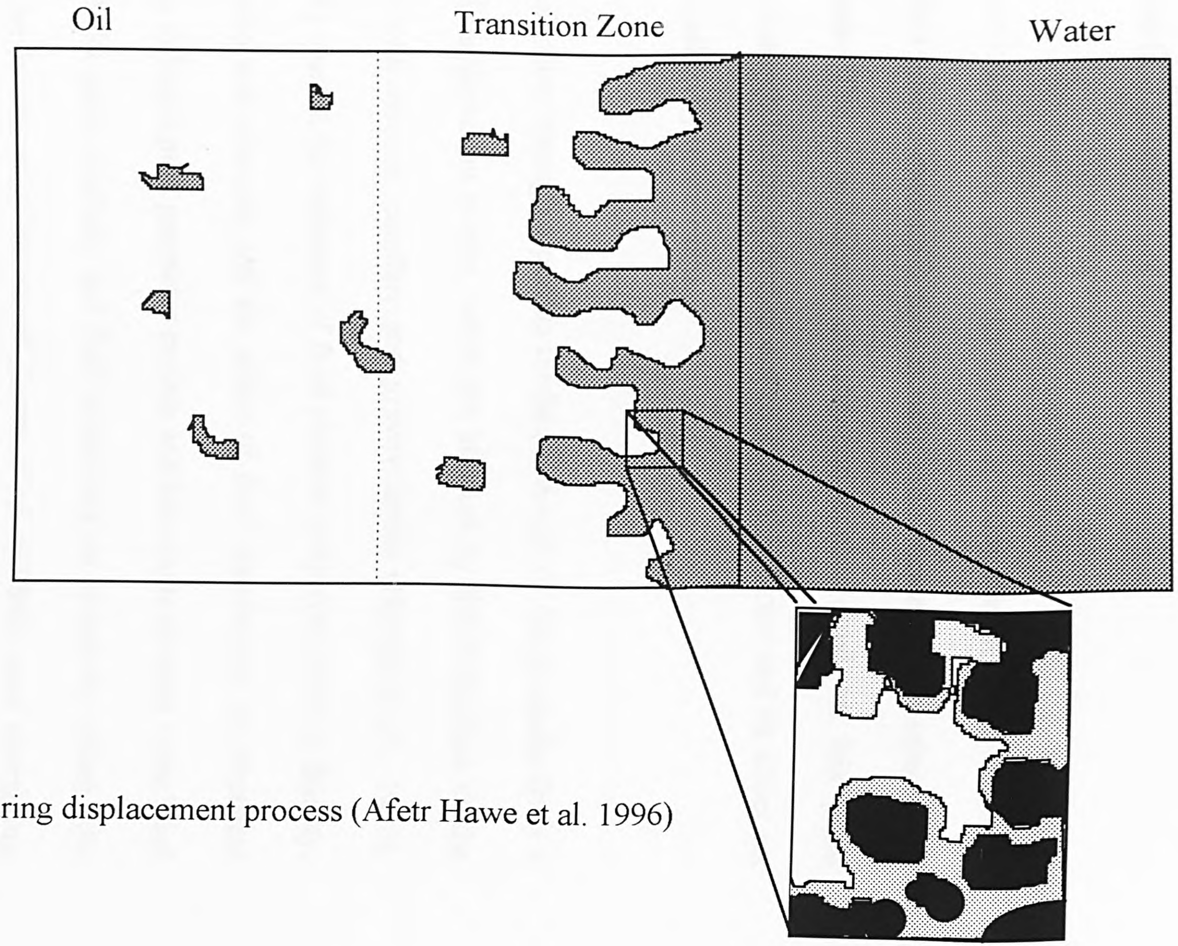

Fig.(5.1) Flow zones during displacement process (Afetr Hawe et al. 1996) resistivity of fluid saturated porous media. The physical properties of the fluids (interfacial tension, viscosity, density) and pore characteristics (pore structure, wettability, pore size distribution, etc.) are the main factors influencing the behaviour of the whole system, especially its resistivity. The three forces involved in the movement and interaction of the fluid phases are (1) capillary force, (2) viscous force and (3) gravity.

As mentioned before, one of the factors affecting the electrical resistivity of the fluid-filled porous medium is the viscosity ratio between the displaced and displacing fluids. The experimental investigation concentrated on this point because little research has been carried out to study this factor and its effect on the saturation-resistivity relationship.

The fluid flow through a porous media (reservoir or core) results from a series of small displacement events, which are affected by the interaction of the pore structure with viscous, capillary and gravity forces (Hawes *et al.,* 1996). Grattoni (1995) studied the influence of fluid physical properties such as density, interfacial tension and viscosity and the effect of fluid distribution on electrical resistivity using different pore geometry models and his results showed some level of influence of the pore structure and fluid properties on resistivity taking into consideration the limitations of the model. Lewis *et al.,* (1986b) used alternating high and low flow rates of the displacing phase and showed the difficulties in achieving uniform distribution.

5.31 Effect of injection rate

5.311 Review

A number of different techniques can be used to measure the electrical resistivity of rocks partially saturated with brine. The porous plate method, the centrifuge method and the continuous injection method are the techniques currently used in the oil industry. Of these, the most recently developed technique is continuous injection, which is powerful, accurate and rapid, and provides a continuous curve of I_R versus S_w. In this technique oil is injected at a constant rate and a fixed viscosity ratio to displace brine. It has the advantage that experimental error can be minimised by automation of the measurement procedure and measurements can be performed at effective reservoir stress.

Maerefat *et al.*, (1990) used the porous plate method to obtain uniform desaturation and a uniform I_R versus S_w relation, and showed that it is essential to allow sufficient time to ensure homogeneous saturation. It is believed that at capillary and electrical equilibrium a uniform saturation distribution can be achieved with the porous plate technique, but small scale permeability heterogeneity can cause non-linearity even after this equilibrium is achieved (Jing *et al.*, 1993b). Lewis et al., (1986b) used the continuous injection technique, initially with low injection rates to minimise fingering, then changed to high rates to minimise capillary end effects; they also recommended the use of the 4-electrode system which is not affected by contact resistance. They tested high porosity and high permeability samples, and concluded that capillary end effects and viscous fingering cause the non-linearity of the I_R versus S_w relationship.

The nonlinearity commonly observed in I_R versus S_w plots may be due to (1) static causes (a vertical, high permeability sample) or (2) dynamic causes (when oil invasion takes place at an end face, the oil saturation profile shows a front moving toward the outlet during the first capillary pressure step (Argaud *et al.*, 1989). de Wall *et al.*, (1991) injected oil into high porosity, high permeability samples at the rate of 1 PV/day and noted that a uniform saturation distribution (constant *n*) was only achieved when S_w fell below 40%. They concluded that the high injection rate and the difference in permeability between the samples and the semipermeable membrane were the causes of the nonlinearity of the I_R versus S_w relationship observed over most of the S_w range. Sprunt et al. (1991) used X-ray CT scans to monitor saturation distribution along their core samples. They varied the capillary pressure (but not the injection rate) and showed that there were problems in achieving homogeneous saturation during resistivity index tests for the two high porosity and high permeability grainstone samples desaturated at constant oil/brine capillary pressure. They concluded that a uniform relation of I_R versus S_w was not obtained because of the created front. Gray et al. (1992) measured resistivity for sandstone samples at a low constant injection rate (0.02 cc/hr), selected so that an insignificant pressure drop existed over the sample throughout the desaturation process. However, a linear I_R versus S_w plot was not achieved except for S_w values less than 45%. Elashahab et al. (1993) used a multiple potential electrode system for resistivity measurement to enable assessment of the saturation distribution and end effects. Jing *et al.*, (1993b) measured resistivity for sandstone samples using a relatively high constant injection rate (0.25 cc/hr) and used X-ray CT scans to monitor the saturation distribution. A linear I_R versus S_w relation was obtained for these samples at $S_w <$ 55%.

However, Lyle and Mills (1989) had previously shown theoretically that the laboratory-derived Archie saturation exponent may differ from the actual reservoir value, and concluded that whenever the core is other than uniformly saturated, the I_R versus S_w log-log plot will exhibit curvature.

On the basis of the work reviewed above the following criteria were chosen for injection rates in the present study. Very high injection rates were avoided as they may cause channelling , and give rise to a significant pressure drop over the sample. Very low injection rates were avoided to prevent significant saturation changes with time in the sample and also to overcome fingering. Four carbonate samples, 1.5" in diameter and 3" long, covering a wide range of porosity and permeability were selected to study the effect of injection rates on the I_R versus S_w relationship. Resistivity index measurements by the continuous injection technique were carried out on these samples at different injection rates.

5.312 Injection Rate Experiments

Low and high oil injection rate experiments were carried out on the selected carbonate samples and the rates chosen were respectively 0.03 cc/hr and 0.15 cc/hr. Fig. 5.2 shows the layout of the apparatus used. The direction of flow injection was selected to be downwards in order to make the flood less stable and so more sensitive to the factors affecting the fluid distribution. Fig. 5.3 illustrates the multiple electrode system used. The samples, fully saturated with

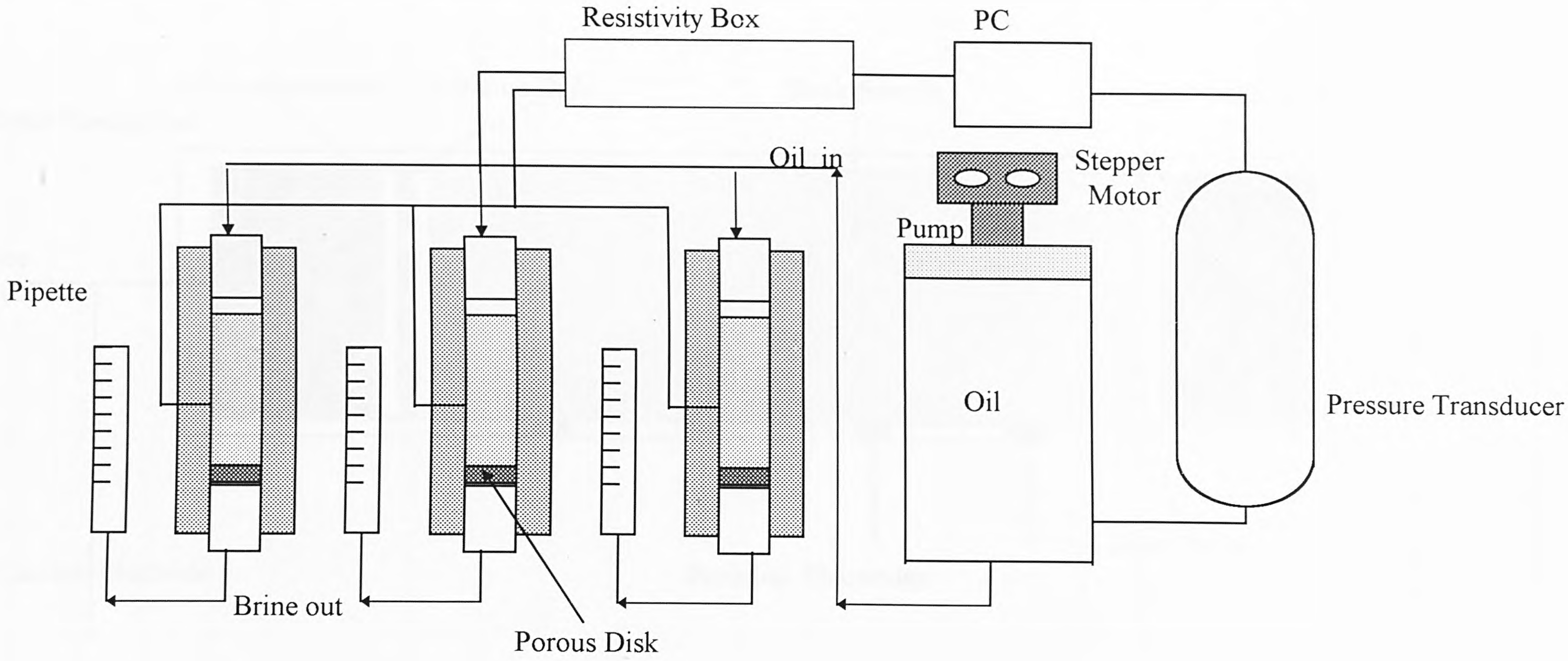

Fig. (5.2) Layout of contiuous injection technique appartus (Core Lab. 1997)

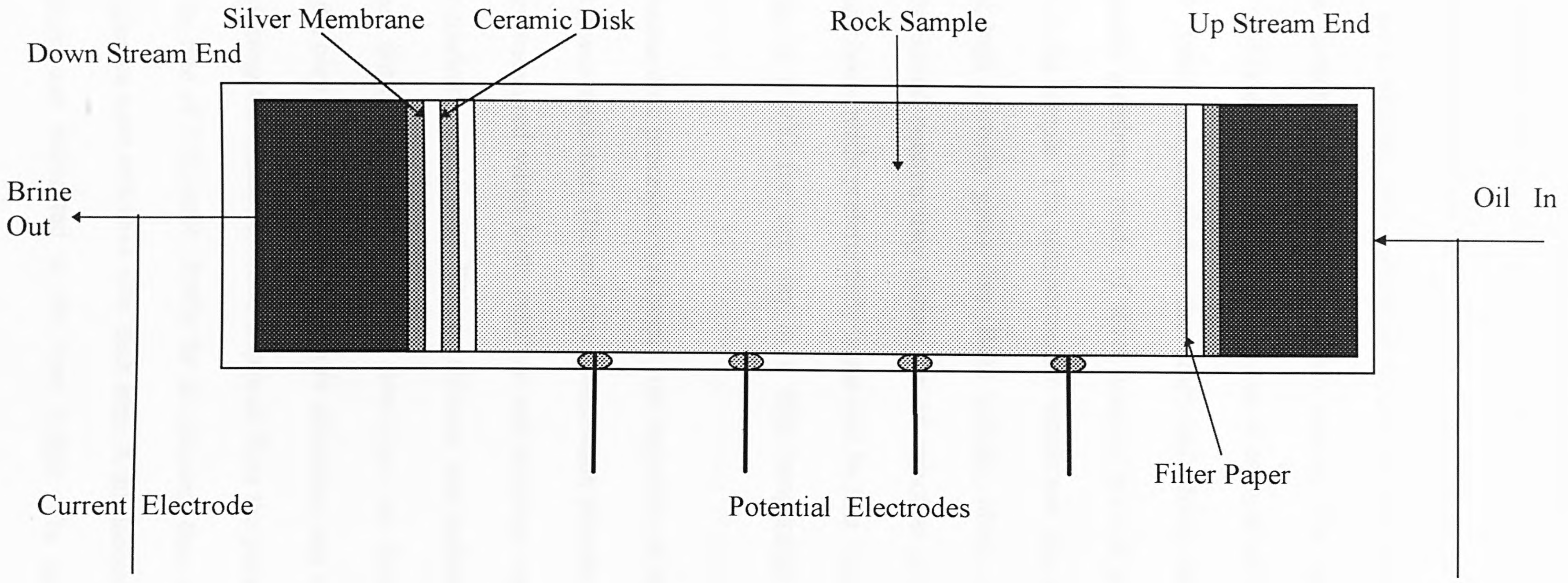

Fig. (5.3) Schematic diagram of multiple electrodes (Continuous Injection Technique) brine of concentration 100 g/l of NaCl, were mounted in a multiple core holder made of aluminium and subjected to an initial confining pressure of 400 psi, which was subsequently increased to 3000 psi before the injection process started.

The sample pore volume was calculated based on the brine volume collected in pipettes attached to the outlet of each sample. The system was allowed to come to equilibrium and oil was then injected at one end of the sample (upstream end) and brine was expelled at the other end (down-stream end) through a semipermeable membrane made of silver, used to prevent passage of the oil at the outlet of the sample. The semipermeable membrane was supported on a brine-saturated high porosity glass disc. Both voltage, phase angle and temperature were monitored continuously during the oil injection process. All samples had previously been made preferentially water-wet by first cleaning with methanol, then firing to 600°C for one day in a high temperature furnace (Morrow, 1990).

Before the desaturation processes was begun, the resistivity of fully brine-saturated samples (R_o) was measured. The oil/brine desaturation process was then started and resistivity measured when both capillary and electrical equilibrium were reached at the confining stress used. This equilibrium was indicated when there was no further change in resistance with time (i.e., no further fluid redistribution along the core length). The average core saturation was calculated volumetrically by deducting the volume of brine displaced from the pore volume. Oil was injected at the rate of 0.03 cc/hr firstly for all samples, then at rate of 0.15 cc/hr, and the samples were recleaned after each step. A displacement pump equipped with a piston was connected to the core holder. The amount of displaced fluid was measured by a calibrated potentiometer connected to the pump piston. The pump was regularly calibrated for the experimental conditions. The samples were subjected to the re-cleaning process to remove oil contamination and to keep them in water-wet condition throughout the experiment. The resistance of the samples was measured at 1 kHz, to minimise polarisation effects (Zeelenberg and Schipper, 1992) and also to minimise any surface conduction contribution (Glover *et al.*, 1996). The resistivity values were corrected for slight temperature variations by using Arps' equation (Arps, 1953).

To begin the continuous injection process, the displacement pump starts to inject the oil into the core holder then into the sample to displace the brine. Initially this was performed at a low rate (0.03 cm^3/hr). This low rate was selected such that an amount of oil corresponding to the pore volumes of samples 1, 2, 3 and 4 will be injected in approximately 22, 13, 26, and 13 days respectively, and for the high rate (0.15 cm^3/hr) the pore volumes of the samples will be injected at 5, 3, 6, and 3 days respectively. The injection of oil was stopped for each sample individually after the given time or when no more brine expelled from the sample. The samples were then cleaned and resaturated (results are shown in Appendix C1).

5.3121 Experimental Results and Observations

The four samples tested gave results as follows (the viscosity ratio being maintained constant):

Sample C1:

This sample has high porosity (34.5%) and permeability (25.1mD). The difference between the I_R/S_w curves at high and low rates is very obvious (Fig. 5.4a), where the percentage difference in *n* between the high and low flow rates reaches about 55% (taking into account the late uniform part of the low rate injection curve). It is observed for this sample that the high injection rate produces a more linear relationship between I_R and S_w. The I_R/S_w relationship for the low rate shows marked curvature. The linear portion of the I_R/S_w curve for the high rate case is longer than the one for the low rate case. The uniform relation for the case of the high flow rate starts as early as $S_w < 82\%$. However, in the very late stages of the desaturation process for the low rate case, the resistivity changes become less, and this can be related to the desaturation of the porous membrane which used in the continuous injection technique. The greater uniformity of the I_R/S_w relationship for the high rate can be attributed to the fact that the high injection rate overcomes the fingering and capillary end effect problems. The pore size distribution which is indicated by capillary pressure and pore size distribution curves (Fig. 5.4b,c) is uni-modal, which usually gives a uniform I_R/S_w relationship.

Sample C2:

This sample has medium porosity (17.7%) and permeability (8.5 mD). It can be observed that the I_R/S_w curves are different for the high and low rates (Fig. 5.5a). Generally, the two cases show good uniformity of the relationship over most of the saturation range. Despite this uniformity, the difference in *n* reaches about 30%. As for the previous sample, the more uniform I_R/S_w relation is obtained for the high injection rate over much of the saturation range ($S_w < 75\%$). The variation in n along the I_R/S_w plots is less obvious than for the other curves.

Fig.(5.4a) I_R vs. S_w for sample C1 at different rates

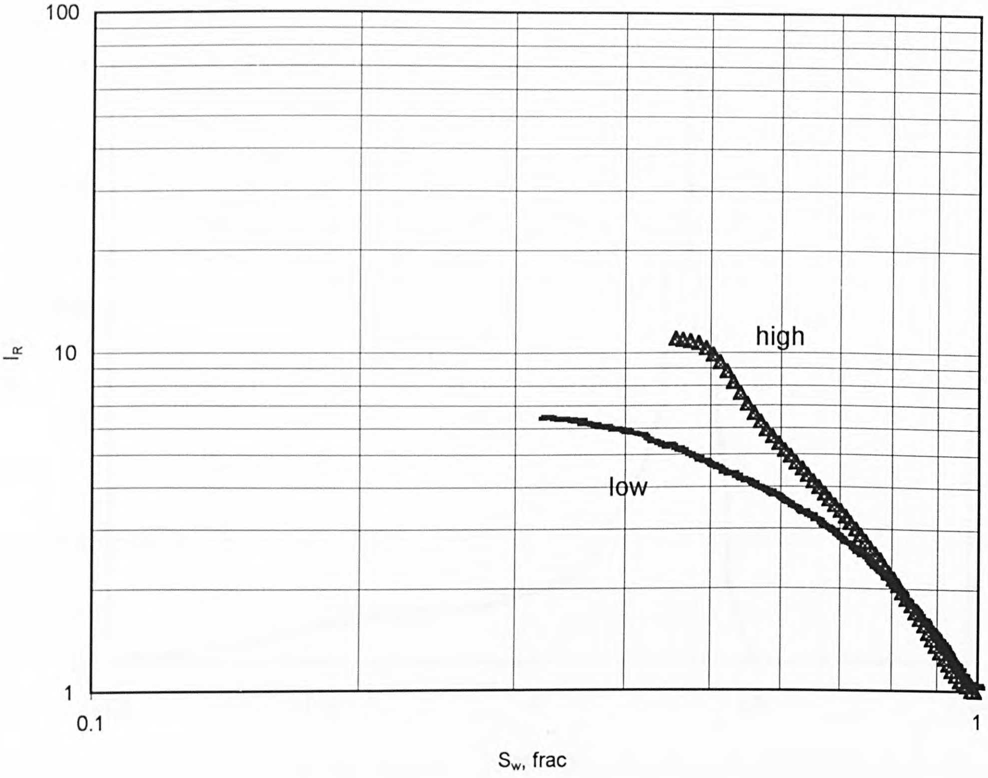

Fig.(5.4b) S_w vs. P_c for sample C1

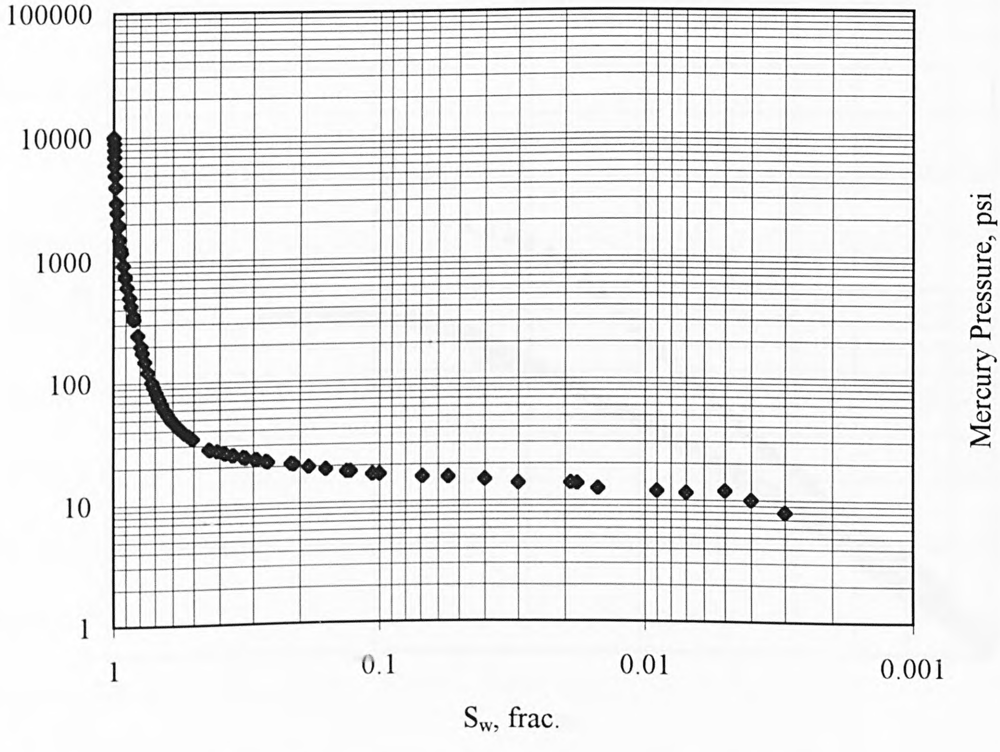

Fig.(5.4c) Pore throat radius vs. Pore distribution for sample C1

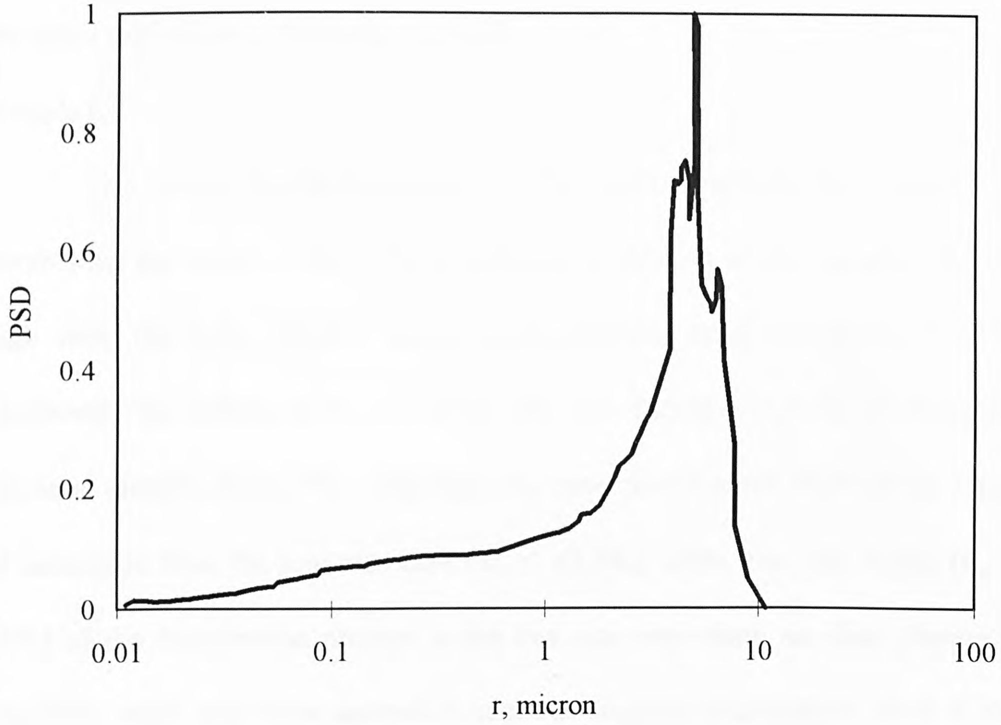

Fig.(5.5a) I_R vs. S_w for sample C2 at differenr rates

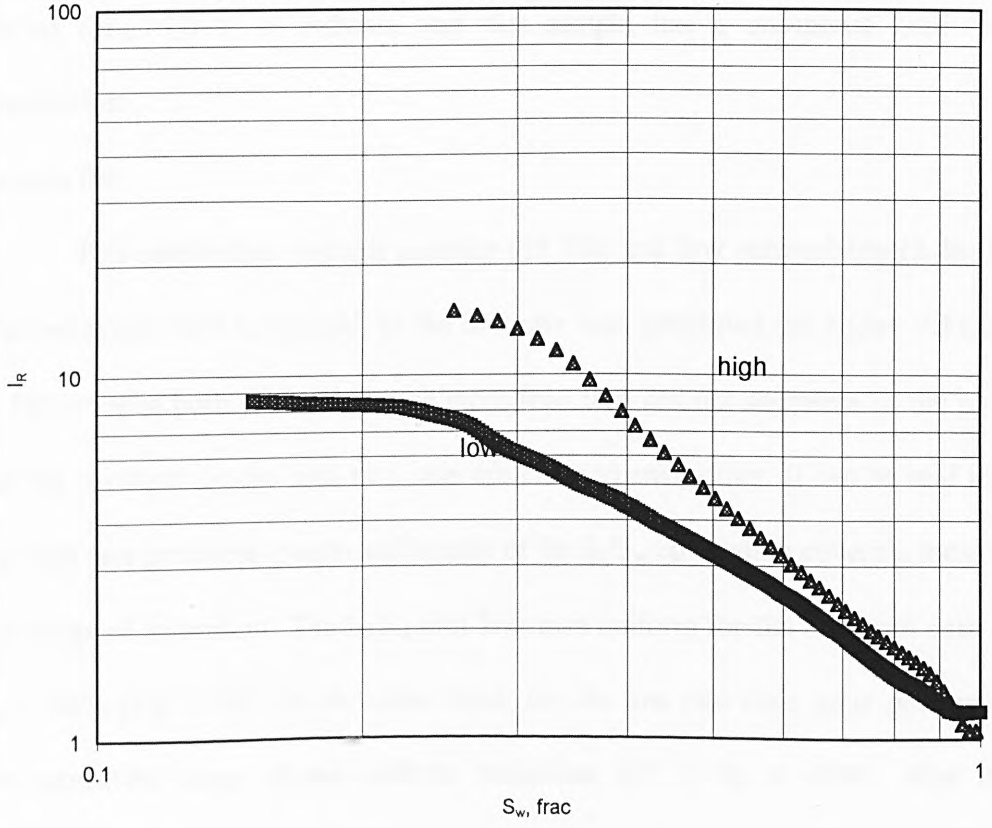

Fig. 5.5 b and c showing capillary pressure curves and pore size distribution indicate clearly that this sample has a uni-modal distribution which is reflected in the good uniformity in the I_R/S_w relationship.

Sample C3:

This sample has high porosity (33.1%) and permeability (23.2 mD). The continuous curvature of the I_R/S_w correlation is obvious in this sample. At the high rate, the I_R/S_w relation seems more uniform, especially at $S_w < 65\%$. Moreover, the difference in *n* between the two curves is not as much as for previous samples, being 8% . The high rate case covers much more of the range of saturation than the low rate case ($S_w < 62.5\%$). Also, the late stages ($S_w < 35\%$) of the desaturation process in the low rate case show no clear change in resistivity index with brine saturation, and this suggests instrumental error at the low saturation value (Fig. 5.6 a). The capillary pressure and pore size distribution curves (Fig. 5.6 b, c) indicate that this sample has a uni-modal pore size distribution.

Sample C4:

This sample has medium porosity (15.1%) and low permeability (2.4mD). The behaviour here is unusual, as the low rate case generated the higher value of *n*. However in both cases, there are more than two distinct segments to the plot, but the *n* values for the high rate case are close to each other. It can be said that the high rate produces greater uniformity of the I_R/S_w correlation covering most of the range of saturation. The I_R/S_w plot becomes uniform for the high rate case at $S_w < 88\%$ (Fig. 5.7a). On the other hand, for the low rate case some portion of the saturation range shows uniform behaviour ($35 < S_w < 65$)%. Also the

Fig.(5.5b) S_w vs. P_c for sample C2

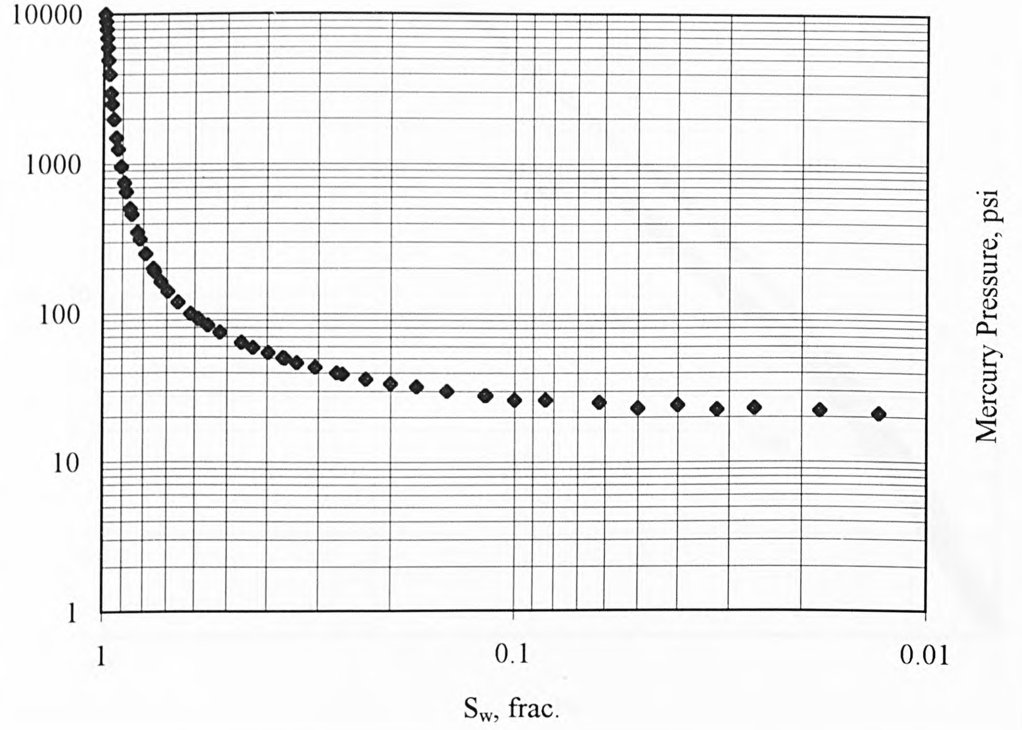

Fig.(5.5c) Pore throat radius vs. Distribution function for sample C2

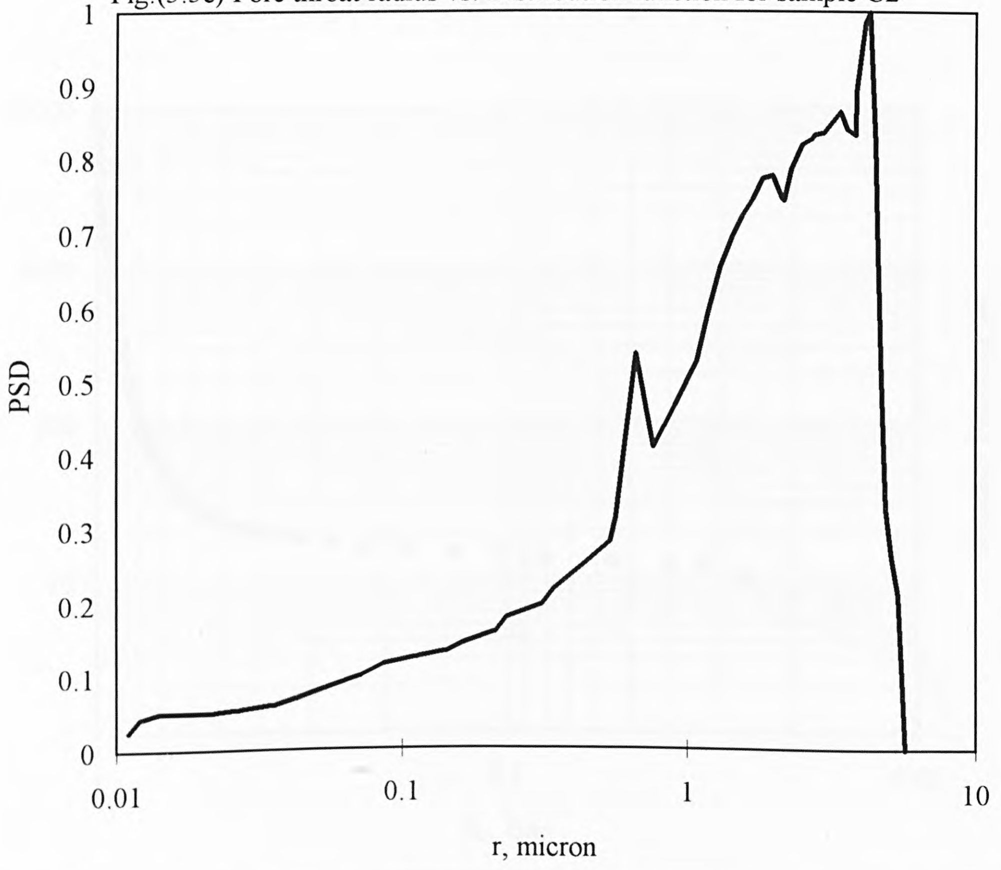

Fig.(5.6a) I_R vs. S_w for sample C3 at different rates

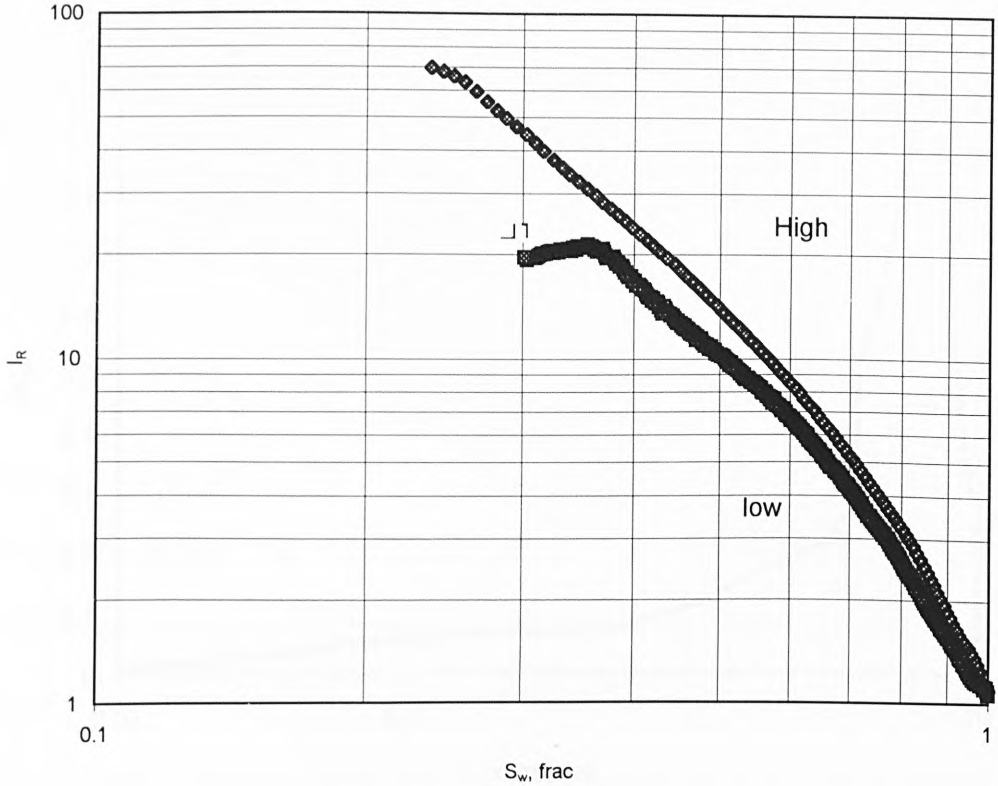

Fig.(5.6b) S_w vs. Pc for sample C3

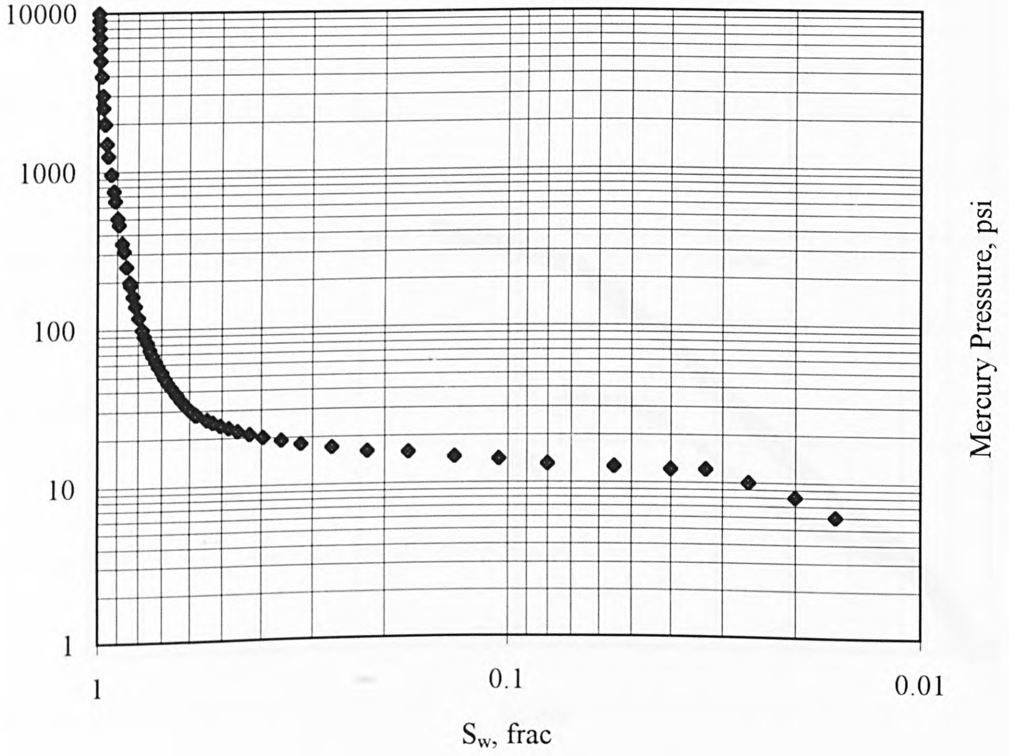

Fig.(5.6c) Pore throat radius vs. Distribution function for C3

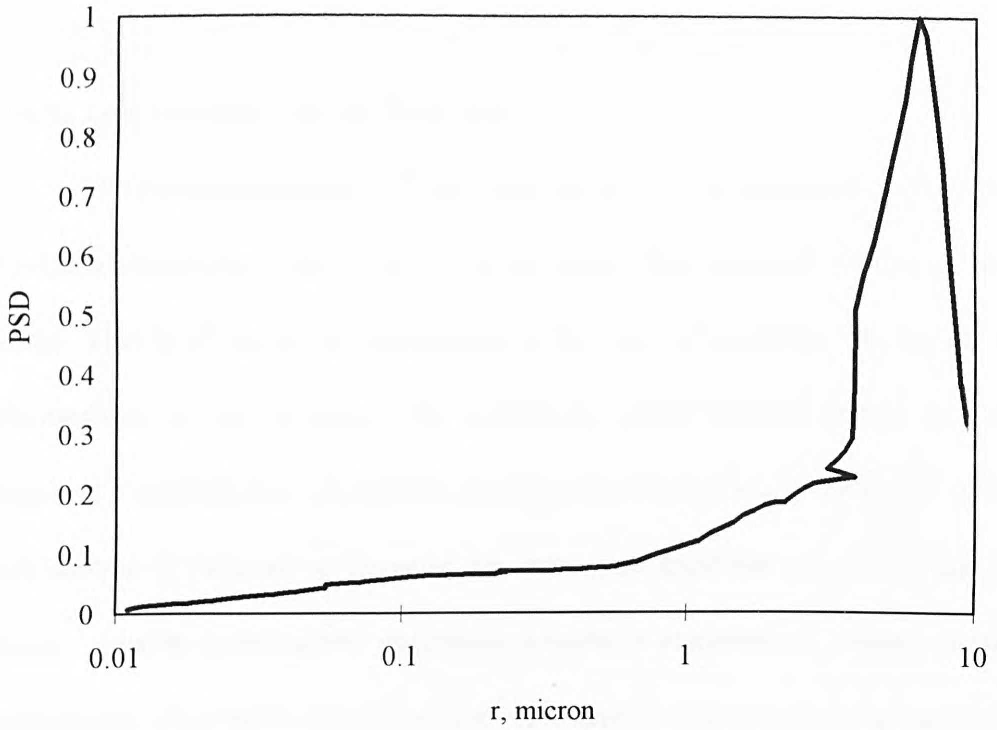

Fig.(5.7a) I_R vs. S_w for sample C4 at different rates

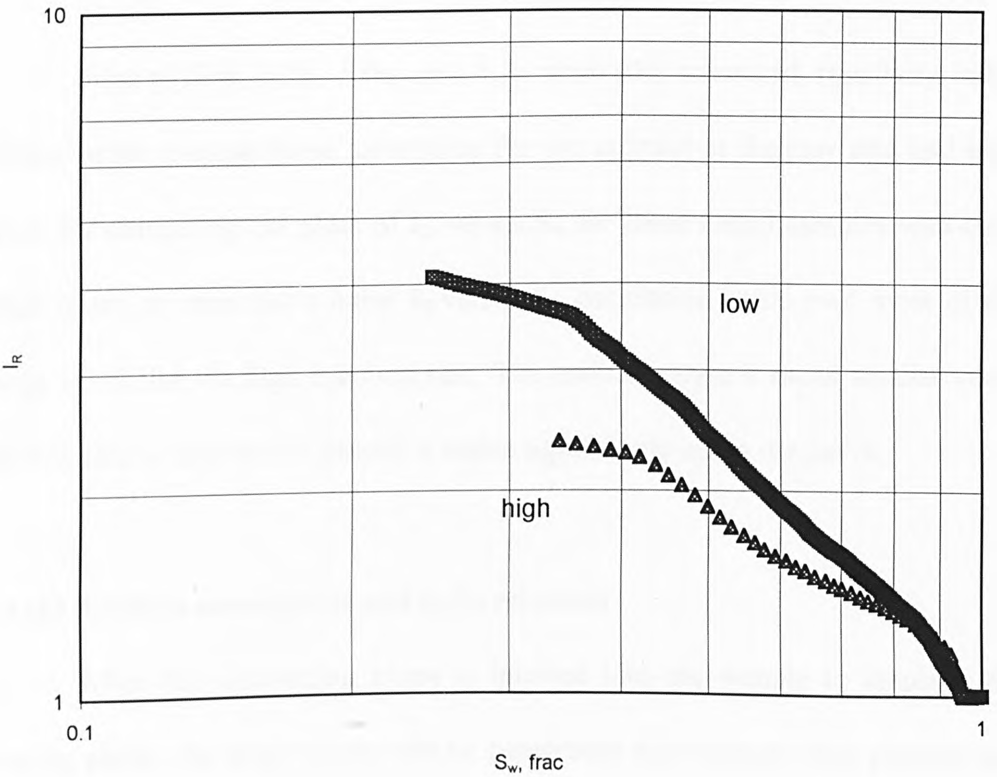

difference in n is marked. The capillary pressure curve is shown in Fig. 5.7 b, and the pore size distribution (Fig. 5.7 c) curve indicates that this sample is bi-modal.

5.3122 Low injection rate vs. High rate

The principal advantage of the continuous injection technique is that it can provide a continuous curve of I_R versus S_w rather than a limited number of data points. This is of particular importance in the case of nonlinear I_R versus S_w relationships. In this technique, the nonwetting phase (oil) is injected into the sample at a constant rate. A uniform saturation distribution along the length of the core sample is required to measure the saturation exponent accurately and so obtain reliable hydrocarbon evaluation (Archie's assumption). Based on the experimental observation mentioned above, it appears that a uniform I_R versus S_w relationship can be obtained by using the high injection rates.

Figures 5.4a, 5.5a, 5.6a, and 5.7a show the measured resistivity index values versus average brine saturations for the samples at the low rate and high rates. By comparing the plots of I_R versus S_w for these tested samples with each other it can be seen that a linear I_R versus S_w correlation holds over most of the range of S_w for the high injection rate. The uniform range is much smaller when the low rate is used and in general n varies significantly along the curve.

5.3123 Archie's assumption and I_R/S_w relations

When the nonwetting phase is injected into the sample to displace the wetting phase, the larger pores will be penetrated first because they present less

Fig.(5.7b) S_w vs. P_c for sample C4

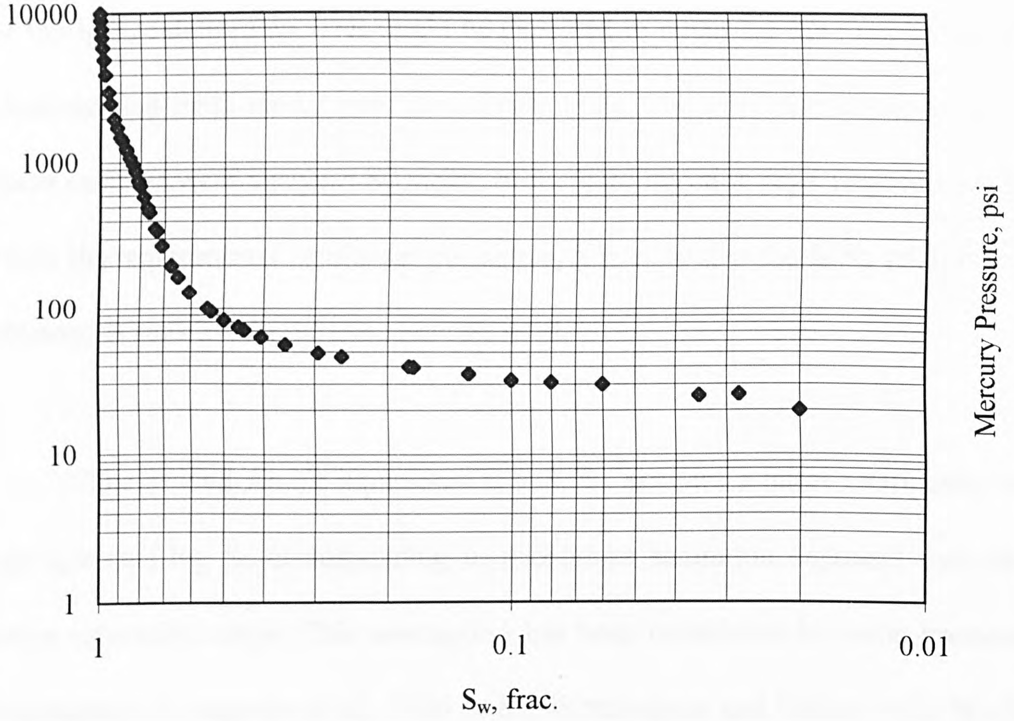

Fig.(5.7c) Pore throat radius vs. Distribution function for sample C4

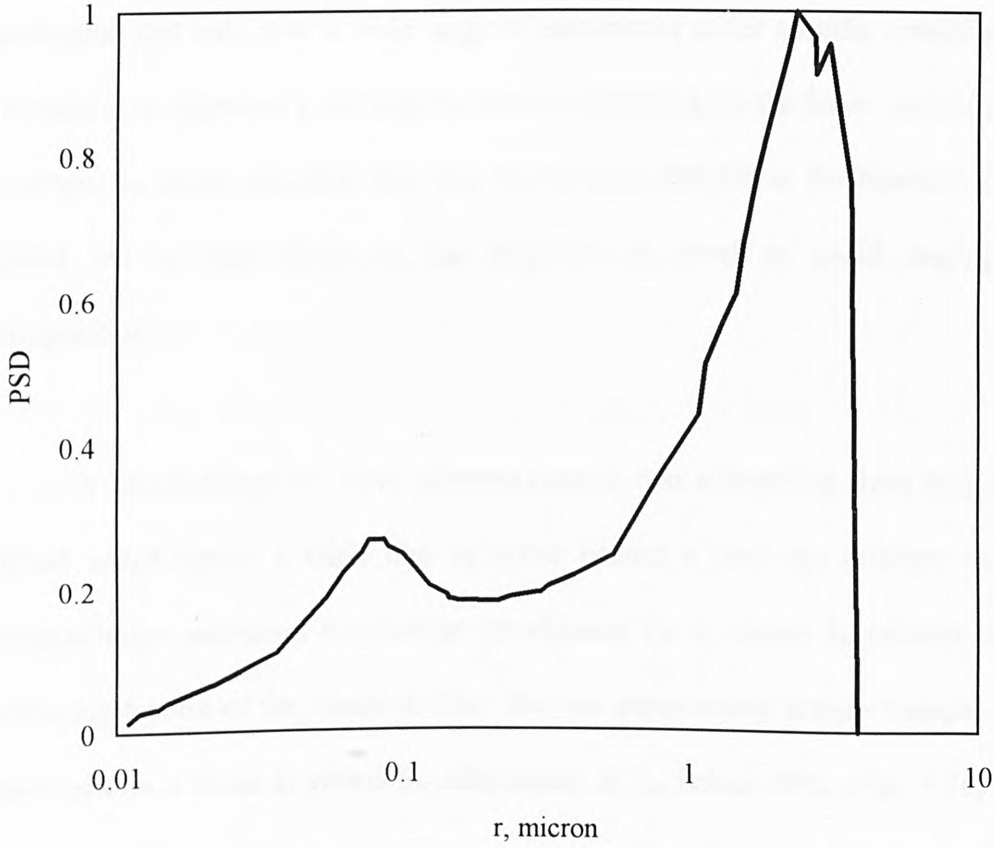

physical resistance. As desaturation progresses, a saturation heterogeneity may develop due to the bypassing of smaller pores, and this will lead to nonlinearity of the I_R/S_w relationship. This might be expected to occur for the samples having bi-modal and multi-modal pore size distributions. The pore size distributions of these samples were analysed by means of mercury injection tests (Appendix C3). From the experimental results set out above, it is clear that the I_R/S_w relationship obtained is sensitive to the injection rate used.

The second Archie equation, $I_R = S_w^{-n}$, assumes a linear relationship of log I_R versus log S_w corresponding to a constant saturation exponent over the entire saturation range. This assumption has been considered by some previous investigators (Longeron *et al.,* 1986 & 89, Worthington and Pallatt 1992, Watfa 1987, Argaud *et al.,* 1989) as "not valid". The above results demonstrate that this assumption can hold over a wide range of saturations under specific conditions. The saturation exponent n can then be reliably obtained from the linear part of the I_R versus S_w curve, provided that the desaturation process in the laboratory is carried out at least down to the reservoir S_w level to avoid improper extrapolation.

A disadvantage of slow injection rates is that a fingering front may be formed which leaves a thick film of water behind it that can produce to a nonequilibrium saturation distribution, invalidating the I_R versus S_w relation. An interesting feature of the results is that the low permeability sample (sample 4) clearly shows a linear I_R versus S_w relationship at S_w below 88%, (Fig. 5.7a) in contrast to the nonlinear relation usually reported for low permeability samples (Argaud *et al.*, 1989).

5.313 Summary

From the above experimental observations, the influence of flow injection rate upon the I_R/S_w relationship and upon the saturation exponent can be summarised in the following points:

a- The electrical resistivity and saturation exponent are dependent on the flow mechanism used to change the saturation within the rock samples.

b- The degree of uniformity and nonuniformity of I_R versus S_w depends on many factors as well as the injection rate used in the desaturation process. For the tested samples, it has been found that the high rate normally gives the more uniform I_R/S_w curves. A large percentage difference in n was found between the high and low injection rate cases.

c- The early and very late stages of the desaturation process show different behaviour in terms of resistivity changes with saturation. This is related to the initial desaturation of the large pores and the desaturation of porous membrane in the later stages.

d- For the tested samples, any nonlinearity of I_R/S_w curves is related not only to the pore size distribution but also to the forces which control the flow mechanism.

5.32 Effect of Viscosity Ratio

5.321 Review

Water saturation is commonly determined from electric well logs based on the second Archie equation (1942) , $I_R = S_w^{-n} = R_t / R_o$. This equation is empirically based. The Archie's parameters are usually obtained from laboratory measurements on core samples. It is assumed in laboratory measurements that the saturation is distributed uniformly throughout the sample, and that the saturation exponent n is constant over the saturation range. However, many cases are encountered where the resistivity index (I_R) shows a non-linear relationship with brine saturation (S_w). Wettability, microporosity and capillary end effects are the main factors which influence this nonlinear behaviour.

The above equation assumes that the same value of water saturation should give same value of resistivity whatever the characteristics of the fluids used, because S_w and R_t are the only variables in the equation. However, experimental conditions, (and especially the viscosity ratio between the displaced and the displacing fluids in the continuous injection technique) may have an important influence on the form of the I_R versus S_w curves. If inappropriate oil and brine viscosities are used in resistivity index measurements, an erroneous value of saturation exponent may be obtained. The influence of viscosity ratio on I_R versus S_w relationships has received very little attention in the past, probably on account of the time and cost involved in such experiments. However, unreliable values of saturation exponent can result in large errors in hydrocarbon determination as described by de Wall *et al.*, (1991).

5.322 Viscosity Ratio Experiments

Experiments using low and high viscosity ratios (viscosity of brine divided by viscosity of oil) were carried out on the six carbonate samples and the ratios chosen were respectively 0.1 and 0.6. The samples, fully saturated with brine, were mounted in a multiple core holder and subjected to maximum pressure of 3000 psi. The sample pore volume was calculated based on the brine volume collected in pipettes attached to the outlet of each sample. The system was allowed to come to equilibrium and oil was then injected at one end of the sample and brine was expelled at the other end through a semipermeable membrane supported by a high porosity glass disc. Both voltage, phase angle and temperature were monitored continuously during the oil injection process. All samples were in a water-wet condition. Before the desaturation process began and the brine-saturated samples (μ_w =1.2 cp) were loaded into the core holder, the resistivity of the fully saturated samples (R_o) was measured. The oil/brine desaturation process was then started (μ_o = 12 cp) and resistivity measured when the capillary and electrical equilibrium was indicated (i.e., no further change in resistance with time). The average core saturation was calculated volumetrically by deducting the volume of brine displaced from the pore volume. Oil was injected first using the low viscosity ratio (μ_R = 0.1). When this run was completed, the samples were subjected to the re-cleaning process and the high viscosity ratios (μ_w = 1.2 cp and μ_o = 2 cp) experiments were carried out. The resistivity values were corrected for temperature variations in all cases (injection rate was kept constant). All results are shown in Appendix C2.

5.3221 Experimental Results and Observations

The six samples tested gave results as follows:

Sample D1:

This sample has medium porosity (14.89%) and low permeability (2.1 mD). The plots of I_R versus S_w for the low and high viscosity ratios is shown in Fig. 5.8a. The non-linearity of the I_R/S_w relationship is obvious especially in case of high μ_R. The I_R/S_w relationship is uniform for low μ_R at $S_w < 43\%$. Two segments are evident in both cases, but in the case of low μ_R, *n* is uniform over most of the range of saturation. The difference in n between the two cases is small. The early part of the curve shows irregularities due to the influence of the desaturation of the larger pores. The capillary pressure and distribution function curves (Fig. 5.8b,c) show a bi-modal pore size distribution for this sample.

Sample D2:

This is more porous and permeable than the previous sample. The uniformity in the I_R/S_w relationships is more clearly obvious in this sample, although it does not cover such a wide range of saturation in the case of high μ_R. The I_R/S_w relationship becomes uniform for low μ_R at $S_w < 70\%$. The desaturation process for low μ_R ends later than the high μ_R case (Fig. 5.9a). The difference in saturation exponent between the two cases is about 15%. This sample has a uni-modal pore size distribution (Fig. 5.9b,c)

Sample D3:

This is a low permeability sample (1.9mD). The I_R/S_w relationship (Fig.5.10 a) is non linear for both cases at the early stages of desaturation, but subsequently, the low μ_R case developed good uniformity at $S_w < 57\%$. The short uniform range of

Fig(5.8a) I_R vs. S_w for sample D1 at different viscosity ratio

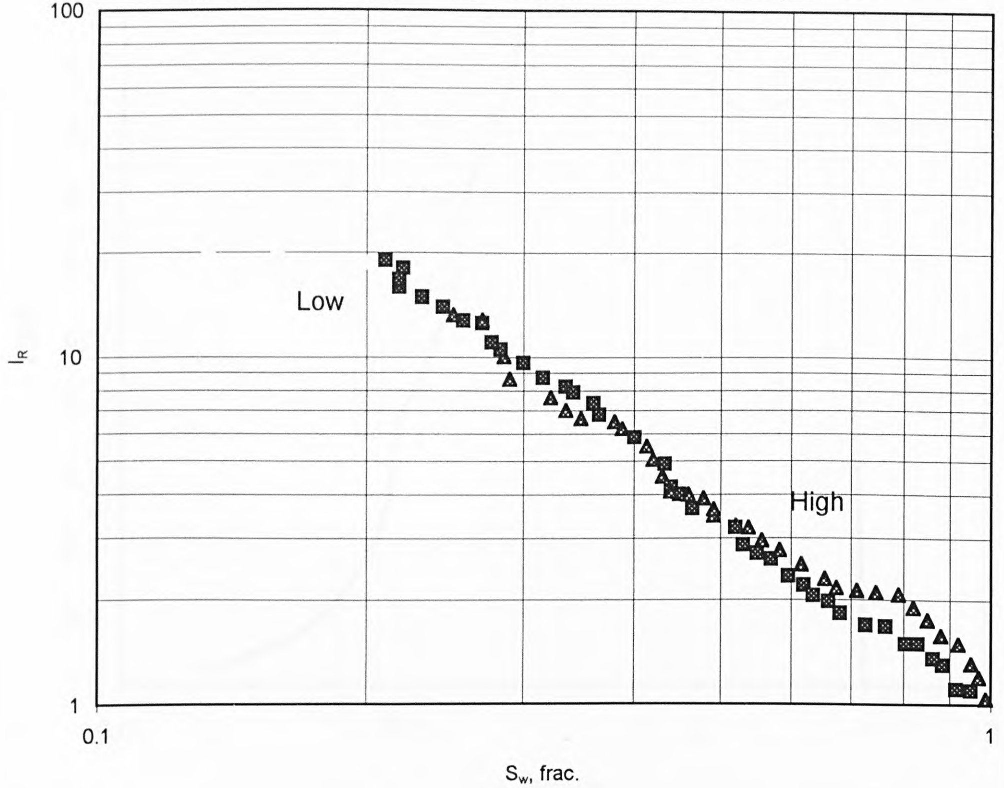

Fig.(5.8b) S_w vs. P_c for sample D1

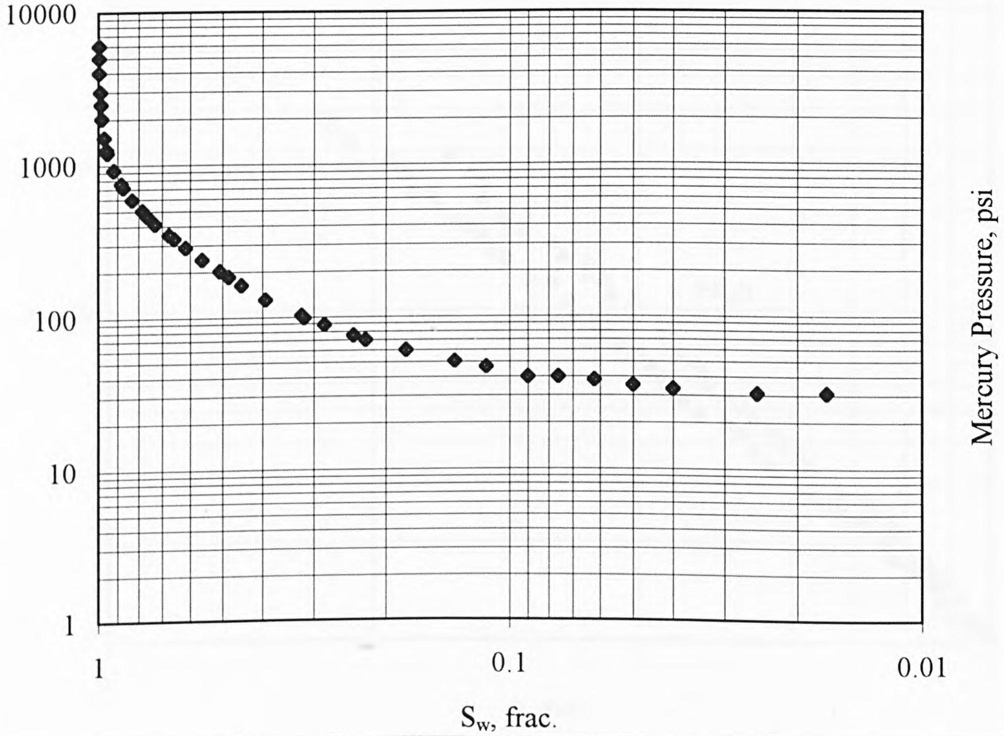

Fig.(5.8c) Pore throat raduis vs. Distribution function for sample D1

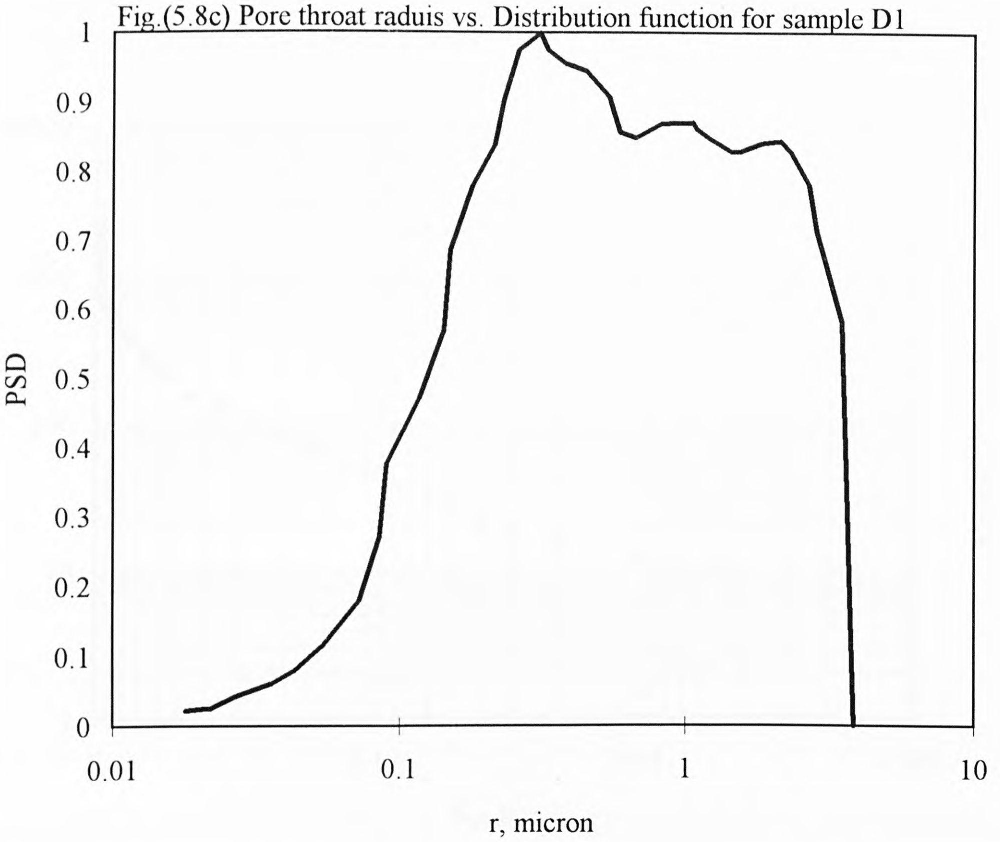

Fig(5.9a) I_R vs. S_w for sample D2 at different viscvosity ratio

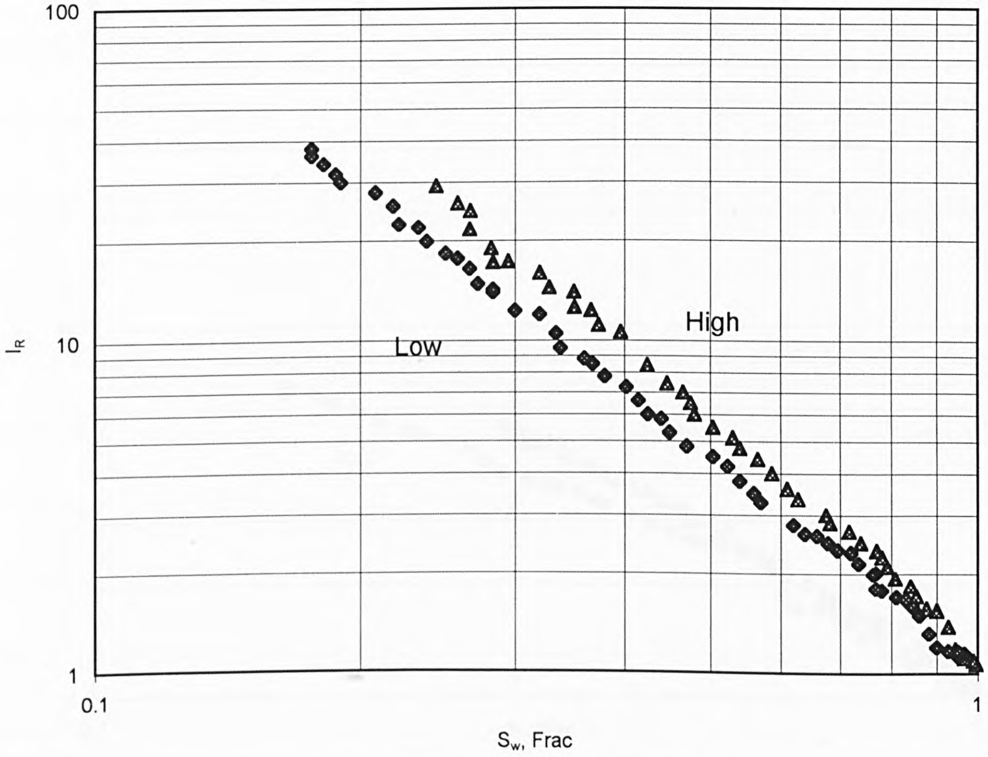

Fig.(6.9) S_w vs. P_c for sample D2

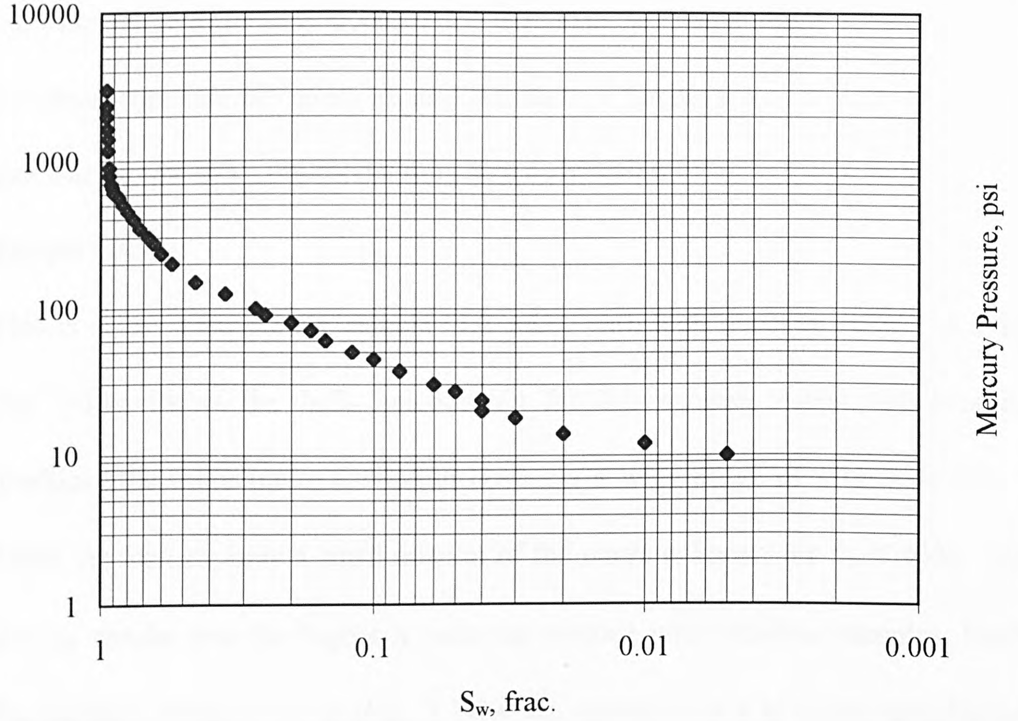

Fig(5.10a) I_R vs. S_w for sample D3 at different viscosity ratio

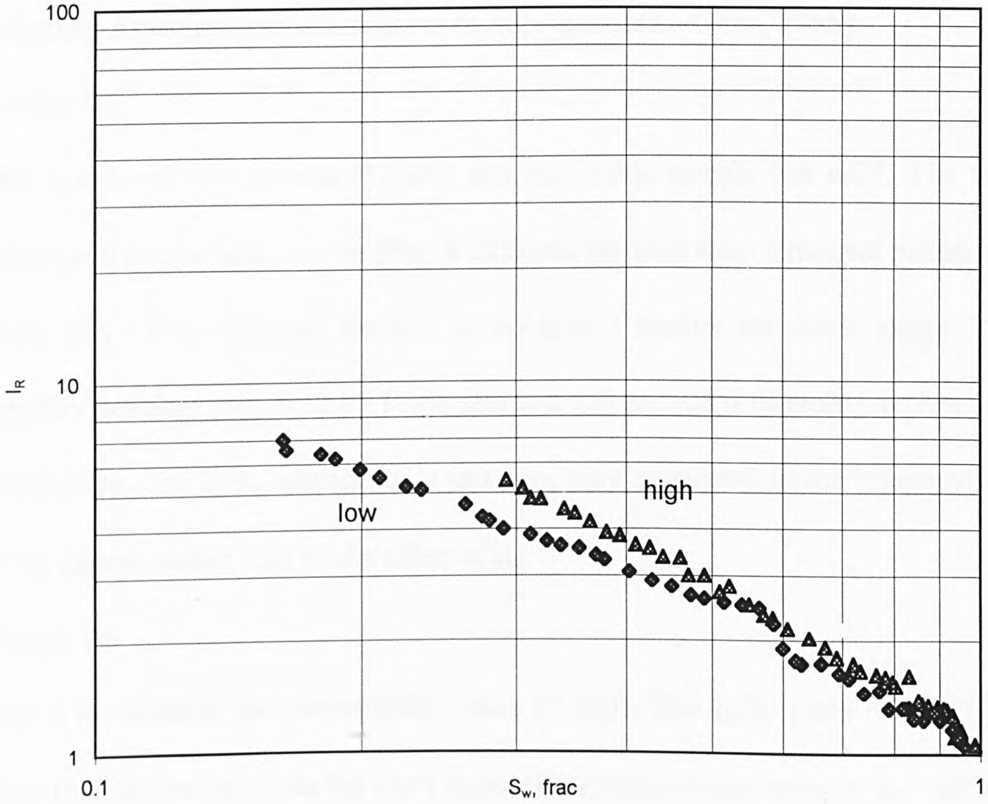

I_R/S_w for high μ_R starts as early as $S_w < 74\%$ but does not cover a wide range of saturation, and the desaturation ended at $S_w = 32\%$ (Fig.5.10 a). In this sample, the percentage difference in saturation exponent has reach about 12%. Fig. 5.10 b,c shows the capillary pressure and distribution function curves, and it is found that this sample has a uni-modal pore size distribution.

Sample D4:

This is a low permeability sample (1.2 mD), with high porosity value (16.3%). Fig. 5.11a shows the I_R/S_w relationship for this sample. Again, the low μ_R produces the more uniform relation covering a wide range of saturation ($S_w <$ 74%). At high μ_R only a small portion of the curve is linear, for $S_w < 45\%$. The low μ_R results give the higher *n* value in contrast with previous samples. From the capillary pressure curve (Fig. 5.11b), the existence of a bi-modal distribution can be recognised at the inflection point where the curve trend starts to change, indicating a change from macropores to micropores (Swanson, 1985).

Sample D5:

This sample is very porous (32.6%) and permeable sample (66 mD). The two cases gave similar I_R/S_w curves (Fig. 5.12a) and the saturation exponent values are close, ($\Delta n = 1\%$), although the low μ_R covered a smaller saturation range. The capillary pressure (Fig. 5.12 b,c) indicates that this sample is bi-modal in pore size distribution. The I_R/S_w uniformity in this case may be related to the homogeneity of the sample rather than to the effect of μ_R.

Sample D6:

This is a relatively low permeability value (8 mD). The I_R/S_w plots (Fig. 5.13a) show that the low μ_R gives the more linear relationship which starts at $S_w < 86\%$

Fig.(6.10b) S_w vs. P_c for sample D3

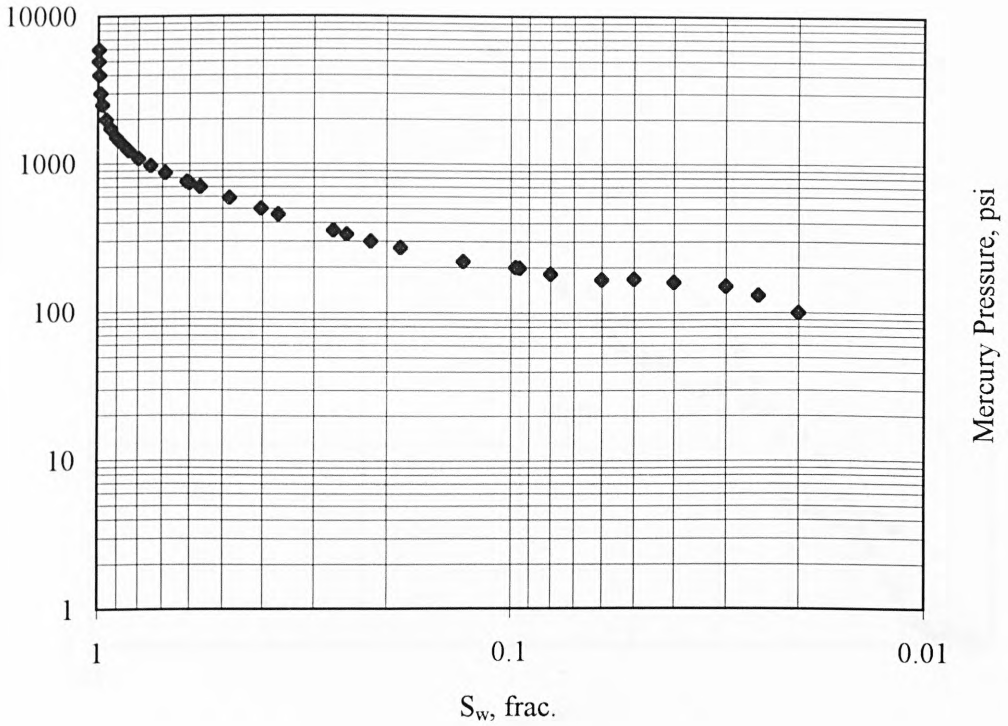

Fig.(5.10c) Pore throat radius vs. Distribution function for sample D3

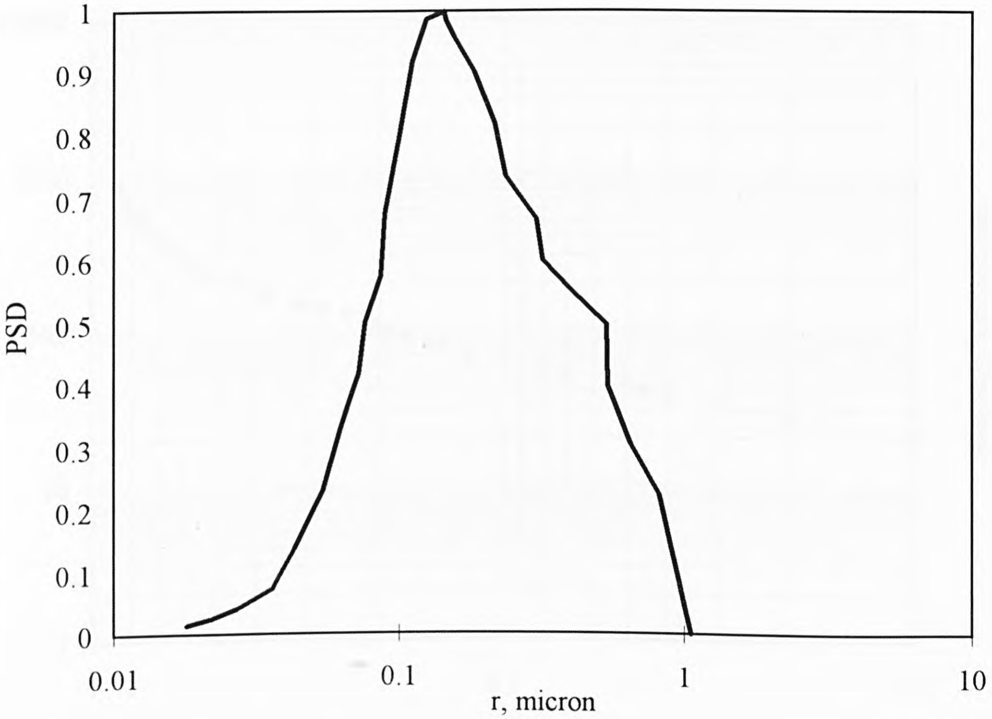

Fig.(5.11a) S_w vs. I_R for sample D4 at different viscosity ratio

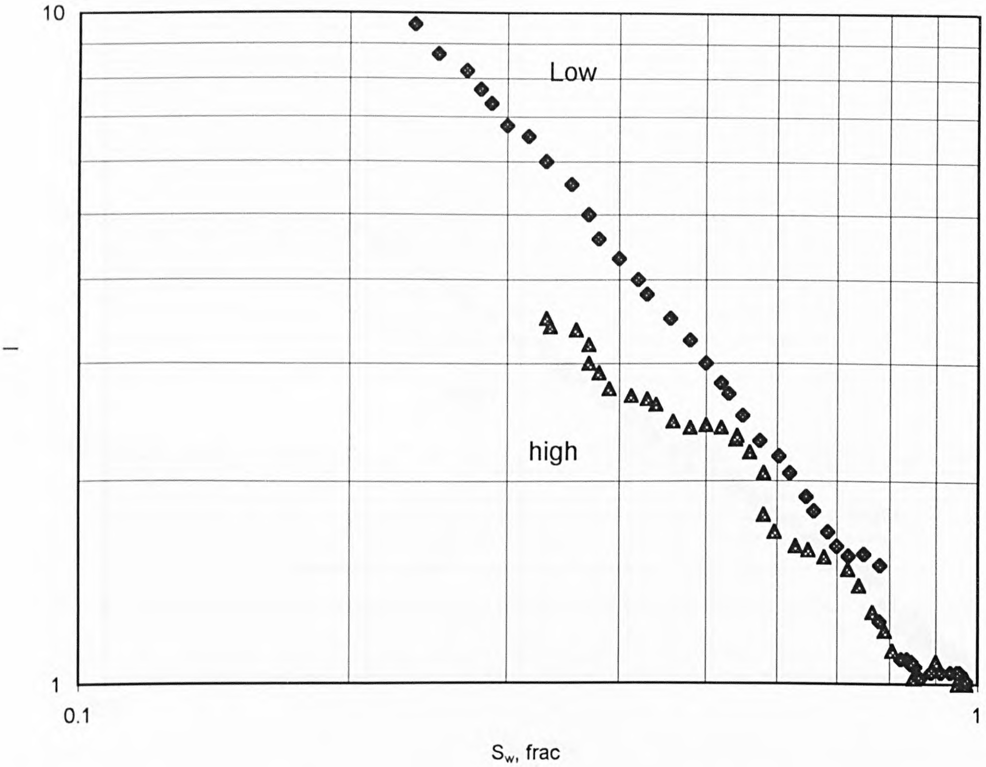

Fig.(5.11) S_w vs. P_c for sample D4

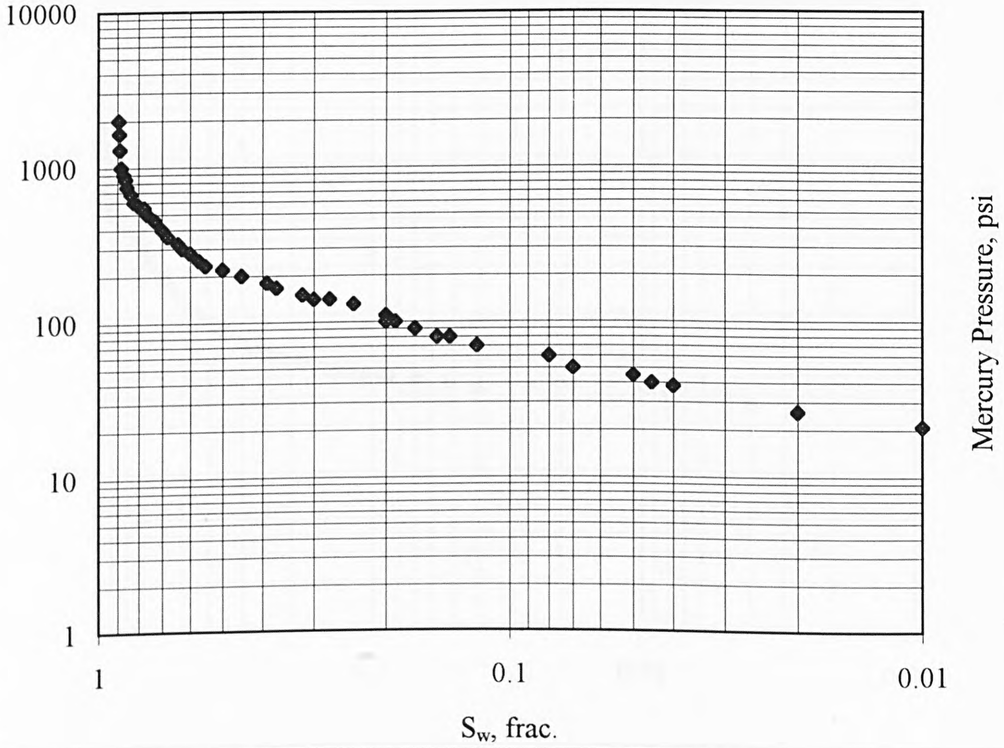

Fig.(5.12a) S_w vs. I_R for sample D5 at different viscosity ratio

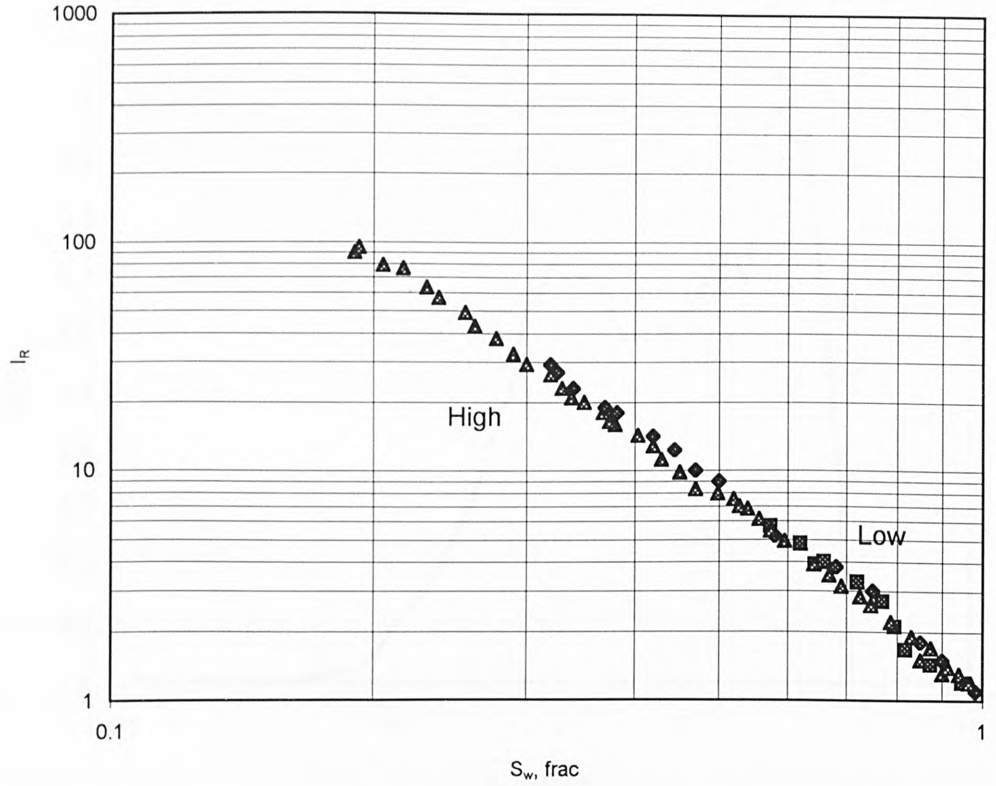

Fig.(5.12b) S_w vs. P_c for sample D5

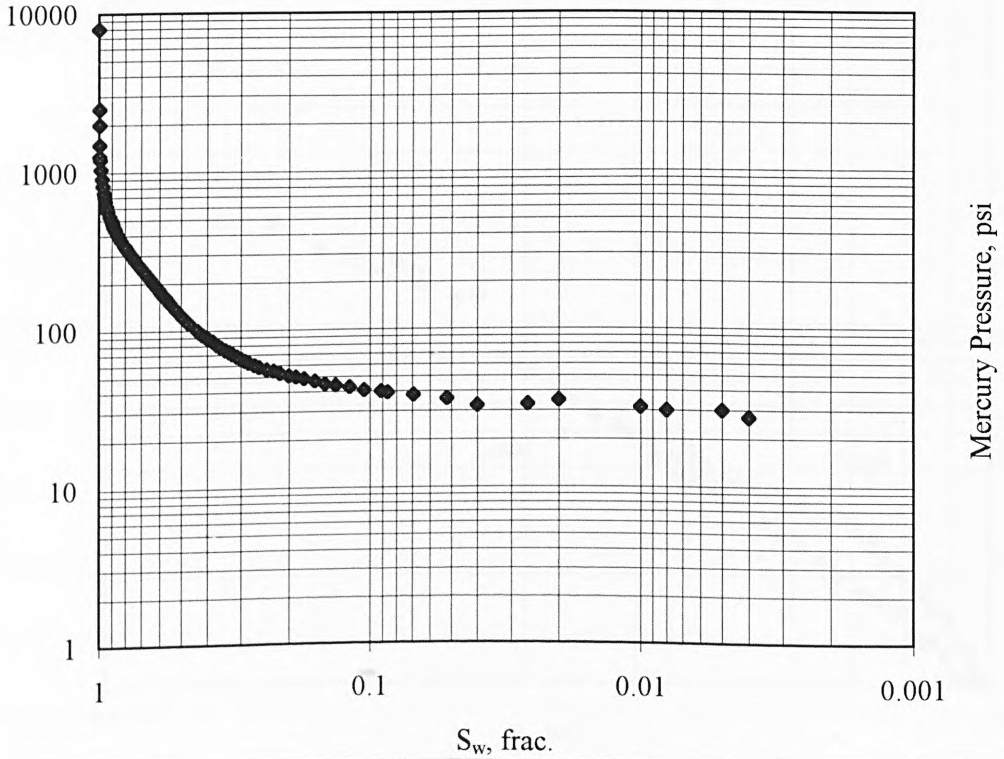

Fig.(5.12c) Pore throat radius vs. Pore Size Distribution for sample D5

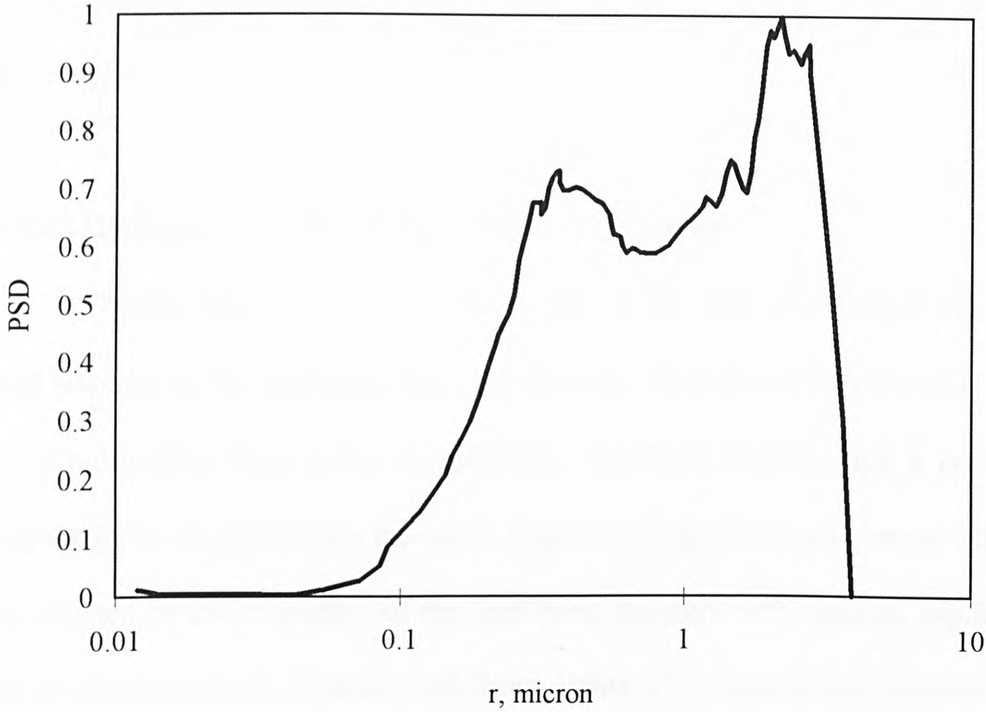

Fig.(5.13a) S_w vs. I_R for sample D6 at different viscosity ratio

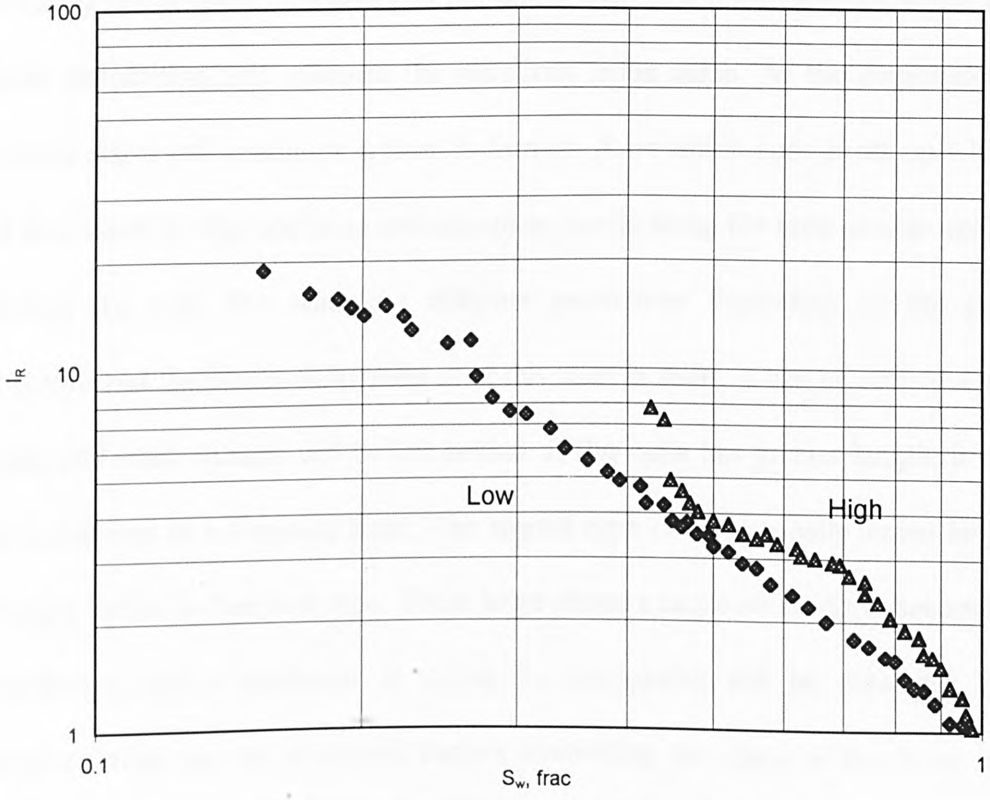

(excluding the very late desaturation stage). Only limited uniformity of I_R/S_w was obtained for the case of high μ_R, which showed two distinct segments (two n values or more). Figures 5.13 b and c indicate the bi-modal pore distribution of this sample.

5.3222 High and low viscosity ratio and I_R/S_w relations

The viscosity ratio (μ_R) is defined here as the ratio of displaced (brine) fluid viscosity to the displacing fluid (oil) viscosity. High ($\mu_R = 0.6$) and low ($\mu_R = 0.1$) ratios were used in this investigation. The fluid flow through a porous medium (core or reservoir) is the result of pore level displacement events, which are affected by the interaction of the local pore structure with viscous, capillary and gravitational forces (Grattoni and Dawe 1996). The displacement of water by oil in a porous medium is not a simple process and depends on many factors including the physical properties of the fluids. The fluid characteristics affect the fluids distribution and influence the resistivity index value. As the displacement process starts and continues, a front is formed. A transition zone is set up where oil first starts to displace brine and this zone travels along the core sample until it reaches the end. The zone has different geometries depending on the pore structure and the forces controlling it. If this zone is short, it can be termed a flat front, and small clusters will be left behind. If this zone has greater length, it can be considered as a fingering front. The second type of front usually leaves larger clusters behind it than first type. These large clusters cause nonuniform saturation distribution and a non-linear I_R versus S_w relationship will be obtained. The viscous forces are one of several factors controlling the shape of the front, and consequently different I_R versus S_w plots are obtained at different viscosity ratios.

Fig.(6.13b) S_w vs. P_c for sample D6

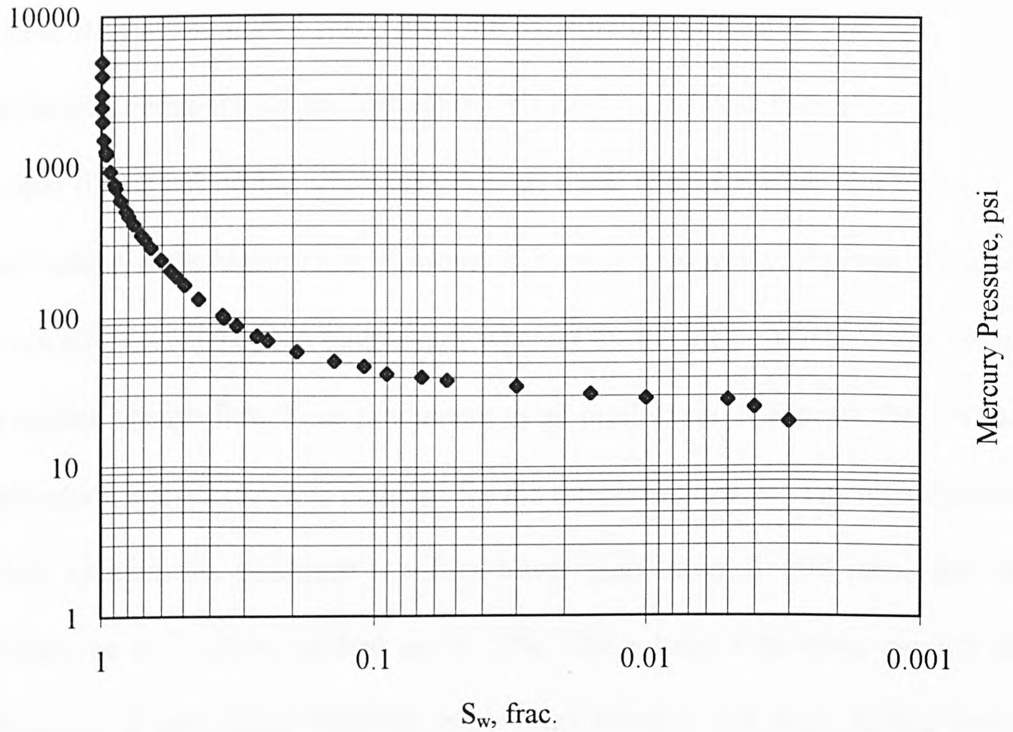

Fig.(5.13c) Pore throat radius vs. Pore Size Distribution for sample D6

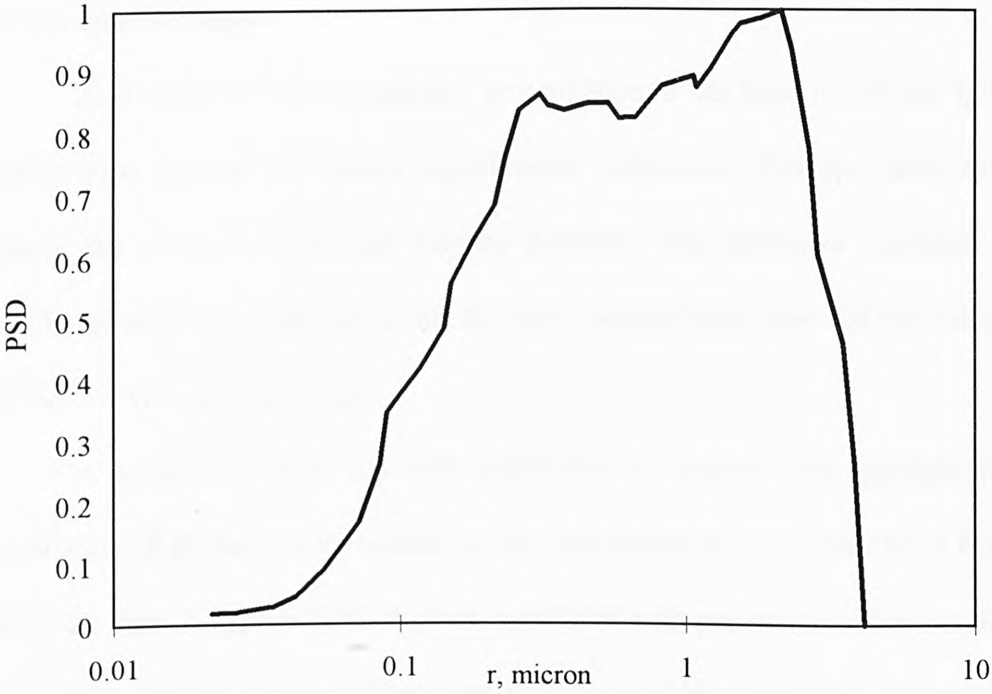

Figures from 5.8a to 5.13a represent I_R/S_w plots for all the tested samples at two viscosity ratios. At the lower ratio, the I_R versus S_w relation is markedly more linear than at the higher ratio. Also the desaturation process at low μ_R covers a greater S_w range than at the high ratio. This can be attributed to the fact that a thin water film is left behind when the lower μ_R used, while a thicker film of water is left behind at the higher ratio. However water was produced in the case of high μ_R even after oil reached the sample end, whereas for the lower μ_R, there was usually a sudden change from brine production to oil production. It appears that uniform saturation distribution was obtained for the samples at low μ_R. The high viscosity ratio experiments produced n values lower than those at low ratio, and the difference in n values reached up to 13%. These large differences confirm the necessity of performing resistivity index measurements with fluids having similar characteristics to the fluids of the reservoir or formation under investigation.

5.4 Parametric Study

As a result of this experimental investigation, it has been found that I_R/S_w relationships depend on various experimental parameters. For the same rock sample the saturation exponent may be different. The saturation exponent is usually found to have high values for the high viscosity ratio case and low values for the low viscosity ratio case.

A parametric study has been performed to quantify and highlight the importance of all the factors studied on the calculation of water saturation from resistivity logs. A hypothetical reservoir is selected with parameters close in value to those in a typical reservoir. The water saturation of this reservoir is determined from the Archie equation using the different values of *n* obtained from this research.

The parameter values selected are as follows;

$R_w = 0.4$ ohm-m

$m = 2$

$\phi = 18\%$

$R_t = 70$ ohm-m

5.41 Injection Rate

Two different injection rates were used in this parametric study for the displacement process. Saturation exponents obtained from the two cases can be different. Inaccuracies in water saturation evaluation may be introduced if the process that mimics the actual reservoir case is not applied during the laboratory measurements.

Results from this research Table 5.2 show that the calculation of water saturation based on I_R/S_w relationships obtained from the two tests can differ by about 19%. Using the proper I_R/S_w relationship is, therefore important. Otherwise, the water saturation determined from resistivity logs can be either over or under estimated.

Table 5.2 S_w calculation for different Injection Rates

Injection Rate	Saturation exponent	S_w %	ΔS_w %
High	2.24	46.1	18.7
Low	1.34	27.4	

5.42 Viscosity Ratio

Table 5.3 shows the water saturation calculated from the Archie equation using data obtained from log measurements and data obtained from core analysis before and after viscosity ratio consideration. A saturation exponent difference of 6.26 % was found between two cases of viscosity ratio (low and high). Therefore the use of nonrepresentative fluid characteristics for a reservoir or formation under consideration would result in an over or under estimation of oil initially in place. The results indicate that the saturation exponent should be measured on representative core samples using fluids with properties close to those in the reservoir.

Table 5.3 Effect of viscosity ratio on the calculation of Sw

Viscosity Ratio	Saturation Exponent	S_w %	Δ S_w%
High	2.15	44.6	6.26
Low	1.81	38.34	

5.5 Conclusions

A study has been conducted in order to investigate the effect of the experimental conditions upon the resistivity-saturation relationships, and this experimental investigation was performed using the continuous injection technique. Based on the experimental results of this chapter, the following conclusions can be drawn for water-wet rocks during drainage conditions:

a. The assumption of Archie's equation that the saturation exponent is independent of fluid characteristics and flow displacement mechanism has been demonstrated in this work as unrealistic. The viscosity ratio between displaced and displacing phases and the injection rate of displacing phase have an obvious influence on the fluid distribution within core samples and hence produce different resistivity-saturation relationships and different saturation exponent values.

b. The effect of the injection rate of the displacing phase was observed for the samples tested. A disadvantage of low injection rates is that a fingering front may be formed which leaves thick films of water behind it that may produce a nonequilibrium saturation distribution, invalidating the I_R versus S_w relation and leading to varying values of the saturation exponent over a wide range of S_w.

c. For most of the core samples tested, it has been found that resistivity-saturation relationships show a more uniform trend at the low viscosity ratio than at the high ratio. It was also noticed that the desaturation process at the low viscosity ratio covered a much greater water saturation range. This is attributed to the formation of a flat front which leaves small clusters behind it leading to a relatively uniform saturation distribution.

d. Because the saturation distribution within the core sample is controlled by capillary and viscous forces, it is recommended that whenever resistivity index measurements are performed in the laboratory, fluid characteristics close to those of the reservoir under investigation should be used.

Generally, in order to achieve precise and accurate evaluation of S_w from resistivity logs, one needs to have in depth understanding of various factors affecting the determination of the saturation exponent in the laboratory. Core samples should be tested using fluid characteristics representing actual reservoir condition of reservoir or formation. Laboratory desaturation techniques and procedures should be designed to represent the actual cases. In addition to this, the experiments should be performed at simulated reservoir conditions of pressure and temperature, so that the pore geometries can be restored as closely as possible to the *in situ* state.

CHAPTER 6

ARCHIE'S PARAMETERS FOR CARBONATE ROCKS

6.1 Introduction

The effects of pore geometry on the electrical properties of fluid-saturated rock were recognised almost from the initial studies (Archie, 1942; Winsauer, *et al.*, 1952). These effects, however, tended to be concealed by the arbitrary manipulation of the constants and exponents in Archie's equations, especially the cementation factor m. Many attempts have been made at quantifying this important parameter. Although there are at least a dozen properties which researchers have related to this parameter, the present study seeks to examine the dependence of the cementation factor and the saturation exponent on the geometry and tortuosity of a carbonate pore system. Large errors can be generated in water/hydrocarbon saturation determinations whenever the parameters used in interpretation are arbitrarily treated as constants. In particular, the use of constant values of the Archie parameters (cementation factor and saturation exponent) in Archie’s equation may introduce major errors.

Core samples from a Libyan carbonate reservoir have been studied in order to determine Archie's parameters by experimental measurement and to examine the effects of porosity type on these parameters. The potential evaluation of this reservoir was made initially on the basis of $m = n = 2$ (National Oil Corporation, 1988b). The choice of a carbonate reservoir for study was due to three reasons; firstly, very little work has so far been carried out in order to investigate *m* and *n* for carbonates at large scale, therefore a gap in the literature has to be filled. Secondly, since more than half of the world's oil production comes from carbonate rocks, and approximately 40% of the oil produced in the history of petroleum industry has come from carbonate reservoirs (Western Atlas 1992a), more attention should be paid to the study of carbonates. Thirdly, this particular reservoir rock is a carbonate exhibiting several different porosity types, so the influence of these upon Archie's parameters can be studied.

The electrical resistance to current flow through the pore space depends on the geometry of the electrical path. The greater the path length, the higher the resistance will be, and the value of Archie's parameters will reflect this. The electrical flow path geometry is determined by the porosity type. As the flow path becomes more convoluted, the reservoir has greater tortuosity, and the Archie's cementation factor will increase due to the increase in resistivity. The laboratory measurements of Archie's parameters for this specific reservoir were performed using a porous plate method. A four electrode system was used to measure the resistivity index of core samples collected from this reservoir.

The pores in this Libyan carbonate reservoir show variations in shape and size which may contribute to variations in the values of m and n. In this chapter, a case study is investigated and presented to examine the influence of porosity type (interparticle, intercrystalline, vuggy, fracture, etc.) on the Archie's parameters, and the results suggest a valuable recommendation for the evaluation of carbonate reservoirs with double or multiple porosity systems. In the next sections, details of carbonate porosity types, the relation between the resistivity and pore geometry and the basis of variations in Archie's parameters are examined and discussed.

6.2 Porosity Types of Carbonate Formations

Pore systems in sedimentary carbonates are generally complex in their geometry and genesis and commonly differ markedly from those of sandstones. Pore systems in carbonate rocks have been classified comprehensively with particular emphasis on their genetic aspects (Choquette and Pray 1970). Other attempts at carbonate pore geometry classification were made by Wardlaw (1971), Nurmi (1984) and Lucia (1983).

Carbonate reservoirs can have several types of porosity including intergranular, intercrystalline, vuggy, moldic and fracture types. The variety of pore types in carbonates results from both depositional and diagenetic processes. In their remarkable book, Rieke et al. (1972) have generally classified carbonate porosity types into three main categories: 1) intergranular-intercrystalline porosity, 2) vugular solution porosity, and 3) fracture-matrix porosity. In the following section more detailed descriptions of these categories are given:

6.21 Intergranular-intercrystalline porosity

This is found in carbonate pools having intergranular porosity which are comparable to unfractured sandstone reservoirs in behaviour. The spatial distribution and the general configuration of the pores are more orderly than in systems falling in the second and third categories. Commonly, the basic particles of the system are well-rounded. In this type the size and shape of allochems have a direct bearing on the nature of the void space. The sedimentary units may also be crystals precipitated from solution to form an intercrystalline porosity. The flow path of fluids or electrical current through this type of porosity has a gently curved shape.

6.22 Vugular solution porosity

Vugular-solution porosity systems are inherently more complex than either intergranular-intercrystalline porosity or fracture-matrix porosity systems. In such systems, the original pore structure has been altered by the formation of solution cavities and channels. The fluid or electrical flow through such a system has a more complex geometry, and the flow path is more tortuous than in the other two cases. The performance of carbonate pools with vugular-solution porosity may closely resemble sandstone pool performance, but commonly differs considerably.

6.23 Fracture-matrix porosity

In reservoirs having fracture-matrix porosity, the double-porosity system may be well developed. The fractures allow the reservoir to produce at an economically attractive rate. Pool performance is markedly different from that of sandstone reservoirs. The flow path shape through the fracture system approaches a linear form. The matrix usually has a low permeability and contains most of the oil, with little occupying the fractures.

Summarising, the flow of fluids or electric current has a path geometry depending on the porosity type. The resistivity variations for each porosity type is discussed in next section.

6.3 Electrical Resistivity Versus Pore Geometry

Oil and gas are nonconductors, and water is a conductor when it contains dissolved salts. The electrical current is conducted in water by the movement of ions. The resistivity of a material is a measure of its ability to conduct electrical current. For a porous medium containing multiple fluid saturations, the resistivity will be influenced by the pore geometry and the distribution of the fluids. The types of porosity in water-bearing carbonate formations, and the paths taken by an electric current flowing through samples from such formations are illustrated schematically in Fig. 6.1 (Asquith 1985). Fig. 6.2 shows how the presence of the hydrocarbons affects the flow of an electric current in a carbonate reservoir with intergranular porosity.

In a simple pore geometry such as that of a plane fracture, the Archie's cementation factor was found to be equal to unity (Aguilera 1980, Ransom 1984). From the schematic in Fig. 6.1, it can be seen that as the electrical flow path becomes more convoluted, the reservoir becomes more tortuous, and *m* will change. With greater tortuosity the resistivity and cementation factor increase.

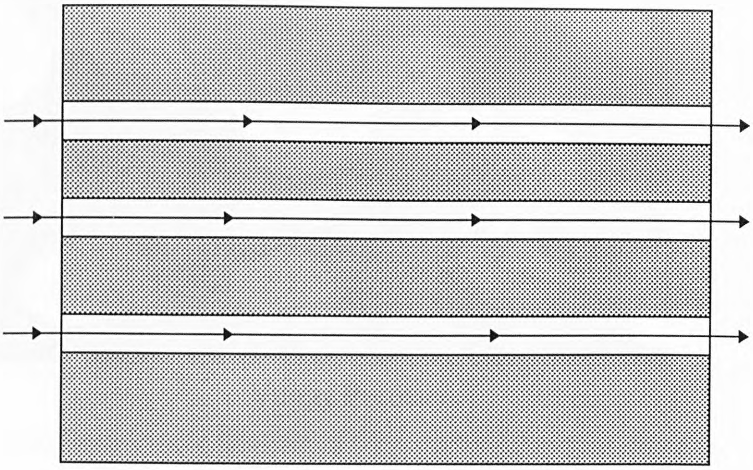

Fracture Porosity

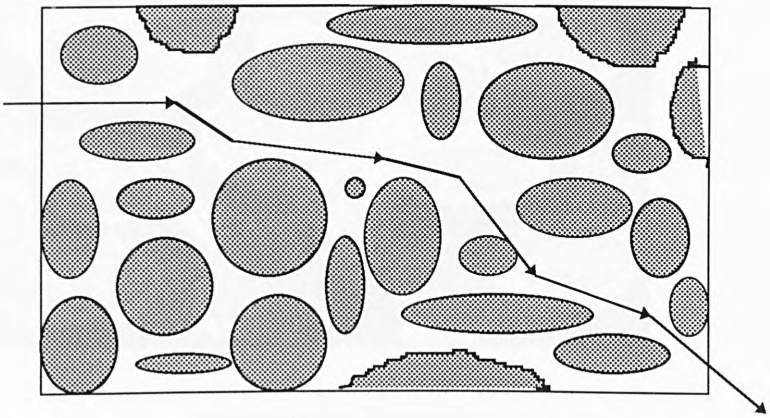

Intergranular
Porosity

Fig.(6.1) Schematic of Electrical Path through different type of porosity (After, Asquith 1985)

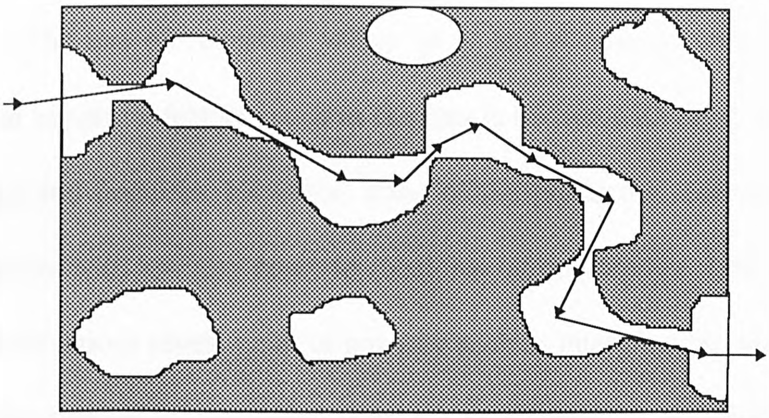
Vuggy Porosity

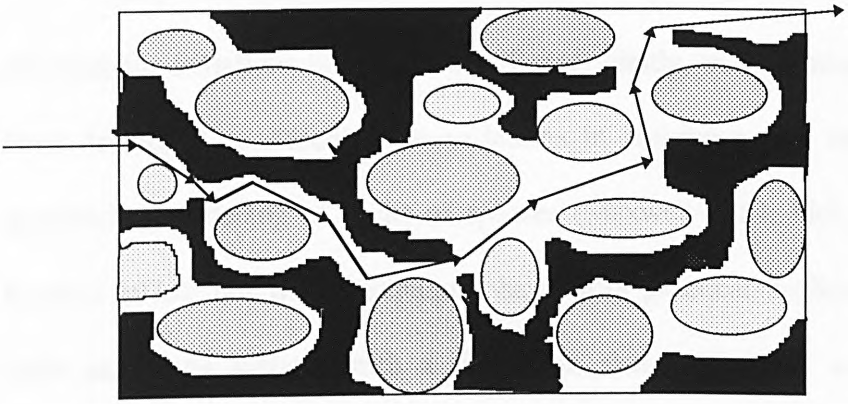
Intergranular Porosity

Fig.(6.2) Schematic of Electrical Path through different type of porosity (After, Asquith 1985)

6.4 Variations in the Archie Parameters

6.41 Variations in Cementation Factor

The use of constant values of m and n over a whole formation may conceal important features such as changes in texture with depth and the presence of vugs and fractures. However, some of the producing reservoirs in Libya are carbonates with low clay contents (National oil corporation, 1980). Core analysis and observations reveal types of porosity such as intergranular, vuggy, moldy and microfracture, which can affect the Archie's parameters, especially m. Variations in m for carbonates result from variations in texture and facies and it has been shown that m can range from 1.2 to 5.5 in such reservoirs (Focke and Munn 1985).

Many attempts have been made in the past to develop flow models allowing for variations in cementation factor. Firstly, mathematical models have been developed to describe the variations in resistance and m based on the geometrical modelling of packs of spheres (Maxwell 1954, Ficke 1924, Rerez-Rosales 1976), but these techniques have little practical application except to clean sandstone systems with a fine grain size, compacted and well sorted (homogeneous systems). Secondly, empirical approaches have been used where correlations between m and ϕ were derived on the basis of core analysis and field studies (Winsauer 1952, Shell 1984, Borai 1987). The so-called "Shell formula" for m (Neustaeder,1968) was derived in a similar fashion from core studies on low porosity dolomite formations; however, this approach predicts an increase in m with a decrease in porosity which in opposite to the trends observed in carbonates (Borai 1987). The Humble formula (Winsauer *et al.*, 1952) is generally applied for unconsolidated sands and has little value for carbonates. Thirdly, many approaches have been made based on log data analysis (Nurmi 1984, Nugent *et al.*, 1978, Mitchell-Tapping 1983, Rasmus 1983). A review of these approaches and techniques can be found in Asquith 1985. However these approaches do not take in account the fact that m can vary from point to point, reflecting variations in porosity and lithology (Watfa 1987). Generally the evaluation of carbonate reservoir potential is based on the assumption that $m = 2$ ($F = 1/\phi^2$), and therefore incorrect judgements and poor decisions can easily be made (Al-Mahtot et al. 1998).

6.42 Variations in Saturation Exponent

For a water-wet reservoir, Anderson (1986) concluded that the saturation exponent n has a narrow range of variation. Sweeney and Jennings (1960) found that n for a particular water-wet carbonate reservoir ranged from 1.3 to 2.2. However, in log formation evaluation, n is usually taken as equal to 2.0, and this in general yields reasonable results. It appears however, that this assumption may lead to pessimistic values of total water saturation (Aguilera, 1980). Generally speaking, the variation in n is less significant than that in m. These variations result from the effects of (1) wettability (Anderson 1986, Donaldson and Siddique 1987), (2) pore size distribution (Worthington *et al.*, 1989, Swanson 1985), (3) reservoir conditions (Archer and Jing 1991, Hilchie 1964), and (4) experimental measurement conditions (Elashahab *et al.*, 1993, Grattoni and Dawe 1996, Al-Mahtot *et al.*, 1997-98). The effect of pore structure upon the Archie parameters requires more investigation to extend earlier work (Pittman 1984, Rasmus 1983, Worthington *et al.*, 1989).

6.5 Libyan Carbonate Reservoir Description

Libya has a number of large reservoirs, some of which are carbonate formations. Due to the large size of these formations, the nature of their pore systems has often been considered simple. Detailed examination of these rocks and studies of the problems in their formation evaluation have revealed a significant degree of complexity similar to that in formations from North Africa and the Middle East. This Libyan reservoir is comprised of five zones A, B, C, D and E. The lithology of these zones is a mixture of dolomite and limestone commonly with nodules of anhydrite. It is mainly dolomite with occasional limestone intervals. Zone D is the thickest zone of this reservoir and mainly has intergranular porosity; it is also the most homogeneous zone. Secondary pores are most common in Zone B which typically contain grains and/or skeletal moldic. Values of m as high as 4.5 in similar zones have been reported (Watfa, 1987). Zone C is a low porosity zone containing mainly intercrystalline pores with a few vugs and fractures. The upper reservoir zones A and B are more heterogeneous with large vugs and expected to have correspondingly large m values. Moreover, zone A contains some intercrystalline porosity types with medium to low values. The lower part of the reservoir is zone E which is of low porosity and may generate low m values (Watfa 1987, Focke and Munn1985); it also contains some fractures and micofractures which cause the porosity to be low (Idris, personal communication, 1995-96, Petroleum research centre, 1985).

The pore structure of most of these zones is not simple, showing large changes in texture and the presence of vugs molds, and fractures which can introduce large changes in *m* values, and may influence the *n* value as well.

6.6 Measurements of Archie's Parameters

6.61 Experimental Procedure

Many plug samples have been collected from four wells of this of the selected Libyan reservoir (Fasha Formation) for measurement of their Archie parameters and their properties are shown in Appendix D. The Archie's parameters were determined in the laboratory by resistivity measurements. A four electrode system was used to measure the formation resistivity factor and resistivity index. Some two electrode measurements were taken at frequency values between 1 - 2 kHz, and compared with the results for the four electrode system in order to test the reproducibility of the measurements, and some small differences were found, but these were not significant. However, the four electrode readings were used for the calculations rather than the two electrode data, for which the electrode polarisation can occur. Before the resistivity measurements, the samples were cleaned, dried and evacuated (See Chapter 3), then saturated with brine appropriate to this formation. The electrical resistance of brine-saturated core plugs and saturant brine were measured at room conditions on consecutive days till results stabilised, indicating ionic equilibrium with the core plugs. Then the formation resistivity factor and the cementation factor were calculated.

In order to determine the saturation exponent, the porous plate method was used to measure the resistivity index for core samples partially saturated with brine. In this method, the resistivity measurements and the desaturation process take place separately, and many samples can be desaturated simultaneously by placing them on a porous plate in a pressure chamber and applying gas pressure. The gas can enter the samples from all directions (except the end face in contact with the porous plate) because no sleeve is placed around the samples. Gas pressure is maintained until brine production stops, indicating that the capillary equilibrium has been reached for all the samples. The gas pressure is then released, and the samples are removed from the pressure chamber. The desaturation of each sample is determined by measuring its change in weight. Then the resistivities of the samples are measured using a four electrode system. This procedure is repeated for each gas pressure increment to obtain the resistivity index at each change in saturation point. Ten core samples among the eighty were chosen for final analysis and their properties are shown in Table 6.1.

Table 6.1 Petrophysical data of Libyan Carbonate samples

Sample	K, mD*	ϕ, %	GD, g/cm^3	Sample	K, mD	ϕ, %	GD, g/cm^3
1	2.37	20.34	2.84	6	3.58	26.33	2.84
2	3.3	12.43	2.84	7	10.3	13.25	2.84
3	31	16.2	2.86	8	6.94	31.21	2.85
4	0.25	10.84	2.84	9	158	27.92	2.86
5	1.46	11.12	2.84	10	145	37.36	2.85

* Confining pressure = 400 psi

* Mean pressure = (1 - 2) atm

6.62 Results and Discussion

Formation resistivity factor data plotted versus ϕ for the samples from this specific reservoir is shown in Fig. 6.3. The Archie's formula which represents this formation can be written as follows

$$F = \phi^{-2.15} , \qquad 6.1$$

where 2.15 is the average value of m, and

$$I = S_w^{\ -2.44} , \qquad 6.2$$

where 2.44 is the arithmetic average value of n, the arithmetic average being calculated for all samples investigated.

It can be seen, therefore, that for this reservoir the average values of the cementation factor and the saturation exponent are respectively 2.15 and 2.44. Water saturation values were determined by Archie's equation using three different procedures; firstly assuming a value of 2 for both m and n, secondly using the average values of m and n for the whole formation as shown above, thirdly using the average values of m and n for the zone concerned.

From visual microscopy and scanning electron microscopy (SEM) (examples shown in Figures 6.4 to 6.8), it was observed that the plugs mainly having granular textures (intergranular porosity type) with anhydrite and low clay contents such as sample 2 (zone C), sample 3 (zone D) and sample 8 (zone E)

Fig. 6.3 Formation Factor vs. Porosity of Libyan Reservoir

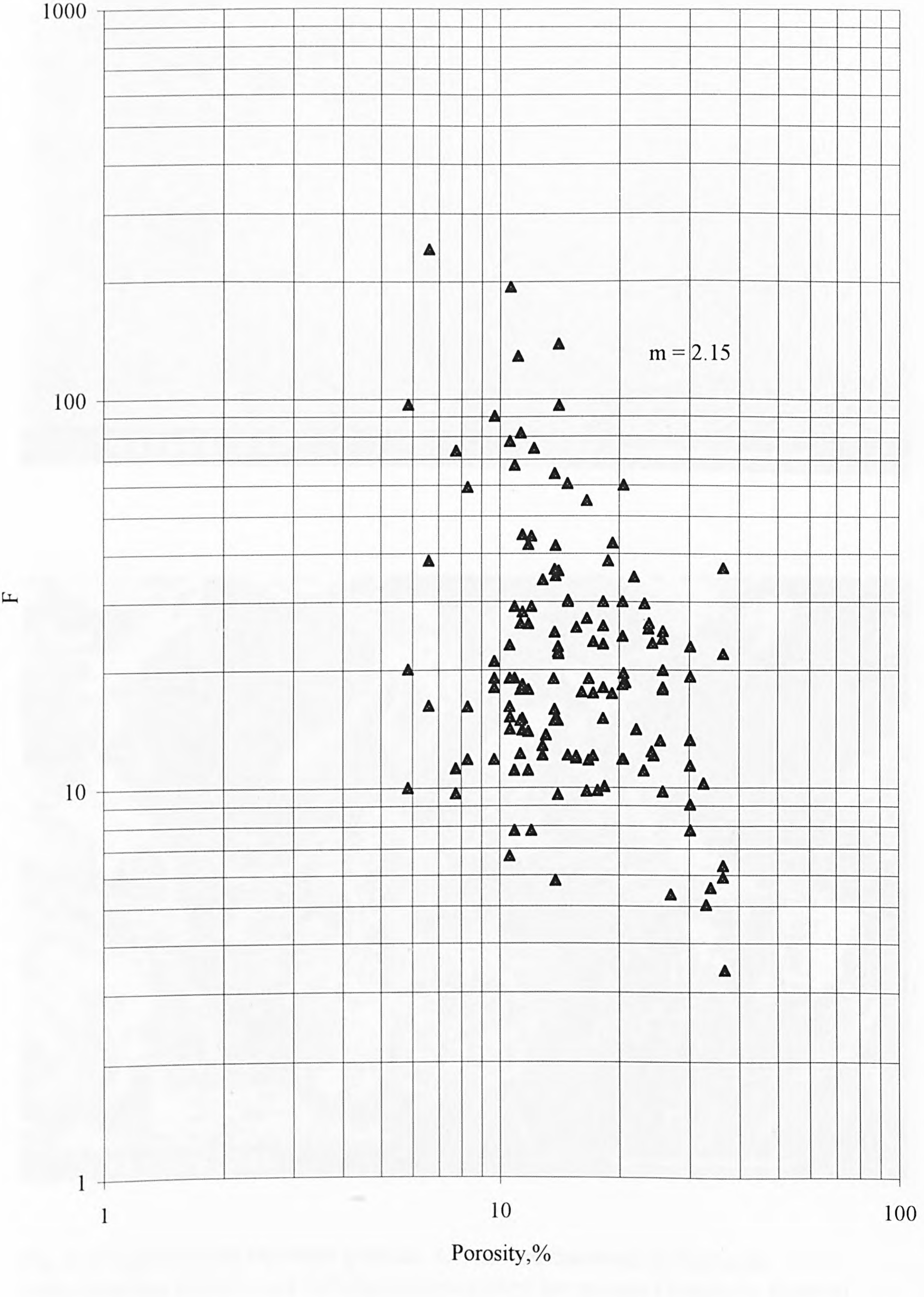

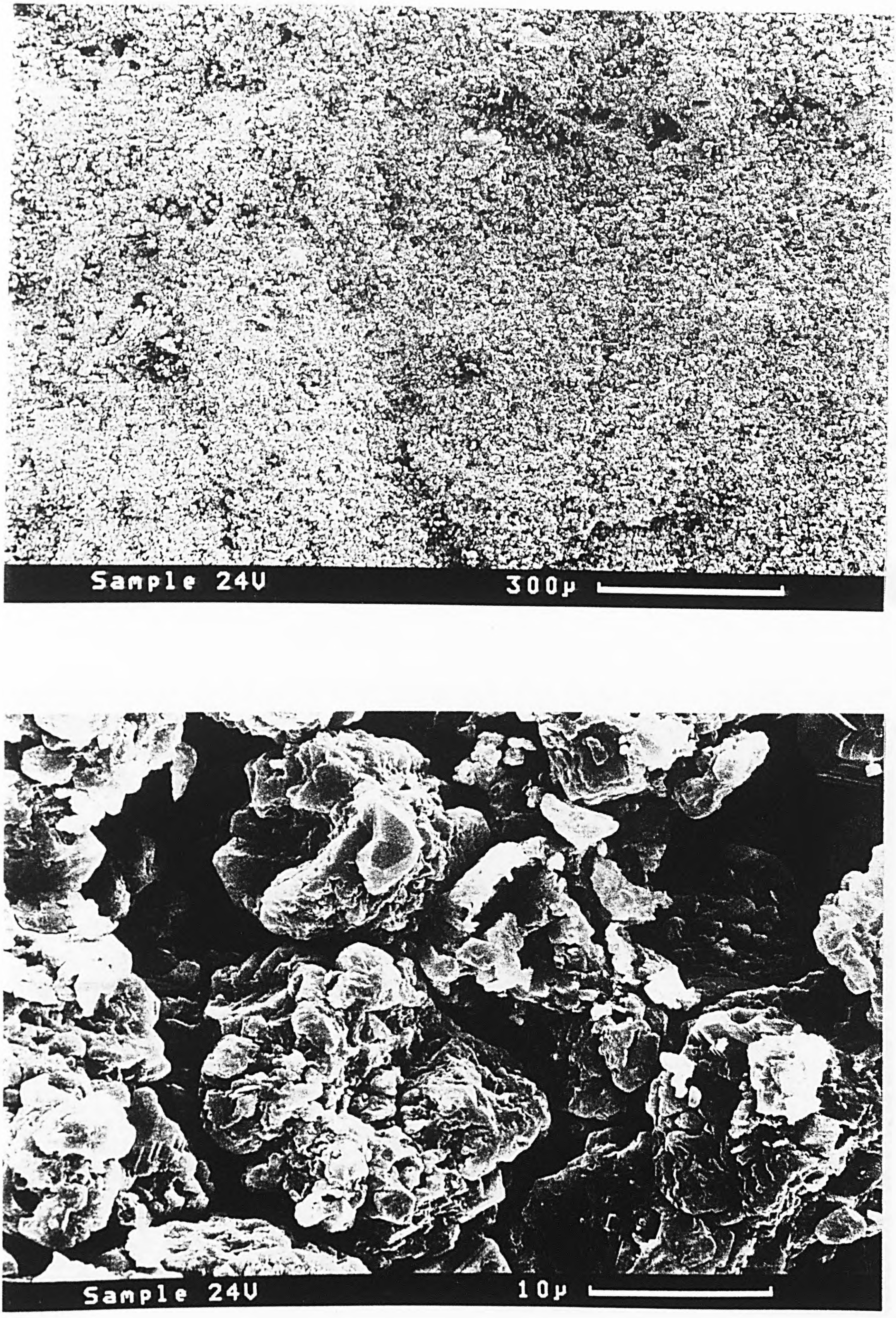

Fig. 6.4 Typical of the Dolomite granular. Crystal are dissolved or fractured. Intercrystalline porosity and variation in pore system are present (Sample 6; Zone A).

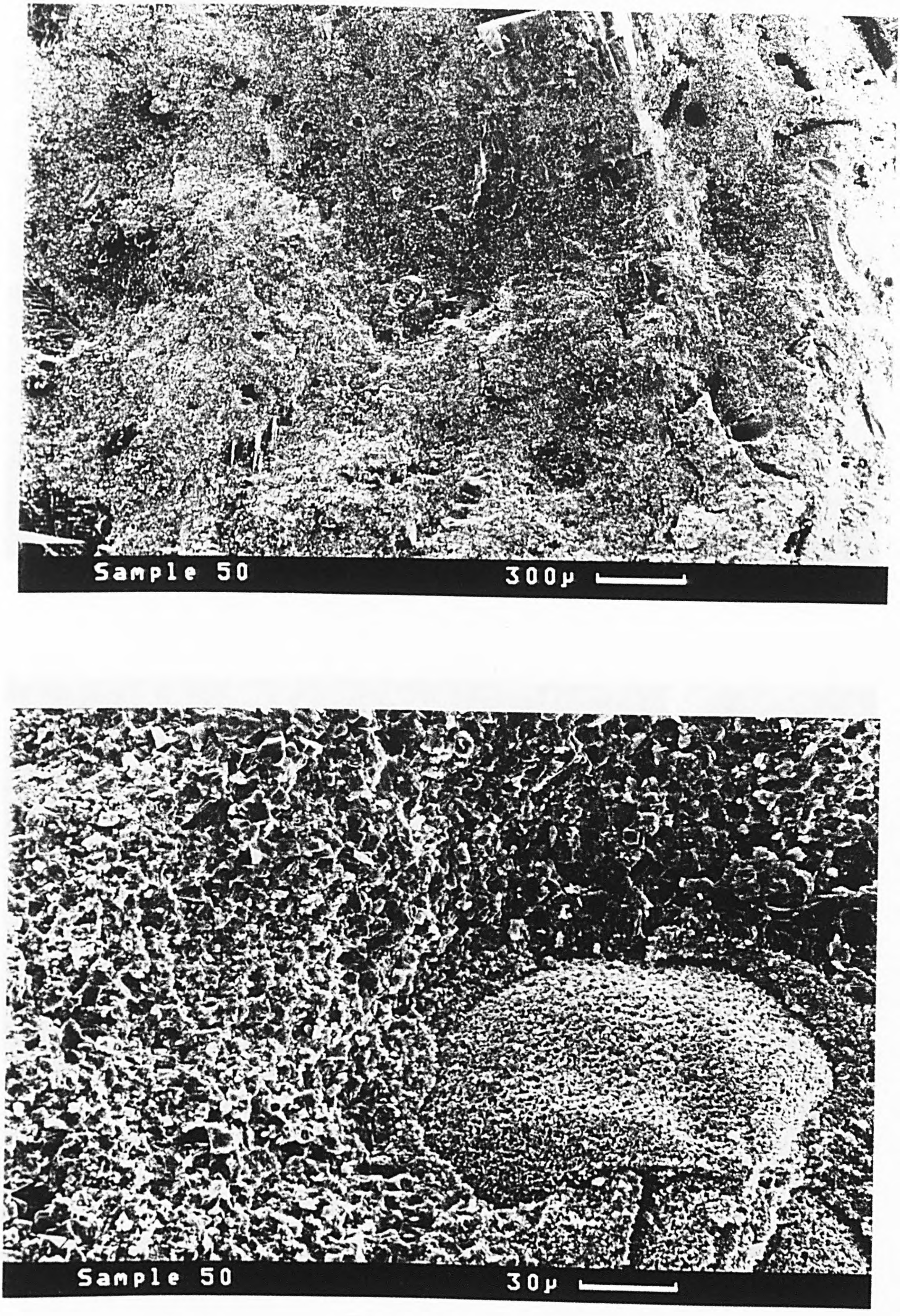

Fig. 6.5 A low porosity dolomite sample with Anhydrite and moldic porosity system with presece of Kaolite, it is heterogeneous sample (Sample 7; Zone B).

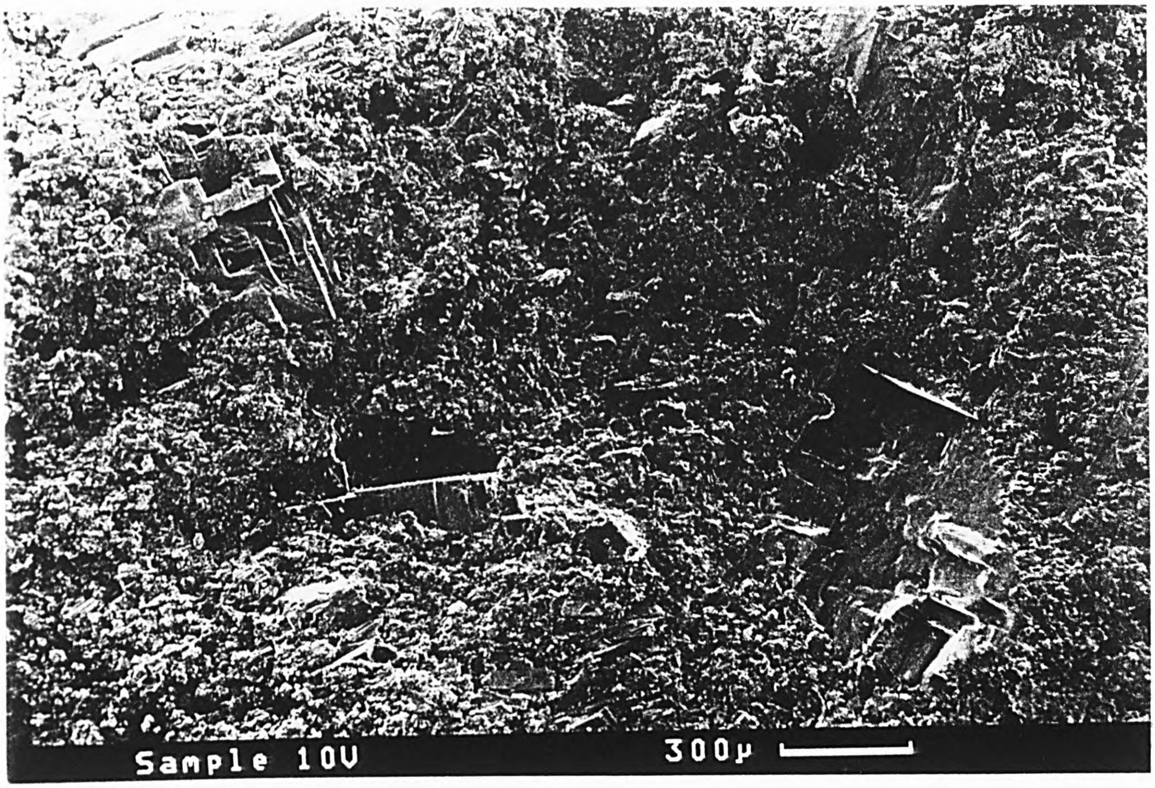

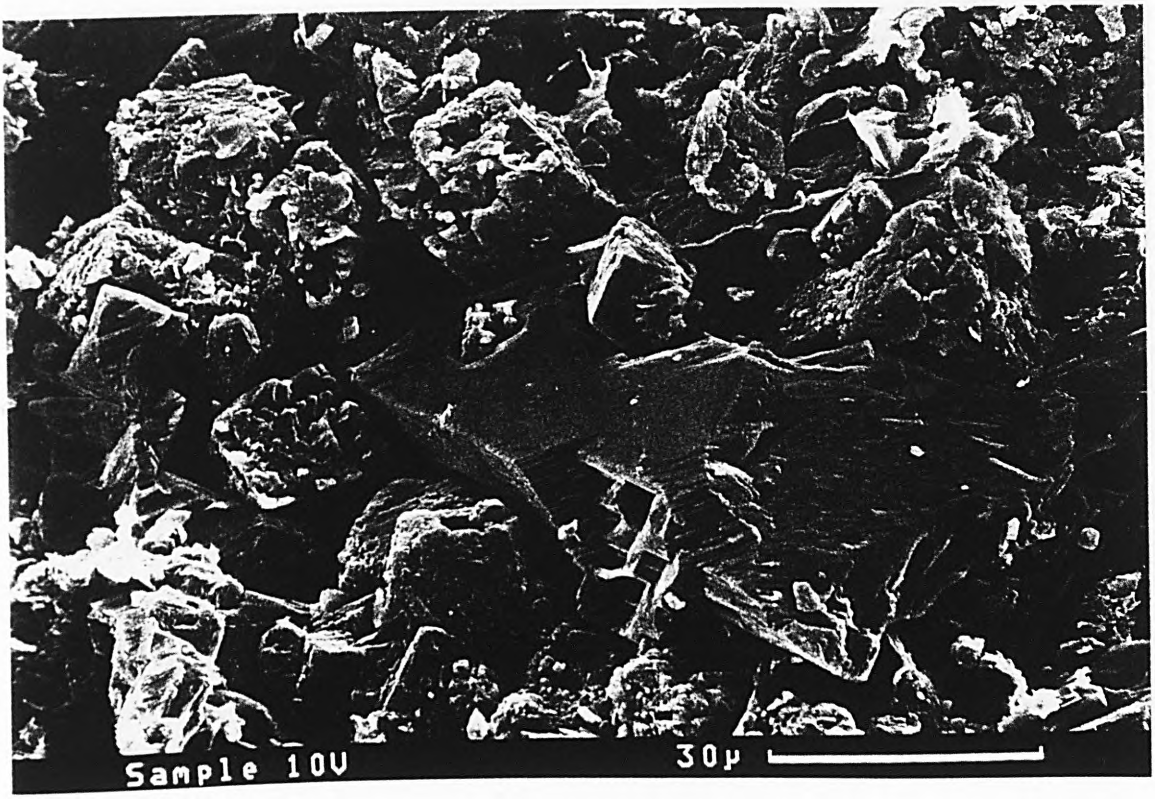

Fig. 6.6 Coarse stepped crystals are anhydrite which may formed replacively. Micropores and macropores are presence and it reflect heterogenity of this sample. Large pores may be related to dissolution-precipitation process. (sample 2; Zone C).

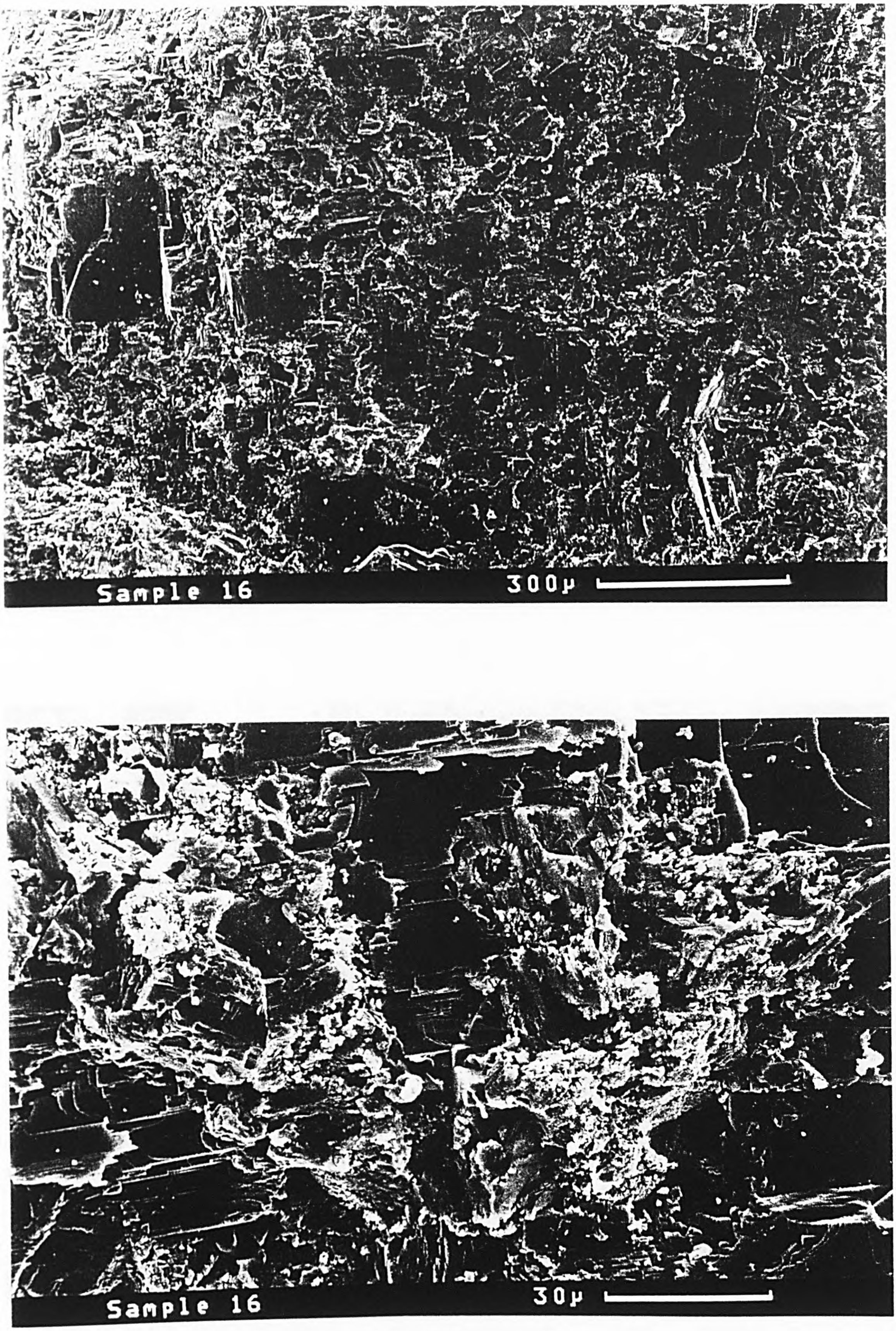

Fig. 6.7 A very low porosity sample having poorly interconnected micropores. Anhydrite is present as tight coarse crystals. Typical of the remnant porosity associated with partially dissolved carbonate. (sample 3; Zone D).

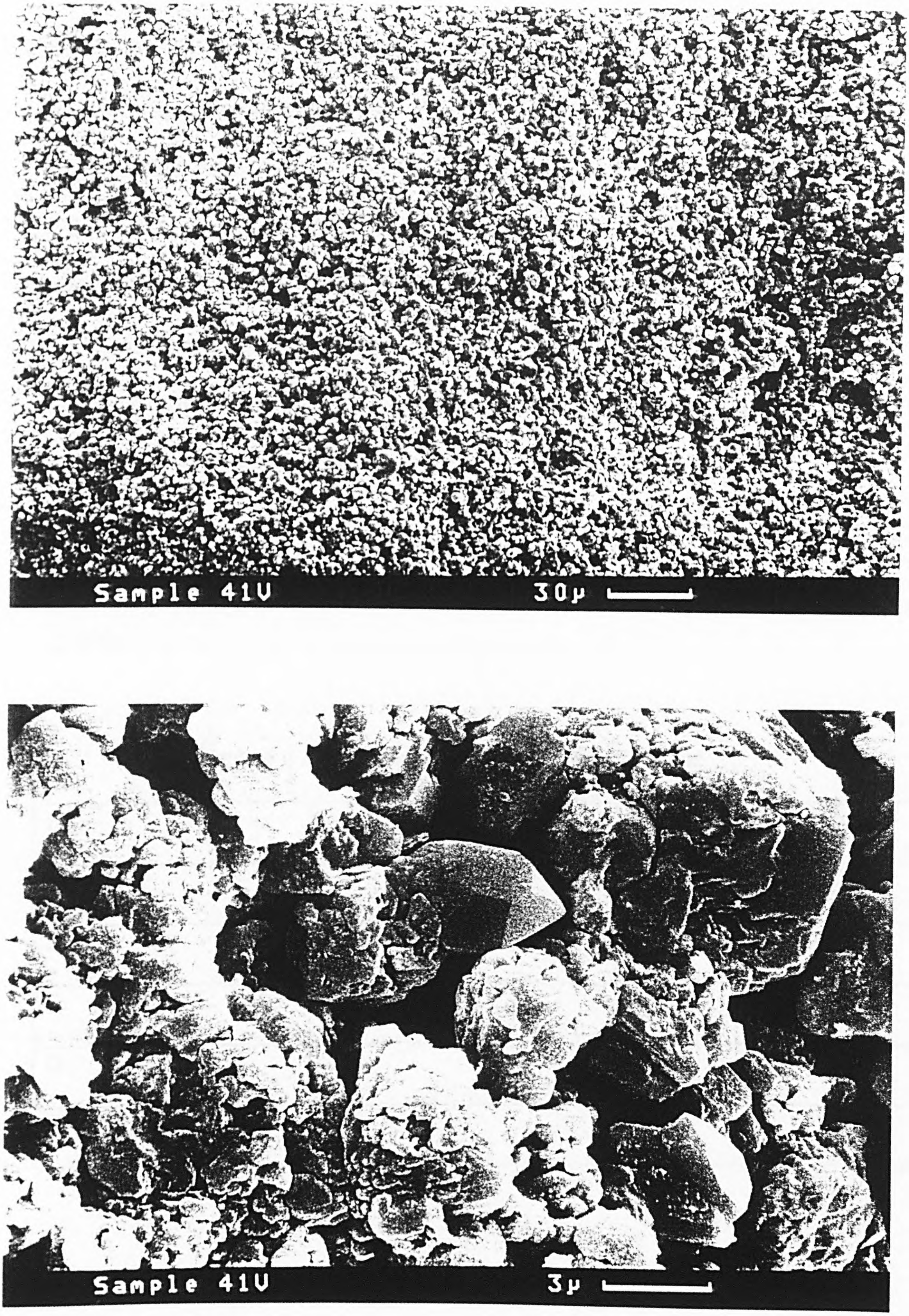

Fig. 6.8 It showing typical range of surface texture and morphologies of dolomite with multifacted forms. It is homogeneous sample and porosity is high and well interconnected, but pore throats are narrow. (Sample 8; Zone E)

had *m* values around 2 or lower. Samples having intercrystalline porosity type had *m* values significantly greater than 2 such as sample 6 (zone A). The samples having moldic or/and vuggy texture had relatively high values of m such as sample 7 (zone B). The saturation exponent values for all zones were in the medium range, varying from 2.16 to 2.78. Table 6.2 presents the average values of *m* and *n* for each zone and Table 6.3 presents the water saturation calculations and the errors which could result from the use of unrepresentative values of m and n. The error in water saturation was found to range from 3.33% to 23.26% when assuming $m = n = 2$. The errors were found to be smaller when average values of m and n for the whole formation and m, n of zone concerned are used (0.6% to 13.6%).

Table 6.2 Average values of *m* and *n* for each zone

zone	cementation factor, *m*	saturation exponent, *n*
A	2.2	2.41
B	2.5	2.78
C	2.03	2.47
D	2.04	2.23
E	1.89	2.33

Table 6.3 Water saturation calculations for each zone

Zone	R_t (Ω/m)	ϕ (%)	S_w1^* (%)	S_w2^* (%)	S_w3^* (%)	$\Delta S_w3\text{-}1$ (%)	$\Delta S_w3\text{-}2$ (%)
A	210	17	12.39	19.76	20.34	7.95	0.58
B	12	28	31.47	41.14	54.73	23.26	13.59
C	26	25	23.95	33.11	31.38	7.43	1.73
D	15	16	49.27	61.48	54.17	4.90	7.31
E	57	21	19.26	27.99	22.59	3.33	5.4

In the above table:-

Rw = 0.089 ohm/m

S_w1 indicates the saturation calculated assuming $m = n = 2$,

S_w2 indicates the saturation calculated using average values of m and n determined for the whole reservoir ($m = 2.15$, $n = 2.44$)

S_w3 indicates the saturation calculate using the average values of m and n for zone

$\Delta S_w3\text{-}1 = S_w3 - S_w1$

$\Delta S_w3\text{-}2 = S_w3 - S_w2$

It is clear that, when evaluating the potential of this carbonate reservoir, the use of the assumption that $m = n = 2$, or of an average value of m and n for the whole reservoir could lead to serious errors in water saturation determination. Some intervals or zones could be evaluated as dry when in reality they could produce hydrocarbons and vice versa.

This Libyan reservoir shows an increase of cementation factor towards its top. This increase in *m* can be attributed to variations in pore geometry which affects the water saturation determination. The Archie *m* is influence by pore geometry. It is obvious that the geometry of secondary pores can vary from zone to zone and from well to well. Even if average values of *m* and *n* for the whole formation are obtained, these should not be used to determine the water/hydrocarbon saturations.

6.7 Conclusions

The Archie cementation factor commonly varies in different rock types of the major carbonate reservoir formations. In the carbonate reservoir under investigation, which is mainly composed of dolomites with primary and secondary porosity types, Archie's parameters were found to be affected by porosity type. Dolomites and limestones that are dominated by interparticle pore systems have *m* values of approximately 2.0, also the intercrystalline porosity type has a similar *m* value. Moldic and vugular generally have *m* values greater than 2.

As a result of this work, it is strongly recommended that in log interpretation for evaluation of carbonate reservoir potential, samples from each porosity type interval or zone or facies should be collected and analysed and their *m* and *n* values used in water saturation calculations. It is concluded also that Archie's parameter can change not only from zone to zone or well to well but even point to point in the reservoir, and it would be a great achievement if m and *n* could be determined continuously throughout the reservoir in a similar manner to the porosity.

Moreover, in the absence of core data, Archie's parameters (especially *m*) can be selected more accurately by taking into account porosity type rather than using $m = n = 2$ or averaging m and n for the whole reservoir. By considering this important factor, errors in reserves and oil initially in place would be reduced. It recommended that this approach should be applied for similar carbonate formation and the results compared with other evaluation tools such as well tests and production data.

CHAPTER 7

DISCUSSION AND CONCLUSIONS

Previous chapters in this thesis dealing with different phases of the experimental work have already discussed the results presented and drawn appropriate conclusions. In this chapter these conclusions will be reviewed and assessed from the point of view of the overall objectives of the work, and recommendations will be made for further study.

In this research a variety of reservoir rock samples (sandstones and carbonates) having a wide range of petrophysical properties (porosity, permeability, pore structure, pore size distribution, etc.) have been studied in order to investigate experimentally the effects of overburden pressure, porosity type, flow displacement and fluid characteristics upon the resistivity-porosity and resistivity-saturation relationships (Archie's parameters). A case study of the Archie parameters was carried out for a carbonate formation and recommendations have been made to ensure more reliable formation evaluation for carbonate systems (sections 6.5 and 6.6).

An existing rock sample testing system was further developed and used to measure the electrical resistivity of five core plugs simultaneously under various overburden pressures. Twenty-two rock samples were tested and their Archie's parameters were measured. An experimental study was conducted to identify the effects of the flow displacement mechanism and the fluid characteristics on the resistivity - saturation relationships and on the values of Archie's saturation exponent (which is usually assumed to be independent of these factors).

7.1 Experimental Techniques

The introduction of this modified sample testing sample system speeds up rock testing and eliminates experimental errors caused by fluctuations in pressure. The apparatus was designed to permit rock samples to be tested at typical overburden pressure conditions.

Two different experimental techniques for making measurements of the electrical resistivity of rocks have been utilised, namely; the porous plate method and the continuous injection technique. These techniques are designed to represent the desaturation processes which occur in many hydrocarbon reservoirs, and to allow study of the desaturation mechanism and the effect of fluid properties on the process. The advantages and disadvantages of both methods have been discussed and evaluated (sections 3.42, 3.43, 5.3 and 6.6).

7.2 Effect of Overburden Pressure On the Electrical Rock Properties

The effect of overburden conditions of pressure on the electrical properties of rocks was investigated. A marked difference was observed between the behaviour of sandstones and the behaviour of carbonates.

7.21 Effect of Overburden Pressure on the Electrical Properties of Sandstones

An increase in the formation resistivity factor F, and the cementation factor m, with overburden pressure has been widely observed and shown to be significant for most sandstone samples studied by previous workers, and this was verified by the current study. The changes in the electrical properties of sandstones are related to the changes in porosity and the pore constrictions caused by rock deformation. The increase in resistivity due to the applied pressure was shown in the present study to depend on physical properties such as porosity, permeability, pore size distribution and cementation. A more rapid increase of resistivity with overburden pressure was found at lower pressures than at higher pressures and this is because the rocks are more compressible at lower pressures. This is due to the fact that the rocks contain a spectrum of pores having various geometries and these pores are very pressure sensitive, so that they deform significantly even at low pressures (Glanville, 1959, Jing 1990, Glover *et al.*, 1994). It was shown that considerable errors in porosity estimation (up to 18%) can be generated in log calibration if the effect of overburden pressure on m is ignored. The effects of overburden pressure on F and *m* were found to be considerably more pronounced for the less porous and permeable samples, whilst the effects for high porosity samples were relatively insignificant. This may be due to the fact that the less porous samples have a larger percentage of small pores; these undergo a greater percentage reduction in volume on pressure increase than larger pores (section 4.21 and 4.22).

7.22 Effect of Overburden Pressure on Electrical Properties of Carbonates

Significant increases of resistivity formation factor F, and cementation factor m with overburden pressure were observed in the experiments for the majority of carbonate samples. Decreases in F and *m* were however observed for other carbonate samples. Reduction in pore sizes and changes in the tortuosity of current flow paths cause an increase of F with pressure. On the other hand, the decrease in F with pressure observed in some cases may be related to the formation of micro-cracks and collapse of the cementing materials as pressure is increased. The changes in electrical properties of carbonates, however, did not correlate with the porosity and permeability of the samples. Errors in porosity estimation caused by neglect of the overburden pressure effect could reach up to 18%. However, the change in F was more pronounced at low pressures than at higher ones. Generally the changes in F and *m* for carbonates are less significant than in sandstones (section 4.21 and 4.22).

7.3 Hysteresis Effect

A significant hysteresis effect was observed in the overburden pressure experiments; it was found that F values measured as pressure is increasing with time are always smaller than those measured with pressure decreasing. For the samples tested, this effect varied with the magnitude, the increment and the duration of the applied pressure. The hysteresis observed here could be explained by time dependent rock elastic behaviour (Jing 1990, Jaeger and Cook 1977). This hysteresis effect suggested that not only the overburden pressure conditions but also the history of the pressure changes can influence the formation resistivity. More extensive tests should be undertaken to explore this effect further.

7.4 Effect of Experimental Conditions on the I_R/S_w relationships

It was concluded in this study that the resistivity - saturation relationships are affected by experimental conditions including injection rates and viscosity ratios of the fluids involved. The saturation exponent to be used to determine water saturations in log analysis should be evaluated with great caution, since the fluid characteristics and displacement conditions used in the laboratory may not be the same as those in the field and it must be emphasised that Archie's equation does not make allowance for the effects of these variables. The experimental studies carried out in the present work have demonstrated that the flow the displacement mechanism and the fluid characteristics effect on the I_R/S_w relationship significantly. They have also identified the conditions under which Archie's equation is applicable. It is concluded that due to the important influence of fluids characteristics, extra care must be taken whenever electrical resistivity measurements are performed in the laboratory, and it is recommended that fluids having properties close to those of the actual reservoir fluids should be used whenever possible.

The key observations can be summarised as follows:-

a) The electrical resistivity and saturation exponent are dependent on fluid characteristics such as the viscosity ratio between the displaced and displacing fluids and also on the injection rate.

b) The majority of the tested samples show that linearity of the I_R/S_w plots is more well-defined at low viscosity ratios than at high ones and at high injection rate.

c) At low μ_R , a high resistivity is usually observed, while the resistivity is less at high μ_R; this may be due to the effect of water left behind during the desaturation process.

d) The tested samples showed that the linearity observed covers a broad range of saturation values starting from 70 - 85 % downwards.

The experimental observations on the influence of the injection rate can be explained as follows: At low injection rates, the formed front is highly fingered and the fingers are very large because capillary forces dominate. These fingers have little transverse dispersion, and thus leave large areas un-invaded so that when the fingers meet at a point they leave behind large clusters of pores containing water by-passed by the displacing oil; this results in a nonuniform distribution, and a nonlinear I_R/S_w relationship is obtained. As the injection rate is increased, the fingers become shorter, the transverse dispersion is increased and a relatively flat front is formed which yields a semi-uniform distribution and a more linear I_R/S_w relationship is obtained. The observation on the effect of viscosity ratio can be explained as follows. At the low viscosity ratio a quasi-uniform water distribution is achieved and the electrical paths are formed by thin water films. On the other hand, at high viscosity ratios a large cluster and thick films of water paths due to uninvaded pores yield a nonuniform distribution and a nonlinear I_R/S_w relationship is obtained (Grattoni, 1994, Al-Mahtot *at al.*, 1998) (sections 3.31 and 3.32).

7.5 Non-linearity of the I_R/S_w relationship

For some of the samples tested, nonlinear I_R versus S_w plots were obtained, with the slope of each plot decreasing as S_w decreased. Multiple values of saturation exponent can be therefore derived for each sample. In order to further investigate of this effect, high pressure mercury injection tests were performed on each sample to yield pore size distributions. As a result of these tests, it was concluded that bi-modal and multi-modal pore size distributions are likely be responsible for the nonlinearity observed (Worthington and Pallatt 1992). For other samples examined, the effects of injection rate and viscosity ratio were shown to have a clear influence on the linearity of the I_R/S_w relationships even for uni-modal pore size distributions and this new and interesting observation shows that n is not only a function of pore size distribution but is sensitive to injection rate and viscosity ratio. This nonlinearity of the I_R/S_w relationship (or variation of n with Sw) has significant implications in the petrophysical evaluation of water and hydrocarbon saturations. Where a nonlinear I_R/S_w exists, the Archie saturation exponent calculated by forced linear regression can be seriously in error and the desaturation process should be allowed to proceed at least to the reservoir S_w level in order to avoid misleading extrapolation results.

7.6 Archie's Parameters of Carbonate Rocks

7.61 Carbonate Reservoir Evaluation (Case Study)

The majority of Libyan hydrocarbon production has so far come from the Sirte Basin, which has been invaded several times by the sea throughout its geological history. The hydrocarbon accumulations in this basin are associated with almost all geological formations from Pre-Cambrian through the Oligocene. In this basin, the strata are varied and the carbonate rocks mainly of upper Cretaceous and Tertiary ages. The main carbonate rocks are dolomitic limestones and dolomite which are widespread in the Northeast of the basin (where the reservoir chosen for this case study is located). The types of porosity in the Northeast of the basin include intergranular, skeletal secondary porosity, moldic and vuggy porosity as well as intercrystalline porosity, and porosity values range from 2 to 40 % (Krista 1982). In the case study described in the present work, it was found the Archie cementation factor is strongly related to porosity type while the saturation exponent is only weakly dependent on porosity type. It was concluded that in view of the complex structure of carbonate formations, and the frequent presence of multiple porosities further studies should be carried out using larger numbers of samples in order to explore their properties more fully. As a result of this case study, a better understanding of the relationship between the Archie parameters and pore type was gained. Moreover, in the absence of core data for carbonate evaluation, Archie cementation factor can be assumed with greater confidence if the porosity types are known.

7.62 Influence of the Porosity Type on Archie's Parameters

As a result of the complexity of many carbonate reservoirs, it is often difficult to determine S_w precisely, due to the wide variations in pore size, pore shape and especially secondary pores (vug, channel, fracture, mold) occurring in these formations. For effective carbonate evaluation, it is essential in the calculation of m to take into account the changes of the pore type in such rocks.

The standard Archie's equation or its modifications may not be the appropriate option because it can be shown theoretically that the flow of electricity through rock is a function of pore geometry and the flow path is more complicated in the more tortuous sample. However, because the geometry (and volume) of secondary pores in carbonate formations vary from zone to zone and from well to well in the same field, it is essential to investigate Archie's parameters as a function of porosity type. In order to carry out this investigation, carbonate rock samples having different porosity types were collected. Firstly, it was observed that Archie's parameters for these varied widely ($1.44 < m < 2.49$ and $2.16 < n < 2.78$). Secondly, it was found that the samples with mainly interparticle or intercrystalline porosity show m-values less than or equal to 2, while vuggy samples generate higher values of m and relatively high n values. The use of invalid Archie's parameters may lead to considerable errors in porosity and water saturation estimations. As a consequence, it is recommended that in log interpretation for carbonate formations, representative plug samples from each porosity type should be used in order to achieve proper formation evaluation. This will reduce the likehood of errors in the estimation of water saturation and oil initially in place. However, this work has defined a practical system whereby more representative values for m can be determined for application in log analysis to obtain more accurate hydrocarbon/water saturations over intervals with complex carbonate lithologies. The success of this technique of variable m values for carbonates can be examined and evaluated in comparison with other tools such as well tests and production data (sections 6.3 - 6.6).

Generally, in this work, the limitations, assumptions and applicability of Archie's equation have been critically evaluated for different rock types, different porosity types and various experimental conditions. It has been demonstrated that Archie's equation fits well in many cases but not in others, particularly where multiple porosity systems are present. However, many workers following Archie have attempted to established Archie-like empirical equations while unaware of the limitations of this approach.

The present study has clearly demonstrated that Archie's equation has significant limitations, and its validity depends on a number of factors such as those investigated in the current work which were not taken into account in Archie's study. Whenever laboratory experiments and data interpretation are being carried out, these limitations on the validity of the equation should be born in mind in order to ensure that it is applied properly and effectively and that misleading conclusions are avoided.

In conclusion, it is not necessary to emphasise the importance of Archie's parameters for hydrocarbon reserves estimation, commercial evaluation and reservoir management. The universally applied Archie's equation assumes the existence of exponential relationships between formation factor and porosity and between resistivity index and water saturation. The serious limitations of these relationships have been critically examined and evaluated on the basis of the experimental studies described in this work.

7.7 Recommendations

This research has shown the significant influence of various factors upon the resistivity-porosity and resistivity-saturation relationships and their resulting impact on porosity estimation and water saturation calculation from resistivity logs. Further research is recommended directed toward the improvement of the petrophysical models based on the finding of this research to cover the effect of overburden pressure, porosity type, and experimental conditions on the electrical properties of reservoir rocks. The following areas are recommended for future experimental and theoretical studies:

7.71 Suggested Experimental Work:

* The effect of temperature on Archie's parameters and the interaction of pressure and temperature effects. More development and modification in the current sample rock testing system is recommended. This should include the influence of the effective overburden pressure on Archie's parameters taking into consideration the pore pressure. Also the current experimental design should be further developed in order to permit simultaneous study of the electrical and hydraulic properties of rocks.

* The combined effects of injection rate and fluid characteristics (viscosity ratio, density, interfacial tension) should be studied for a large number of rock samples at reservoir conditions in order to gain a more complete understanding of their influence on I_R/S_w relationships. Homogeneous, heterogeneous and outcrop rock samples should be used in order to take into account the influence of homogeneity on resistivity - saturation relationships.

7.72 Suggested Physical and Mathematical Modelling:

Since it is difficult to directly observe pore and fluid distributions within rock samples, so the need to physical model (1-D, 2-D and 3-D) becomes essential. The selection of geometric characteristics is one of the key problem in modelling, because the geometry of the porous medium controls the petrophysical properties of the rocks. By incorporating pores and throats of different sizes, these models can be used to study the effects of pore size, throat size and pore shape, and pore to throat aspect ratio. In chapter 5, the influence of flow mechanism and fluid characteristics on resistivity-saturation relationship and on Archie saturation exponent has been investigated on core samples at macroscopic level. A qualitative study is required to support the findings and the conclusions of the effects of these factors on electrical properties of rock, and the need of an physical model become essential for this type of this study. Varying the experimental condition parameters and/or the structure itself can be carried out with these type of models. Also a mathematical model should be conducted along side with the physical one.

* The application of the improved dual and multiple porosity carbonate formation models and an extensive experimental investigation for wide range of carbonate samples having different types of porosity needs to be undertaken. A model and suitable equations to determine Archie's cementation factor for a carbonate formation containing intergranular, vuggy porosities with a fracture system can be developed by reconsidering the previous models (Aguilera 1980, Rasmus 1983, Watfa and Nurmi, 1987). Such a study could produce a method to measure

volumes of intergranular/vuggy porosity with fractures from well logs which would allow point-to-point calculation of Archie's cementation factor.

7.73 Core Sample Selection:

The careful selection of core samples before any fluid flow experiments are carried out is highly recommended to check their homogeneity/heterogeneity together with geological information and chemical composition which are important in data interpretation. X-ray, CT scanning and NMR are some of the rock imaging techniques that can be used for this purpose.

REFERENCES AND BIBLIOGRAPHY

Aguilera, R., 1976. Analysis of natural fractured reservoirs from convential well logs. Journal of Petroleum Technology, July, 764-772.

Aguilera, R., 1980. Naturally Fractured Reservoirs. PennWell Publishing Company.

Al-Mahtot O. B. and W. E. Mason., 1996. Reservoir description: Core data to identify flow units for a clastic North Sea reservoir. Turkish Journal of Oil and Gas, 1, Feb.

Al-Mahtot, O. B., Mason, W. E. and Nasar, M., 1997. New experimental approach in saturation exponent determination by continuous injection technique. Petroleum Research Journal, 9, 1-7.

Al-Mahtot, O. B., Mason W. E. and Adam A., 1999. Archie's parameters m and n in carbonate reservoir: Case study. An article accepted and approved for publication in Petroleum Research Journal, 10.

Al-Mahtot, O. B. and Mason W. E., 1995. Theoretical Investigation on cementation factor variations. Paper presented at the 14th Turkish Oil And Gas Conference, Ankara, Turkey, April.

Al-Mahtot O. B. and Mason W. E., 1997. Effect of viscosity ratio upon Archie's saturation exponent. Paper presented at Meditererian Petroleum Conference MPC 97, Tripoli - Libya, November 21-23.

Al-Mahtot O. B. and Mason W. E., 1998. Determination of Archie saturation exponent by continuous injection technique). *DiaLog* Magazine of London Petrophysical Society, August - September, 4, 8-9.

Al-Mahtot O. B. and Mason W. E., 1998. Effect of fluid characteristics and flow mechanism on Archie saturation exponent. Paper (#9814) presented to Society of Core Analysis SCA, International Symposium, Huge, Netherlands, September.

Amin, S. A., Watfa, M. and Awad, A., 1987. Accurate estimation of water saturation in a complex carbonate reservoir. SPE paper 15714, presented at the 5th Middle Eastern Oil Show, Bahrain, March 7-10.

Amott, E., 1959. Observation relating to the wettability of porous rock. Trans. AIME, 216, 156-162.

Amyx, J. W., Bass, D. W. and Whiting, R. L., 1960. Petroleum Reservoir Engineering. New York: McGraw-Hill.

Anderson, W. G., 1986. Wettability literature survey - Part 3: the effects of wettability on the electrical properties of porous media. JPT, 1371 - 1378.

Archer, J. S. and Jing, X. D., 1991. The influence of reservoir condition measurements of shaly sand electrical properties on equity studies. Paper L, Trans. of the 14th European Formation Evaluation Symposium, London, December.

Archer, A. S. and Wall, P. G., 1992. Petroleum Engineering Principles and Practice. London: Graham and Trotman.

Archie, G. E., 1942. The electrical resistivity log as an aid in determining some reservoir characteristics. Trans., AIME, 146, 54 - 62.

Archie, G. E., 1947. Electrical resistivity as an aid in core-analysis interpretation. AAPG Bull., 31, (2), 350-366.

Archie G. E., 1952. Classification of carbonate reservoir rocks and petrophysical considerations. AAPG Bull., 36 (2), 278 - 298.

Argaud M., Giouse, H., Straley, C., Tomanic J. and Winkler, K., 1989. Salinity and saturation effects on shaley sandstone conductivity. SPE paper 19577 presented at the 64th SPE Annual Technical Conference and Exhibition, San Antonio, October 8-11.

Arps, J. J., 1953, The effect of temperature on the density and electrical resistivity of sodium chloride solutions. Trans. AIME, 198, 327-330.

Asquith, G. B., 1985. Handbook of log evaluation techniques for carbonates reservoir. AAPG, Tulsa, OK.

Asquith, G. B.,1982. Basic well log analysis for geologists. AAPG, Tulsa, OK.

Asquith, G. B. and Gibson., 1982. Basic well analysis for Geologists: AAPG Methods in Exploration. No. 3.

Baldwin, B. A. and Yamanashi, W. S., 1989. Persistence of nonuniform brine saturation distribution in SCA electrical resistivity study core plugs after desaturation by centrifuging. The Log Analyst, January - February, 45-49.

Borai, A. M., 1987. A new correlation for the cementation factor in low-porosity carbonate. SPE Formation Evaluation, Dec., 120-132.

Brace, W. A., Orange, A. S. and Madden, T. R., 1965. The effect of pressure on electrical resistivity of water saturated crystalline rocks. Journal of Geophy. Res., 67, 5669.

Brace, W. F. and Orange, A. S., 1968. Further studies of the effects of pressure on electrical resistivities of rocks. Journal of Geophy. Res., 73, 5407.

Britains Offshore oil and gas, 1988. UK offshore operators association (UKOOA) and the Natural History Museum Booklet. First Edition.

Carmen, P. C., 1937. Fluid flow through granular beds. Tans. Inst. Chem. Eng., (15), p. 150, London.

Carothers, J. E., 1968. A statistical study of the formation factor relation to porosity. The Log Analyst, September - October, 9, (5), 13-20.

Carothers, J. E. and Porter, C. R., 1970. Formation factor - porosity relation from well log data. Trans. 11th Annual Logging Symposium, May.

Choquette, P. W. and Pray, L. C., 1970. Geologic nomenclature and classification of porosity in sedimentary carbonates. Bull. AAPG, 54, (2), 207 - 250.

Cornell, D and Katz, D. L., 1953. Flow of gases through consolidated porous media. Ind. Eng. Chem., 45, 2145.

Cosse R., 1993. Basic of Reservoir Engineering. Series: oil and gas field development techniques. France: Editions Technip.

de Wall, J. A., Smits, R. M., de Graaf, J. D. and Schipper, B. A., 1991. Measurements and evaluation of resistivity index curves. The Log Analyst, September - October, 583-595.

Darcy, H., 1856. The public fountains in the Town of Dijon. V. Dalmont, Paris.

Donaldson, E. C., Chilinganan G. V. and Yen T. F., 1985. Enhance oil recovery: I Fundamentals and Analysis. Amsterdam, Oxford: Elsevier.

Donaldson, E. C. and Siddique, T. K., 1987. Relationship between Archie saturation exponent and wettability. SPE paper 16790, presented at the 62nd SPE Annual Conference and Exhibition, Dallas, Texas.

Dolandson, E. C., Thomson, R. D. and Lorenz, P. B., 1969. Wettability determination and its effect on recovery efficiency. SPE J., March, 13-20.

Doveton J. H., 1986. Log analysis of subsurface geology: concepts and computer methods. New York, John Wiley.

Doyen, P. M., 1987. Crack geometry in igneous rocks: a maximumentrpy inversion of elastic and transport properties. J. Geophys. Res. (92), B8, p. 8169 - 8181.

Dunlap, H. F., Bilhartz, H. L., Shuler, E. and Bailey, C. R., 1949. The relation between electrical resistivity and brine saturation in reservoir rocks. JPT, 259-264.

Dullien, F. L., 1992. Porous Medium; Fluid transport and pore structure, 2nd Edition. Academic Press, INC., London.

Elashahab B. M., Jing, X. D. and Archer J. S., 1995. Resistivity index and capillary pressure hysteresis for rock samples of different wettability characteristics. SPE paper 29888, presented at SPE Middle East Oil Show, Bahrain, March 11-14.

Elashahab, B. M., Jing, X. D. and Archer, J. S., 1993. Laboratory determination of Archie saturation exponent of various water-wet and oil-wet sandstone rocks at reservoir conditions. In: Proceeding of the 2nd Mediterranean Petroleum conference, MPC 93, Tripoli-Libya.

Fatt, I., 1957. Effect of overburden and reservoir pressure on electrical logging formation factor. AAPG Bull., 1957, 41.

Fjaer E., Holt R. M, Horsrud P., Raaen A. M and Risnes R., 1992. Petroleum Related rock mechanics. Developments in petroleum sciences, 33. Amsterdam: Elsevier.

Focke, J. W. and Munn, D., 1985. Cementation exponent in Middle East carbonate reservoirs. SPE paper (13735) presented at the SPE 1985 Middle East Oil Technical Conference and Exhibition. Bahrain, March 11-14.

Fricke, H. A., 1924. A mathematical treatment of the electric conductivity and capacity of disperse system. Physical Review, 24, 575 - 587.

Gant, P. L. and Anderson, W. G., 1988. Core cleaning for restoration of native wettability. SPE Formation Evaluation, p. 131-138.

Glanville, R. R., 1959. Laboratory study indicates significant effects of pressure on resistivity of reservoir rock. JPT, April, 20-26.

Glover P. W. J., Baud, P., Darot, M., Meredith P. G., Boon S. A., LeRavalec M., Zoussi S. and Reuschle, T. 1995. α/β phase transition in quartz monitored using acoustic emissions. Geophys. J. Int., (120), P. 775 -782.

Glover P. W. J., Gomez J. B., Meredith P. G., Boon S. A., Sammond P. R. and Murrell S.A., 1996. Modelling the stress-strain behaviour of saturated rocks undergoing triaxial deformation using complex electrical conductivity measurements. Survey in Geophysics, 17, 307-330.

Glover P. W. J., Meredith P. G., Sammond P. R. and Murrell S. A., 1994. Measurements of complex electrical conductivity and fluid permeability in porous rocks at raised confining pressures. In: Proceedings Eurock 94 Conference, Balkema, Rotterdam.

Gomes-Rivero, O., 1976. A practical method for determining cementation exponent and some other parameters as an aid in well log analysis. The Log Analyst, September - October.

Grattoni, C. A., 1995. Influence of pore scale structure on electrical resistivity of reservoir rock. D. Phil. thesis, Imperial College, University of London.

Grattoni, C. A. and Dawe, R. A., 1996. Influence of fluid distribution upon electrical resistivity of partially saturated media. Paper presented at the 36th Annual SPWLA Symposium, Paris, June 26-29.

Gray, R., Trewin, B., Pallatt, N. and Mitchell, P., 1992. Comparison of saturation exponent data by the porous plate and by the continuous injection technique with in-situ saturation monitoring. In: Proceedings Third European Core Analysis Symposium (EUROCAS III), Paris, September 14-16.

Grist D. M., Langley G. O. and Neustadter E. L., 1975. The dependence of water permeability on core cleaning method in the case of some sandstone samples. J. Can. Pet. Technical, 48-52.

Gueguen, Y. and Palciauskas, V., 1994. Introduction to the physics of rocks.Princeton University Press, New Jersey

Guillotte J. G., Schrank J. and Hunt E., 1979. Smackover reservoir: Interpretation case study of water saturation versus production: Gulf Coast Ass. Geo. Societies, Trans., 29, 121 - 126.

Guyod, H., 1944. Fundamental data for the interpretation of electric logs. Oil Weekly, October, 115, 38.

Guyod, H., 1948. Electrical developments in the USSR. World Oil, Aug.

Hausenbles, M., 1995. Stress dependence of cementation factor. SCA paper (9518), presented at the International Symposium of Society of core analysis, San Francisco, September.

Hawes R. I., Dawe R. A., Evans R. N. and Grattoni C. A., 1996. The depressurization of water-flooded reservoir; wettability and critical gas saturation. Journal of Petroleum Geoscience, 2, 117 - 124.

Helander, D. P. and Camble, J. M., 1960. The effect of pore configuration, pressure and temperature on rock resistivity. Paper W, Trans. SPWLA, Tulsa, Oklahoma.

Hilchie, D. W., 1964. The effect of pressure and temperature on the resistivity of rocks. D. Phil. thesis, The university of Oklahoma.

Hilchie, D. W., 1982. Applied openhole log interpretation for geologists and engineers, Department of petroleum engineering, Colorado, School of Mines, Golden, CO.

Idris M., 1995 - 96. Personal Communications. Petroleum Research Centre, Tripoli - Libya.

Ives, D. G. and Janz, G. J., 1961. Reference electrodes: theory and practice. New York: Academic Press.

Jackson, P. D., Taylor-Smith, D. and stanford, P. N., 1978. Resistivity-porosity-particle shape relationship for marine sands. Geophysics, 43, 1250-1268.

Jaeger, J. C. and Cook, N. G., 1977. Fundamental of rock mechanics. London: Chapman and Hall.

Jakosky, J. J. and Hopper, R. H., 1937. The effect of moisture on the direct current resistivities of oil sands and rocks. Geophysics, 2, 33 - 35

Jing, X. D., 1990. Effect of pressure, temperature and clay on the electrical and hydraulic properties of synthetic and natural rocks. D. Phil. thesis, Imperial College, University of London.

Jing, X. D. and Archer J. S., 1991a. Special core analysis consideration in the determination of electrical properties of shaly rocks at reservoir conditions. In: **P. Worthington, and D. Longeron,** eds. Advances In Core Evaluation II; Reservoir Appraisal. Reading : Gordon and Breach Sciences.

Jing, X. D., Archer, J. S. and Daltaban, T. S., 1992. Laboratory study of the electrical and hydraulic properties of rocks under simulated reservoir conditions. Marine and Petroleum Geology, 9, 115-127.

Jing, X. D., Archer, J. S. and Elashahab, B. M., 1993. Experimental investigation of the effect wettability, saturation history and overburden pressure on resistivity index. In: Proceedings 15th European Evaluation Symposium, SPWLA, May 5-7.

Jing X. D., Gillespie A., and Trewin B. M., 1993. Resistivity index from non-equilibrium measurements using detailed in-situ saturation monitoring. SPE paper 26798, presented at the Offshore European Conference, Aberdeen, September 7-10.

Keelan, D. K., 1972. Critical review of core analysis techniques. J. Can. Pet. Tech. (April), p. 42-55.

King, M. S., 1965. Acoustic velocities in rocks as a function of changes in overburden pressure and pore fluid saturants. Geophysics, 31, 50-73.

Klinkenberg, L. J. 1941. Permeability of porous media to liquids and gases. Drill and Prod. Prac., API, p. 200.

Koerperic E. A., 1975. Utilisation of Waxman-Smits equations for determining oil saturation in a low salinity, shaley sand reservoir. JPT, 27, 1204 - 1208.

Moore, J., 1958. Laboratory determined electric logging parameters of Bradford Third sand. Prod. Monthly, p.30-39.

Krista, M. S., 1982. Hydrocarbon geology of Libyan, Western desert and Nile Delta. M. Sc thesis, Aberdeen University.

Lang, W. H., 1976. Porosity - resistivity cross plots can help to evaluate formations. The Oil and Gas Journal, Novomber.

Lewis M. G., Sharma M. M., Dunlap H. F. and Dorfman M. H., 1986. Wettability and stress effect on saturation and cementation exponents Paper K, Trans. SPWLA, 29th Annual Logging Symposium, San Antonio, Texas, June.

Lewis, M. G., Sharma, M. M. and Dunlap, H. F., 1988. Techniques for measuring the electrical properties of sandstone cores. SPE paper 18178, presented at the 63rd SPE Annual Conference and Exhibition, Houston, October 2-5.

Leverette, M. C., 1939. Flow of oil-water mixtures through unconsolidated sands. Trans AIME, 132, 149-171.

Longeron D. G., Argaud M. J. and Bouvier L., 1989. Resistivity index and capillary pressure measurements under reservoir condition using crude oil. SPE paper (19589) presented at the 64th SPE Annual Technical Conference and Exhibition, San Antonio, Texas, October 8-11.

Longeron, D. G., Argaud M. J. and Feraud, J. P., 1986. Effect of overburden pressure, nature and microscopic distribution of the fluids on electrical properties of rock samples. SPE paper 15383, presented at the 61st SPE Annual Technical Conference and Exhibition, New Orleans, October 5-8.

Lovell, M. A. and Pezard, P. A., 1990. Electrical properties of basalts from DSDP hole 504B: a key to the evaluation of pore space morphology. **A. Hurst, M. A. Lovell, and A. C Morton,** eds. Geological applications of wirelines logs geological society special publications No. 48, pp. 339-345.

Lucia, F. J., 1983. Petrophysical parameters estimated from visual description of carbonate rocks: A field classification of carbonate pore space. JPT, March , 629-637.

Luffel, D. L. and Randall, R. V., 1960. Core handling and measurements techniques for obtaining reliable reservoir characteristics. SPE paper 1642-G, presented at the 1960 SPE Formation Evaluation Symposium, Houston, November.

Lyle, W. D. and Mills, W. R., 1989. Effect of nonuniform core saturation on laboratory determination of Archie saturation exponent. SPE Formation Evaluation, March, 49 - 52.

Maerefat N. L., Baldwin B. A., Chaves A. A., LaTorraca G. A., 1990. SCA guidelines for sample preparation and porosity measurements of electrical resistivity samples. The Log Analysts, March -April, 68 - 75.

Mahmood, S. M., Maerefat, N. L., and Chang, M. M., 1988. Laboratory measurements of electrical resistivity at reservoir conditions. SPE paper 18179, presented at the 63rd SPE Annual Technical Conference and Exhibition, Houston, October 2-5.

Martin, M., Murray, G. H. and Gillingham W. J., 1938. Determination of potential productivity of oil-bearing formation by resistivity measurements. Geophysics, 3, 258 - 272.

Maute, R. E., Lyle, W. D. and Sprunt, E. S., 1992. Improved data-analysis method determines Archie parameters from core data. JPT, 103-107.

Maxwell, J. Clerk., 1954. A treatise on electricity and magnetism. New York: Dover Publications Inc., 1.

Mitchell-Tapping, H. J., 1983. Petrophysical evaluation of the Smackover Oomoldic porosity of East Taxas of southern Arkansas. The Log Analysts, 24, 4, July - August, p.3 - 13.

Monicard, R. P., 1980. Properties of reservoir rocks: Core analysis. Graham and Trotman.

Moore, J., 1958. Laboratory determined electric logging parameters of Bradford third sand Prod. Monthly, March, p. 30 - 39.

Morrow, N. R., 1990. Wettability and its effect on oil recovery. JPT, December, 1476 - 1484.

National Oil Corporation, 1980a. Geological studies of Libyan carbonate formations: Sirte Basin. Geology Department, Internal Report, NOC, Libya.

National Oil Corporation, 1988b. Core and Log data of some north-east sirte basin carbonate reservoirs. Internal Reports, Formation Evaluation, NOC, Libya, 1988.

Neustaedter, R. H., 1968. Log evaluation of deep Ellenburger gas zones. SPE paper 2071, presented at the Deep Drilling and Development Symposium-Delaware Basin of the SPE of AIME, Monahans, Texas, March.

Noman, R. and Archer J. S., 1987. The effect of pore structure on non-Darcy gas flow in some low permeability rocks. SPE (#16400) presneted at SPE/DOE low permeability reservoir symposuim held at Denver, Colorado, May 18-19.

Noman, R., Shrimanker, N. and Archer J. S., 1985. Estimation of the coefficient of inertial resistance in high-rate gas wells. SPE (#14207) presented at 6oth Annual Conference and Exhibition of the Society of Petroleum Engineering held in Las Vegas, September 22-25.

Nugent W. H., Coates G. R. and Peebler R. P., 1978. A new approach to carbonate analysis. In: Proceedings 19th Annual Logging Symposium, SPWLA, paper O.

Nurmi, R. D., 1984. Carbonate pore system: porosity-permeability relationship and geological analysis. AAPG Annual Meeting, San Antonio, May.

Owen, J. E., 1952. The resistivity of a fluid-filled porous body. Trans. AIME, p. 169.

Parkhomenko, E. I., 1982. Electrical resistivity of minerals and rocks at high temperature and pressure. Review of Geophysical and space Physics, 20, 193.

Perez-Rosales, C., 1976. Generalisation of the Maxwell equation for formation resistivity factor. JPT, 819 - 824.

Petroleum Research Centre, 1985. Geological description of some north-east Sirte basin carbonate reservoirs. Geology and Petrophysics Department. Internal Reports, PRC, Libya.

Pirson, S., 1958. Oil reservoir engineering. Michigan: McGraw-Hill.

Pittman, E. D., 1984. The pore geometries of reservoir rocks. Physic and Chemistry of porous media, Proceedings of AIP Conferences edited by **D. L. Johnson and P. N. Sen,** 107, 1 - 19.

Pittman, E. D. and Thomson, J. B., 1979. Some applications of scanning electron microscopy to the study of reservoir rock. SPE 7550, paper presented at the SPE 53rd Annual full Technical Conference and exhibition. Houston.

Purcell, W. R., 1949. Capillary pressures - their measurement using mercury and the calculation of permeability therefrom. Trans. AIME, (186), p. 39 - 48.

Raiga-Clemenceau, J., 1977. The cementation exponent in formation-porosity relation: the Effect of permeability. In: Proceedings 18th Annual Logging Symposium of SPWLA, June 5-8.

Ransom, R. C., 1984. A contribution toward a better understanding of the modified Archie formation resistivity factor relationship. Log Analyst, 25, (2), 7-12.

Rasmus, J., 1983. A variable cementation exponent for fractured carbonates. The Log Analyst, 24, (2), 7 - 11.

Rasmus, J. C. 1986. A summary of the effects of various pore geometries and their wettability on measured an in situ values of cementation and saturation exponents. Trans., SPWLA, 27th Annual Logging Symposium. Houston, TX.

Redmond J. C., 1962. Effect of simulated overburden pressure on the resistivity, porosity and permeability of selected sandstones. D. Phil. thesis, Pennsylvania State University.

Reynolds H. R., 1961. Rock mechanics. London: Crosby Lockwood and Son Ltd.

Revil, A. and Glover, P. W. L., 1998. Nature of surface electrical conductivity in natural sands, sandstones, and clays. Geophysical Research Letter, (25), 5, p. 691- 694.

Rieke, H. H., Chilinger, G. V., and Munnon, R.W., 1972. Oil and gas production from carbonate rocks. New York: American Elsavier Publishing Company, Inc.

Robertson Research, 1995. Core Analysis. Roberston Publication courses.

Rust, C. F., 1952. Electrical resistivity measurements on reservoir rock samples by the two-electrode and four-electrode methods. Trans. AIME, 195, 217-224.

Sanyal, S. K., 1972. The effect of temperature on electrical resistivity and capillary pressure of porous media. D. Phil thesis, Stanford University.

Sawyer, D. T. and Roberts, J. L., Jr., 1974. Experimental electrochemistry for chemists. New York: John Wiley and sons.

Schlumberger, 1989. Log interpretations principles/applications. Schlumberger Eductional Services.

Serra, O., 1984. Fundamentals of well-logging interpretation, I. The Acquisition of Logging Data. 'Developments in petroleum science, 15A', Translated from the French by **Westaway P. and Abbott H.** Amsterdam: Elsevier.

Shell, 1984. Log interpretation charts, Schlumberger, Houston, 15.

Slawinski, A., 1926. Conductivity of an electrolyte containing dielectric bodies. J. Chem. Phys., 23, 710 - 727.

Sprunt, E. S., Desai, K. P., Coles, M. E., Davis R. M. and Muegge, E. L., 1991. CT-Scan-Monitored electrical resistivity measurements show problem achieving homogeneous saturation. SPE paper 21433 presented at the SPE Middle East Oil Show, Bahrain.

Sonden, E., Bratteli, F., Kolltveit, K. and Normann, H. P., 1992. A comparison between capillary pressure data and saturation exponent at ambient condition and at reservoir conditions. Formation Evaluation, March, 34-40.

Sundberg, K., 1932. Effect of impregnating waters on electrical conductivity of solids and rocks. Petroleum transaction of the AIME, 97, 367 - 391.

Swanson B. F., 1985. Microporosity in reservoir rocks: Its measurements and influence on electrical resistivity. Paper H, Trans. SPWLA 26th Annual Logging Symposium, Dallas, June.

Sweeney, S. A. and Jennings, H. Y., 1960. Effects of wettability on electrical resistivity of carbonate rock from a petroleum reservoir. J. Phys. Chem., 64, 551 - 553.

Timur, A., Hempkins, W. B. and Worthington, A, E., 1972. Porosity and pressure dependence of formation resistivity factor for sandstones. In: Proceedings of 4th Formation Evaluation of Canadian Well Logging Society, Calgary, May 9-10.

Tixier, M. P. and Martin, M., 1954. History of logging and future development. Canadian oil and gas industries, 7, (8).

Tixier, M. P., 1951. Porosity index in Limestone from electrical logs. Oil and Gas Journal.

Unalmiser S. and Funk J., 1998. Engineering core analysis. Distinguished Author Series. JPT, April, 106 - 114.

Wardlaws, H. W. R., 1971. Optimisation of rotary drilling parameters. D. Phil. thesis, University of Texas.

Wardlaw, N. C., 1976. Pore geometry carbonate rocks as revealed by pore casts and capillary pressure. AAPG Bull., 2, 60, p. 245 - 257.

Watfa M. and Nurmi R., 1987. Calculation of saturation, secondary porosity and productivity in complex middle East carbonate reservoirs. Paper cc presented at the 28th SPWLA Annual Logging Symposium, June-July.

Waxman, M. H. and Smits, L. J. M., 1968. Electrical conductivities in oil bearing shaley sands. SPE Journal, (8), p. 107 - 122.

Wendle, D. L., Anderson, W. G. and Meyers, J. D., 1987. Restored state core analysis for the Hutton reservoir. SPE, Formation Evaluation, December.

Western Atlas International 1992. Atlas Wireline Service: Introduction to wireline log analysis. Houston: Western Atlas International, Inc.

Wie, J. Z. and Lile, O. B., 1992. Hysteresis of the resistivity index in unconsolidated porous media. SCA paper (9212), presented at the 33rd Annual Symposium of the SPWLA , Oklahoma City, June 15-17.

Winsauer, W. O., Shearin, Jr., H. M. Masson, P. H. and Williams, M., 1952. Resistivity of brine-saturated sands in relation to pore geometry. Bull. AAPG, 36, (2), 253 - 277.

Worthington, A. E. Hedges, J. H. and Pallatt, N., 1990. SCA guidelines for sample preparation and porosity measurements of electrical resistivity samples. Part I-Guidelines for preparation of brine and determination of brine resistivity for use in electrical resistivity measurements. The Log Analyst, January - February, 23-40.

Worthington, P. and Longeron, D., 1991. Advances in core evaluation II 'Reservoir Appraisal' Reading: Gordon and Breach Science Publishers.

Worthington, P. and Pallatt, N., 1992. Effect of variable saturation exponent on evaluation of hydrocarbon saturation. SPE Formation Evaluation, December, 331 - 336.

Worthington, P., Pallatt, N., and Toussaint-Jackson, J. E., 1989. Influence of microporosity on the evaluation of hydrocarbon saturation. SPE Formation Evaluation, June, 203 - 209.

Wyble, D. O., 1958. Effect of applied pressure on the conductivity, porosity and permeability of sandstones. Trans. AIME, 213, 430.

Wyckoff, R. D. and Botset, H. G., 1936. The flow of gas-liquid mixture through unconsolidated sands. Physics, 7, (9), 325 - 345.

Wyllie, M. R. and Gregory, A. E., 1953. Formation factor of unconsolidated porous media: influence of particle shape and effect of cementation. Trans. AIME, 198, 103 -110.

Wyllie, M. R. J., 1953. Formation factor of unconsolidated porous media: Influence of particle shape and effect of cementation, Trans. AIME.

Wyllie, M. R. J. and Gardner, G. H. F., 1958. The generalised Kozeny-Carman equation. World Oil, March-April.

Wyllie, M. R. J. and Spangler, M. B., 1952. Application of electrical resistivity measurements to problem of fluid flow in porous media. Bull. AAPG, 36, 359-403.

Yale, D. P., 1984. Network modelling of flow storage and deformation in porous rock. D. Phill. thesis, Stanford University, California.

Zeelenberger P. W. and Schipper B.A., 1992. Developments in I_R-S_w measurements. Paper presented at the 3rd European Core Analysis Symposium (EUROCAS III), Paris, September.

PPENDIX A

ROUTINE ROCK CHARACTERISATION

(a) Porosity Measurements

Porosity is defined as ratio of pore volume to the bulk volume of a porous media. It can either be total or effective. Total porosity is defined as the ratio of the total pore volume both interconnected and isolated to the bulk volume whereas effective porosity is the ratio of only interconnected pore volume to the bulk volume. The porosities measured in this study are all effective since they provide the flow path and the storage for the recoverable hydrocarbon.

The helium expansion porosimeter is based on the principle of Boyle's law which describes an isothermal expansion of ideal gas with equation PV = constant, where P and V are the pressure and volume of the gas respectively. It is believed that this technique has the advantage of accurate, non-destructive and fairly rapaid porosity measurements for majority of the rock samples encountered. The reason for using helium gas is that it has one of the smallest molecules and can therefore pentrate all the interconnected pore spaces for any rock sample in the shortest possible time. The absorption of this gas on the surface of rocks is also said to be negligible compared to air (Jing, 1993).

A simple procedure for the derivation of the grain volume based on Boyle's law is as follows (Jing, 1993)

$$P_1 . V_R / T_1 + P_2 . V / T_2 = P_3 . (V_R + V) / T_3 \qquad (B.1)$$

where

P_1 = reference pressure, psi

V_R = reference volume, cm^3

P_2 = pressure in the unknown volume, psi

V = unknown volume, cm^3

T_1, T_2, T_3 = absolute temperatures, K

P_3 = resultant equilibrium pressure, psi

Since P_2 is the atmospheric pressure, under isothermal conditions, i.e. $T_1 = T_2 = T_3$, equation (B.1) becomes:

$$(P_1 + B) \,.\, V_R + B.\, V = (P_3 + B) \,.\, (V_R + V) \qquad \text{(B.2)}$$

where B is the barometric pressure. Thus

$$P_3.\, V = V_R \,.\, (P_1 - P_3) \qquad \text{(B.3)}$$

The above equation can be written as

$$V = V_R \,.\, ((P_1 / P_3) - 1) \qquad \text{(B.4)}$$

The term $(P_1/P_3 - 1) = R$ is defined as the expansion ratio. So when all the dummy pieces are in the core holder, equation (B.4) becomes

$$V_1 = V_R\, R_1 \qquad \text{(B.5)}$$

Similarly, with some dummy cores taken out:

$$V_2 = V_R R_2 \tag{B.6}$$

and with the core plug in place

$$V_3 = V_R R_3 \tag{B.7}$$

where R_1, R_2 and R_3 are all expansion ratios. Therefore,

$$V_2 - V_1 = V_R (R_2 - R_1) = V_D$$

where V_D = dummy core volume. Since V_D is already known, the reference volume (V_R) can be calculated from:

$$V_R = V_D / (R_2 - R_1)$$

So the grain volume (V_2 , V_3) can be found from:

$$Vg = V_R (R_2 - R_3) \tag{B.8}$$

All samples were made with regular shapes and with sharp edges, so the bulk volume can measured using a calliper.

(b) Air Permeability Measurements

Permeability is a measure of the specific flow capacity of a porous media and it is independent of the types of pore fluids present. Permeability of any materials can be determined accurately only by flow experiments. Empirical correlations between the porosity and permeability of rocks may exist only for rocks with the same lithology , pore geometry and pore size distribution (Archer and Wall 1992, Al-Mahtot and Mason 1996).

For flow of fluid, heat and electrical current, a transport equation in the direction of the applied potential gradient is defined as:

$$Q / A = U = - \text{constant}\ d\Phi/dL \tag{B.9}$$

i.e., the rate of transfer is proportial to a potential gradient. Based on the transport equation, Darcy (1856) derived experimentally a relation which is well knon as the Darcy's law for flow of water through beds of sand as follows

$$Q/A = - k\, d\Phi' / \mu\, dL \tag{B.10}$$

and,

$$k = Q \mu \ / \ A (d\Phi' / dL) , \tag{B.11}$$

where k is the permeability of the rock in Darcy which has a dimension of L^2, μ = viscosity of fluid (cp), $d\Phi' / dL$ = datum corrected pressure drop (atm/cm) and A = cross section area of flow (cm^2). Darcy's law is inadequate at high flow velocities due to the effects of inertia and turbulence. A quadratic equation containing a coefficient of inertial resistance which is dependent on the geometry of the porous medium can be used instead (Noman and Archer 1987).

Dry gas such as air, nitrogen or helium is usually used in laboratory determination of permeability in order to minmise fluid-rock reaction and also for convenience. Fig. **A.1** shows a schematic diagram of the Hassler cell for flow measurements. Air permeability can be calculated from the following equation:

$$k_a = 2 \mu L Q_{sc} P_{atm} / A (P_1^2 - P_2^2) \qquad (B.12)$$

where P_1, P_2 are the upstream and downstream pressures (psi), and Q_{sc} is the flow rate measured at standard conditions (cm^3/h). The air permeability measured in this way differs from the true permeability, and requires the application of the Klinkenberg correction (Klinkenberg 1941), but this correction was not used in the present research, since it can readily be evaluated given the confining pressure and mean gas pressure values.

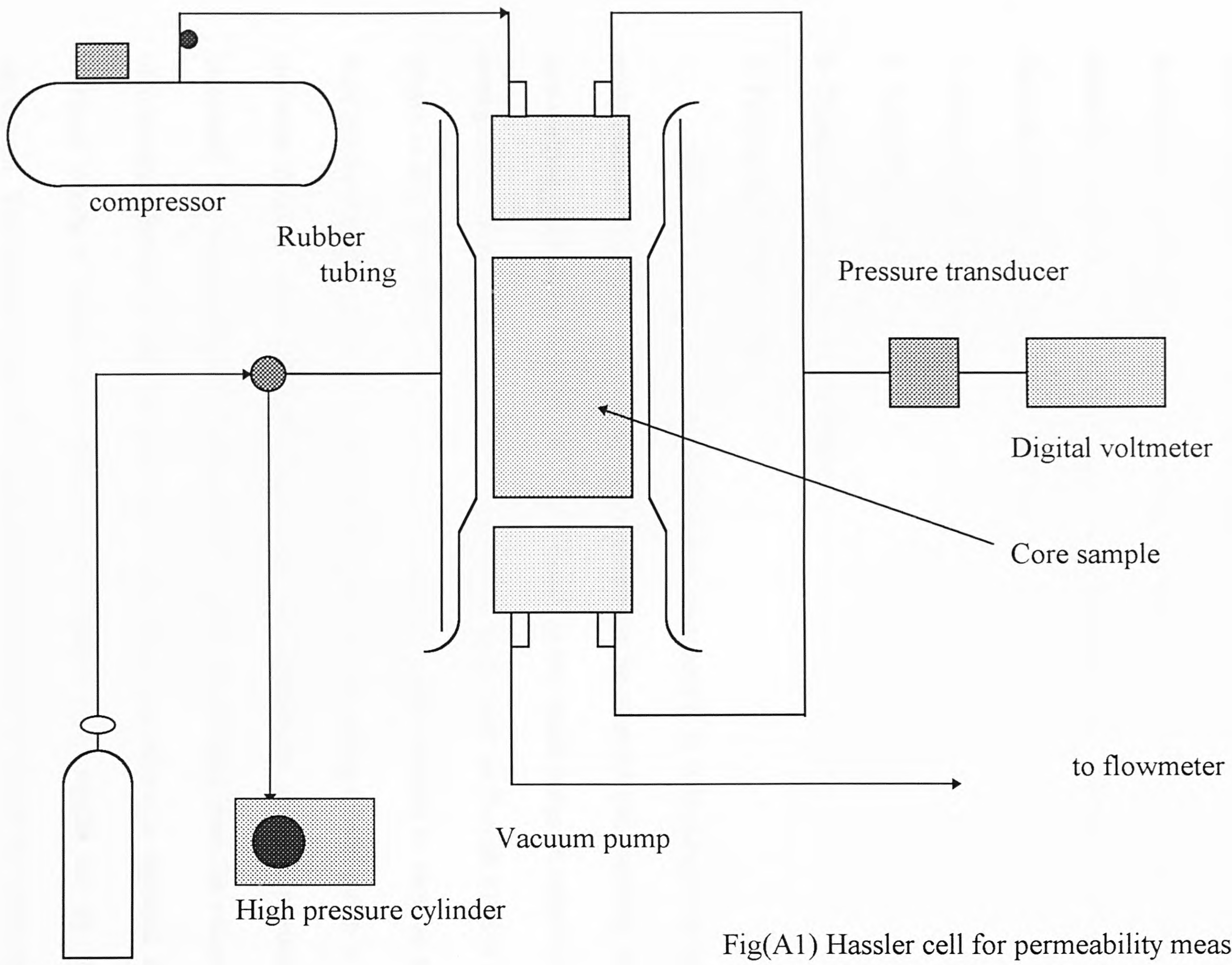

Fig(A1) Hassler cell for permeability measurements

(c) Capillary pressure Measurements

The pore size distribution in a given rock type, which has been shown to influence initial saturation distribution, permeability and electrical resistivity, can be determined using the capillary pressure measurements. There are four basic methods avalible for experimental determination of capillary pressure characteristics of rock samples. These are

1- Mercury injection method

2- Centrifuge method

3- Dynamic capillary pressure method

4- Porous diaphragm method

Although the mercury injection test is destructive, it is employed in this study because of the advatage that high pressure can be attained and mercury, the non-wetting phase with respect to air, can be forced into small pores. A schematic arrangement of the apparatus similar to that originally used by Purcell (1949) is shown in Fig. **A. 2**. The core is placed in a chamber under vacuum to remove air from the pore spaces. Mercury is then forced into the core using a hand pump in a stepwise fashion, with sufficient time given for equlibrium at each pressure increased. The non-wetting phase saturation , can be determined from the volume of mercury injected at each pressure step. The above procedure is repeated till mercury pressure reachs very high pressure (2000 psi), which set by the equipment. The reverse cycle of the withdrawn of mercury is carried out after the maximum pressure has been reached to determine the imbibition capillary pressure and to show the hysteresis (This was not presented in this thesis results). The pore

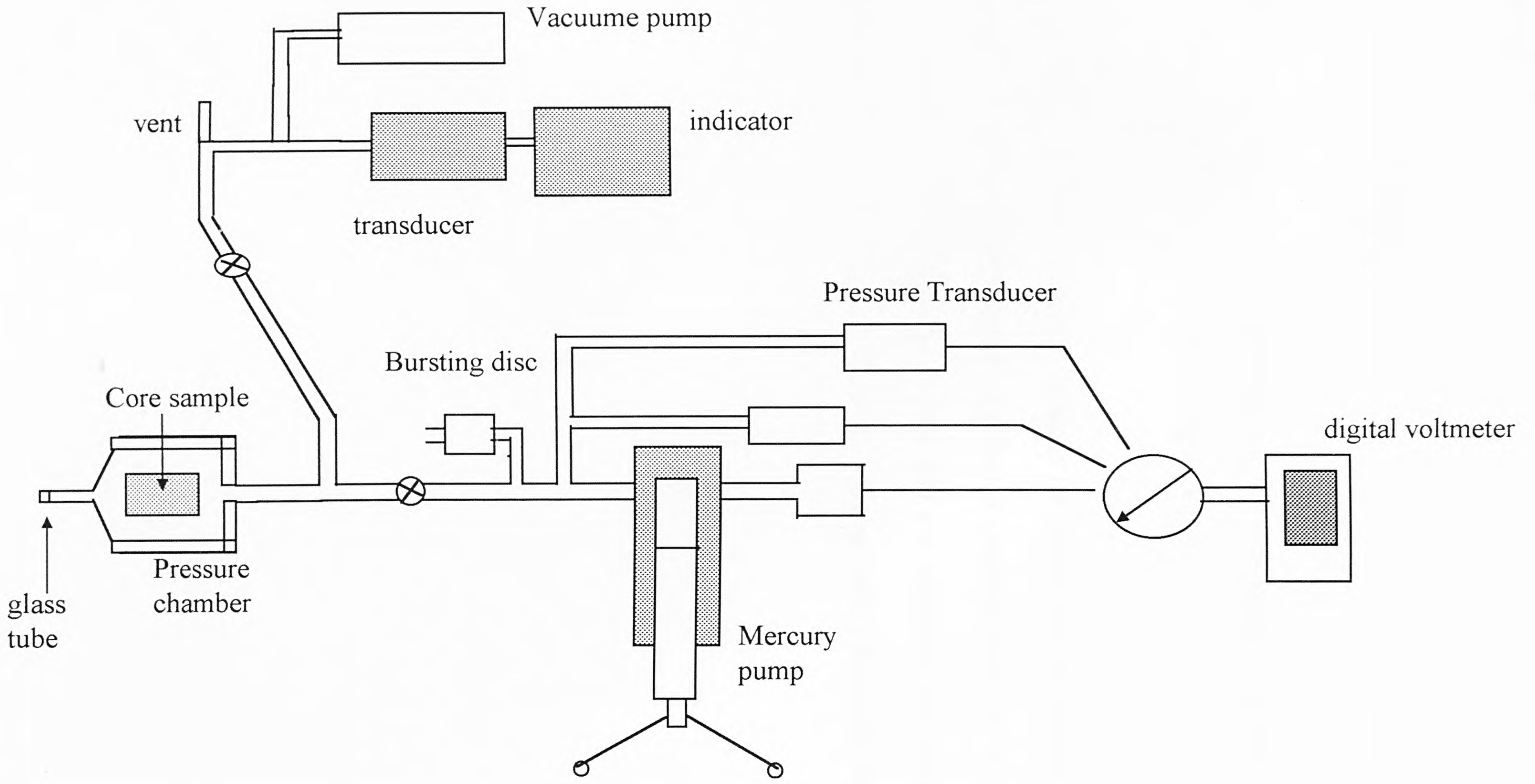

Fig.(A2) Schematic diagram of mercury capillary pressure set-up (after Noman 1988) size distribution function (D_r) is determined from the capillary pressure curve as follows

$$D_r = P_c / r \quad dS/dP_c$$

Where P_c is the capillary pressure (psi), r is the pore radius (μm) and dS/dP_c is the inverse of the slope of the capillary pressure plot.

Although there are various methods for carring out the measurements of porosity, permeability and pore size distribution (capillary pressure) of rocks, for the purpose of the present work only a few are employed and therefore are discussed. More can be found in literature (Keelan 1972, Monicard 1980, Hurst 1987).